分光学俯瞰講義

47+ Years of Spectroscopy on Unstable Species

Yuan-Pern Lee

Department of Applied Chemistry,

National Yang Ming Chiao Tung University, Hsinchu, Taiwan

1952 Born

1973 BS, Dept. Chemistry, National Taiwan University

1975 Dept. Chemistry, U. C. Berkeley
George Pimentel (1922–1989)

Matrix isolation– chemi-luminescence

1978

Chemiluminescence of SO ($\tilde{c}\,^1\Sigma^- \rightarrow \tilde{a}\,^1\Delta$) in solid argon

Yuan-Pern Lee and George C. Pimentel

Department of Chemistry, University of California, Berkeley, California 94720

(Received 23 May 1978)

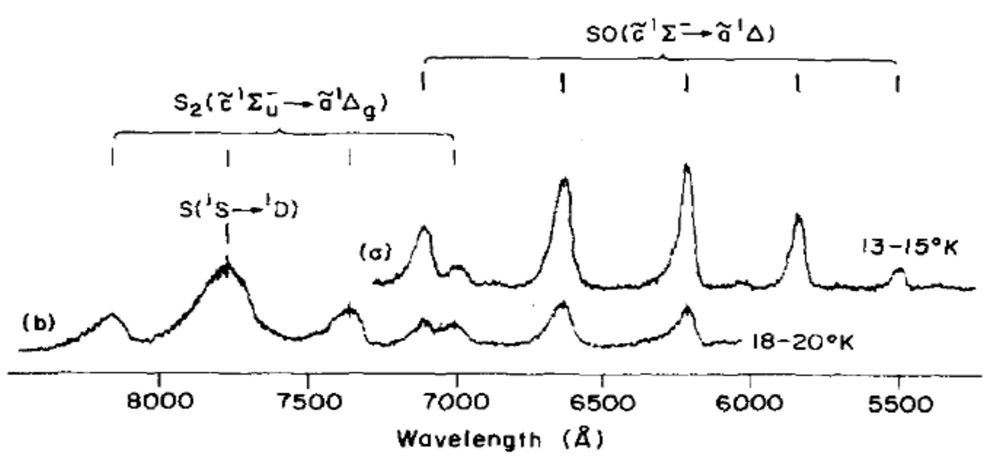

FIG. 1. Thermoluminescence spectra of irradiated OCS/O_2/Ar. Trace (a) 1/1/200; trace (b) 3/1/200.

JCP *69*, 3063 (1978)

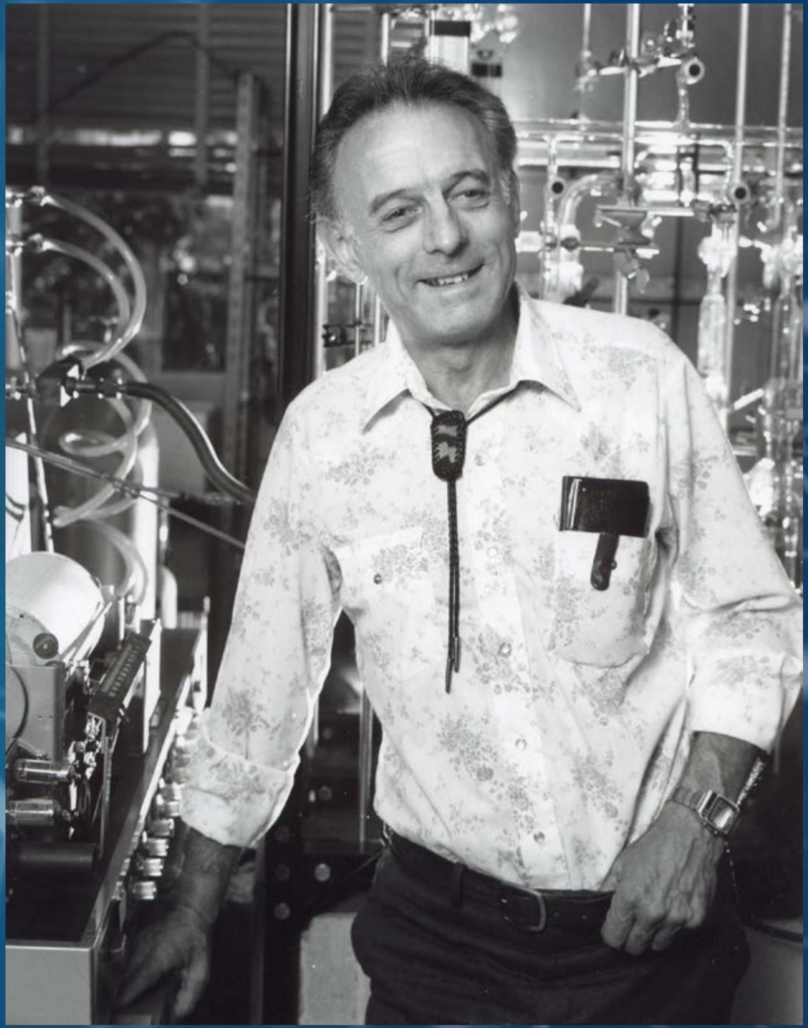

1978

Henry F. Schaeffer (1944–)

Quantum-chemical calculations

1979

Diatomic sulfur: Low lying bound molecular electronic states of S_2 [a)]

William C. Swope, Yuan-Pern Lee, and Henry F. Schaefer, III

Department of Chemistry and Materials and Molecular Research Division, Lawrence Berkeley Laboratory, University of California, Berkeley, California 94720

(Received 22 August 1978)

TABLE IV. Comparison of theoretical and experimental results for 13 electronic states of S_2.

State	Size of D_{2h} CI space	Method[a]	T_e, cm^{-1}	T_0, cm^{-1}	r_e, Å	ω_e, cm^{-1}	B_e, cm^{-1}	α_e, cm^{-1}
$^1\Sigma_u^+$		SCF	72 500	δ + 65 800	2.026	650	0.2566	0.0011
	5529	CI	59 700	δ + 49 900	2.128	500	0.2326	
		CI+	53 800	δ + 44 800				
		Expt.[b]	45 100	δ + 36 624.7	⋯	428.5	⋯	⋯
$f\,^1\Delta_u$		SCF	61 400	a + 54 600	2.030	660	0.2556	0.0011
	5529	CI	49 700	a + 44 300	2.138	500	0.2305	0.0010
		CI+	44 100	a + 39 300				
		Expt.	~41 600	a + 36 875.45	2.1555	438.32	0.22704	0.00178
$e\,^1\Pi_g$		SCF	37 000	c + 24 400	2.160	280	0.2257	
	2915	CI	43 000	c + 25 700	2.143	430	0.2293	
		CI+	43 300	c + 25 400				
		Expt.[c]	(~37 000)	(c + 13 451.8)	(~2.08)	(533.7)	(~0.25)	⋯
$^1\Pi_u$		SCF	49 300	49 300	2.154	500	0.2270	0.0009
	3051	CI	41 600	41 600	2.243	400	0.2094	0.0012
		CI+	37 600	37 600				
		Expt.	⋯	⋯	⋯	⋯	⋯	⋯
$B'\,^3\Pi_g$		SCF	33 900	A' + 20 600	2.120	460	0.2345	
	2939	CI	35 400	A' + 17 100	2.106	450	0.2375	0.0023
		CI+	35 300	A' + 16 200				
		Expt.[d]	35 300	A' + 14 326	2.08	~500	0.244	⋯
$B\,^3\Sigma_u^-$		SCF	50 100	50 100	2.033	650	0.2549	0.0011
	5827	CI	38 300	38 300	2.142	490	0.2296	0.0017
		CI+	32 500	32 500				
		Expt.	31 689	31 689	2.168	434	0.2244	0.0018
$B''\,^3\Pi_u$		SCF	41 400	41 400	2.135	510	0.2310	0.0009
	3078	CI	35 200	35 200	2.219	430	0.2139	
		CI+	32 100	32 100				
		Expt.	≤31 700	≤31 700	<2.28	⋯	>0.2029	⋯
$A\,^3\Sigma_u^+$		SCF	14 000	A' + 710	2.156	510	0.2267	0.0014
	5747	CI	18 900	A' + 640	2.176	580	0.2224	0.0016
		CI+	19 700	A' + 620				
		Expt.[d]	21 971	A' + 997	2.15	482.15	0.2248	0.0014
$A'\,^3\Delta_u$		SCF	13 300	13 300	2.148	520	0.2284	0.0014
	5827	CI	18 300	18 300	2.168	480	0.2242	0.0016
		CI+	19 100	19 100				
		Expt.[d]	20 974	20 974	2.146	488.2	0.2285	0.0015
$c\,^1\Sigma_u^-$		SCF	12 600	12 600	2.140	527	0.2301	0.0014
	5653	CI	17 300	17 300	2.160	489	0.2257	0.0017
		CI+	17 900	17 900				
		Expt.[e]	~20 000	~20 000	⋯	⋯	⋯	⋯
$b\,^1\Sigma_g^+$		SCF	6730	6730	1.877	813	0.2989	0.0012
	4562	CI	9790	9790	1.914	732	0.2874	0.0015
		CI+	8960	8960				
		Expt.	~8500	~8500	⋯	700.82	⋯	⋯
$a\,^1\Delta_g$		SCF	6730	6730	1.877	813	0.2989	0.0012
	4562	CI	5440	5440	1.907	746	0.2897	0.0014
		CI+	4820	4820				
		Expt.	~4700	~4700	1.8987	702.35	0.29262	0.00173
$X\,^3\Sigma_g^-$		SCF	0	0	1.876	819	0.2994	0.0012
	2948	CI	0	0	1.900	760	0.2920	0.0015
		CI+	0	0				
		Expt.	0	0	1.889	725.668	0.29541	0.00158

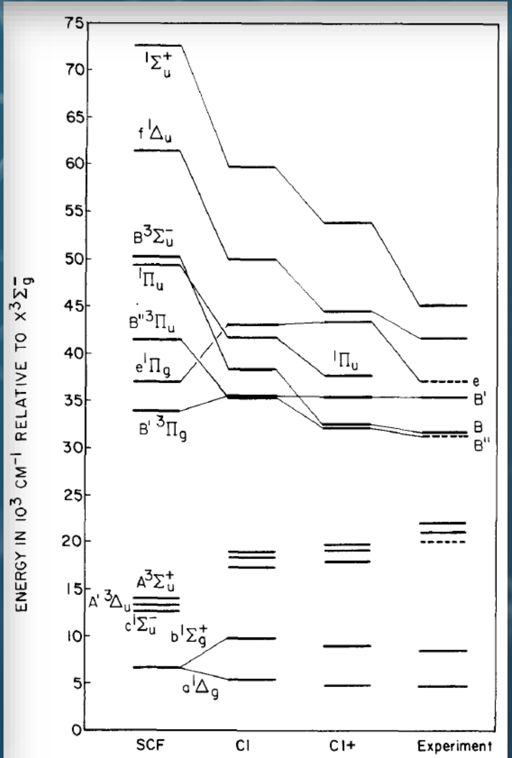

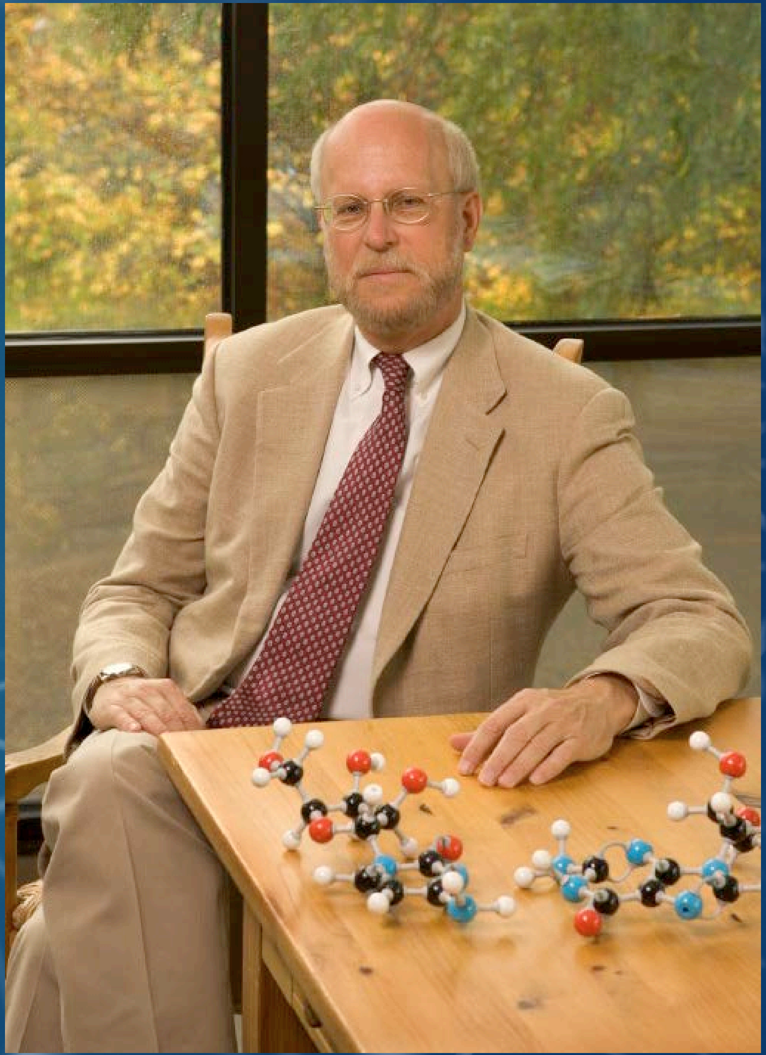

JCP *70*, 947 (1979)

1979 PhD, Dept. Chemistry, U. C. Berkeley

Postdoctor, ERL, NOAA, Boulder, Colorado

Carleton Howard (1945–)

Chemical kinetics & atmospheric chemistry

LMR & discharge-flow tube

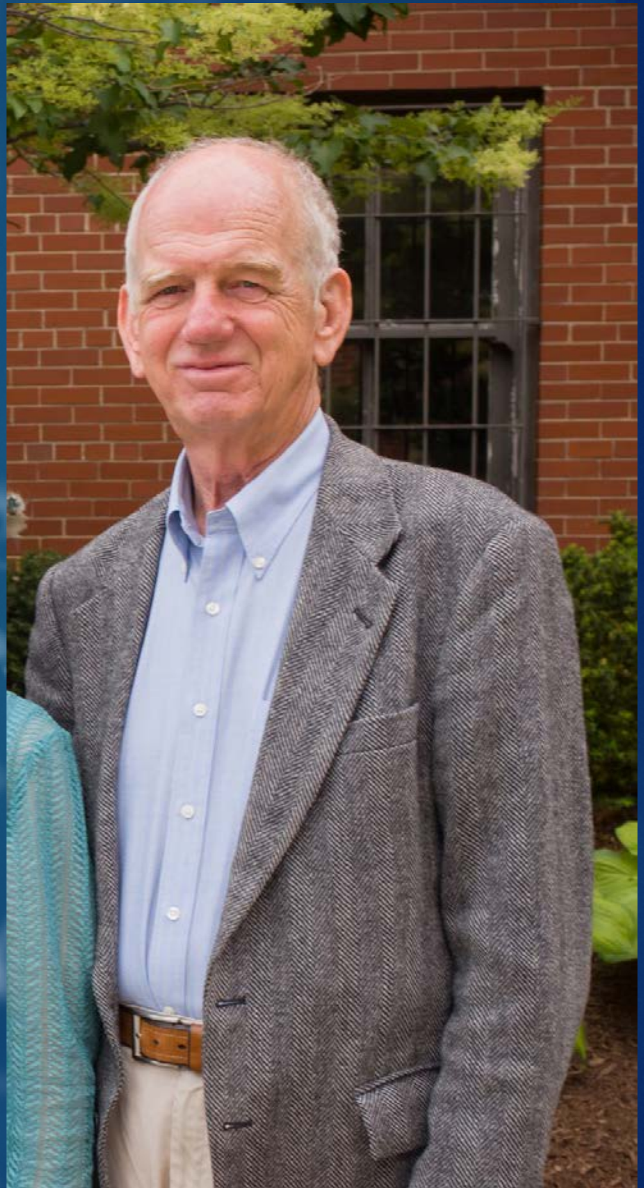

1982

Laser Magnetic Resonance Spectroscopy of ClO and Kinetic Studies of the Reactions of ClO with NO and NO_2

YUAN-PERN LEE,* RICHARD M. STIMPFLE,†‡ ROBERT A. PERRY,** JOHN A. MUCHA,§ KENNETH M. EVENSON,° DONALD A. JENNINGS,° and CARLETON J. HOWARD†

Aeronomy Laboratory, NOAA Environmental Research Laboratory, Boulder, Colorado 80303

Int. J. Chem. Kinet. *14*, 711 (1982)

1981

Assoc. Professor (Unfavorable environments)

Dept. Chemistry, National Tsing Hua University

Matrix isolation– chemi-luminescence

Chemical kinetics– discharge flow tube

1985

JCP *82*, 2942 (1985)

Chemiluminescence of CaO from the Ca+N_2O and Ca+O_3 reactions in solid argon

Chining-Shiang Wei, Sui-Whei Guo, and Yuan-Pern Lee
Department of Chemistry, National Tsing Hua University, 855 Kuang-Fu Rd., Hsin-Chu, Taiwan, Republic of China

(Received 14 November 1984; accepted 11 December 1984)

Int. J. Chem. Kinet. *17*, 1201 (1985)

Temperature Dependence of the Rate Constant for the Reaction OH + H_2S in He, N_2, and O_2

YU-LIN LIN, NIANN-SHIAH WANG, and YUAN-PERN LEE
Department of Chemistry, National Tsing Hua University, Hsinchu, Taiwan 300, Republic of China

1985 **Professor,** Dept. Chemistry, National Tsing Hua University

1986 **First laser- Nd:YAG + dye laser**

1987

JQSRT 38, 163 (1987)

THE S_{21} LINES OF THE $A^2\Sigma^+$ $(v' = 1) \leftarrow X^2\Pi$ $(v'' = 0)$ TRANSITIONS OF OH AND OD

Shiaw-Ruey Lin, Sze-Tsen Lee and Yuan-Pern Lee
Department of Chemistry, National Tsing Hua University, Hsinchu, Taiwan 30043, Republic of China

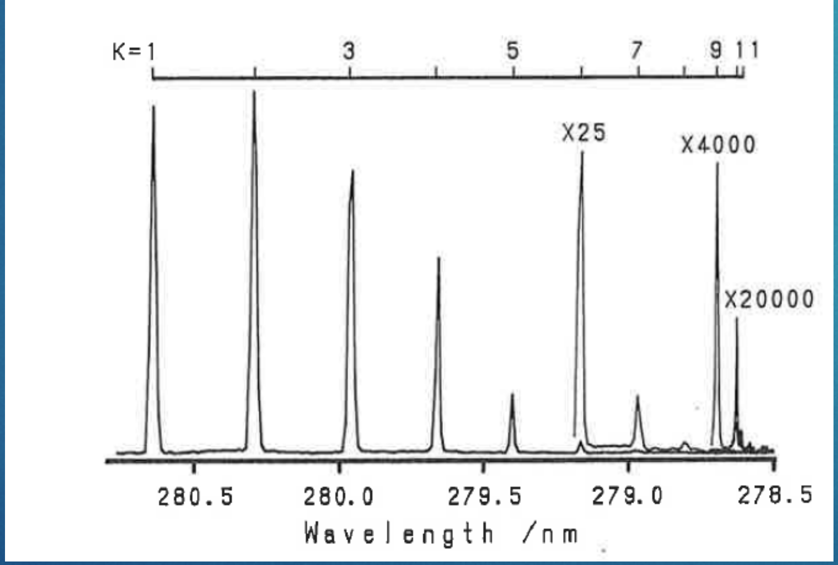

1986

First FTIR: Bomem DA3.002 (Regional Instrument Center)

1987

JCCS *34*, 161 (1987)

PRODUCT DETERMINATION OF GASEOUS RADICAL REACTIONS USING MATRIX ISOLATION–FTIR DETECTION

YU-PING KUO (郭玉苹), SHAN-SHAN JU (朱姍姍) AND YUAN-PERN LEE (李遠鵬)
Department of Chemistry, National Tsing Hua University, Hsinchu, Taiwan 30043, R.O.C.

$ClO + HO_2 \rightarrow$
Observed HO_2, ClO, ClO_2,
HOCl, HCl

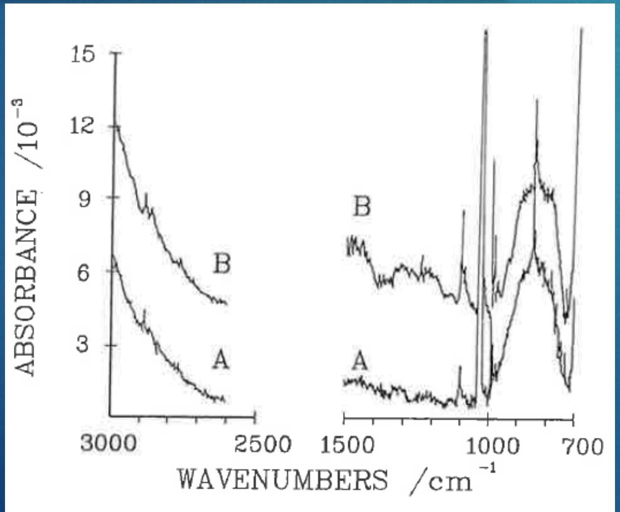

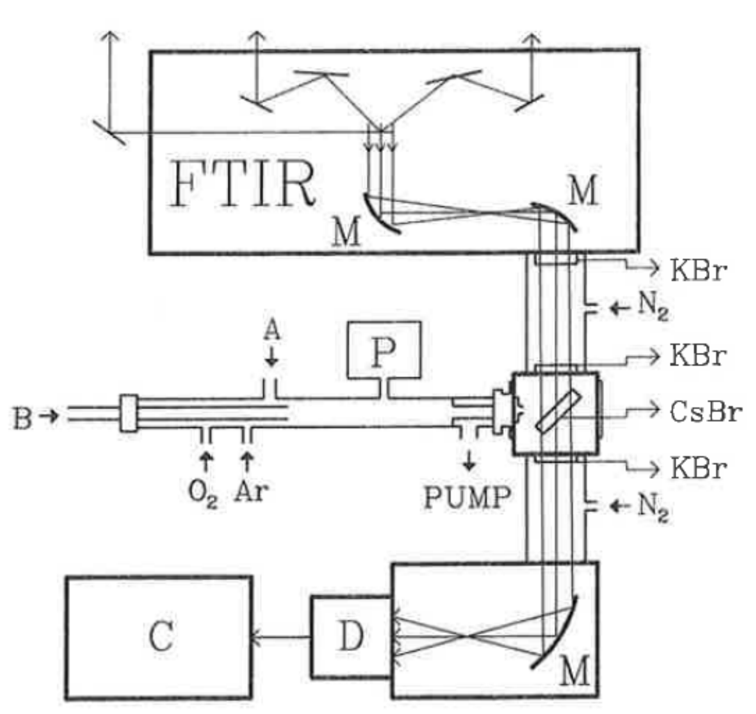

1988 Chung-Shan Academic Research Award
中山學術著作獎

1990 Academic Achievement Award in Science
(教育部理科學術獎, Ministry of Education, Taiwan)

1991 21st International Symposium on Free Radicals, Williamstown, Massachusetts, U.S.A. (Plenary talk)
"*Spectroscopy and kinetics of radicals of atmospheric interest*"

1999 Fellow (American Physical Society)

2008 Academician (Academia Sinica)中央研究院第二十七屆院士

2018 George C. Pimentel Prize for Advances in Matrix Isolation

2019 Presidential Science Prize, Taiwan

Techniques in Spectroscopy

1987	Supersonic jet, laser-induced fluorescence
1988	Matrix isolation, Laser-induced fluorescence
1995	VUV absorption / ionization
1995	Degenerate four-wave mixing Two-color resonant four-wave mixing
1995	Step-scan FTIR in emission mode
1997	Step-scan FTIR in absorption mode
2004	*Para*-hydrogen matrix isolation
2005	NIR Cavity ringdown
2011	VUV/IR ionization TOF detection
2018	Quantum-cascade laser absorption

Techniques in kinetics/dynamics

1985	Discharge-flow tube / Resonance fluorescence
1990	Flash (Laser) photolysis / Laser-induced fluorescence
1995	Step-scan FTIR in emission (2001)
1997	Step-scan FTIR in absorption (2006)
2002	Diaphragmless Shock tube
2018	Quantum-cascade laser absorption

Matrix Isolation

Inert-gas matrices

Pimentel & Porter, 1954

Sample diluted in inert gas and deposited onto a cold (4–20 K) target

guest : sample

host : Ar, Ne, Kr, Xe, N_2, O_2, H_2

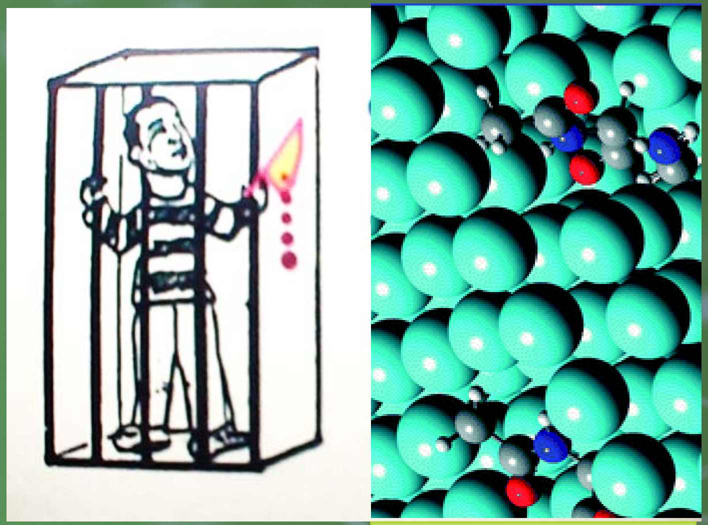

Pohl et al.
PCCP 9, 4698 (2007)

Characteristics

1. Requires minimal samples
2. Simplified spectra– no rotation, no hot bands
3. Small matrix shift of vibrational wavenumbers from gas phase
4. Cage effect– higher photo-dissociation threshold
   recombination of dissociation fragments
5. Rapid energy relaxation

Matrix Isolation — Electronic transitions

Chemi-luminescence

S_2, SO, C_2N_2, BaO, CaO, CaCl

Laser-induced fluorescence

S_2, SO, SO_2, CH_3O, CH_3S, CS_2^+, S_2^+, OClO, C_{60}

JCP *70*, 692 (1979)

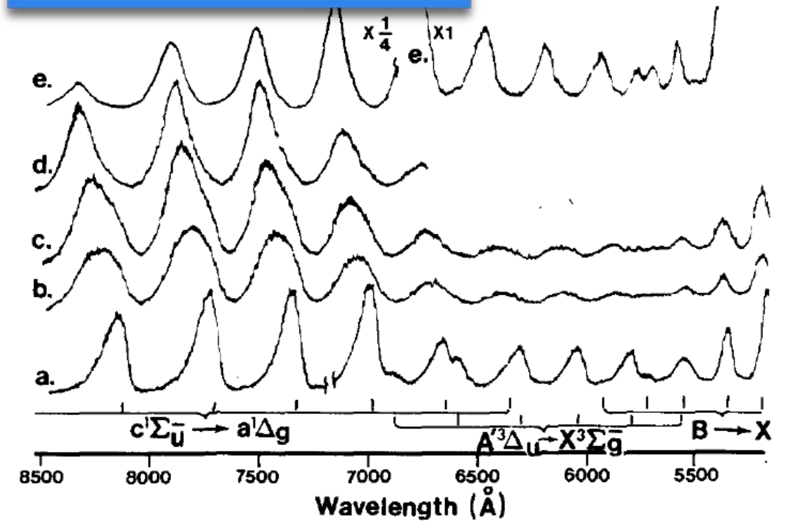

JCP *89*, 13 (1988)

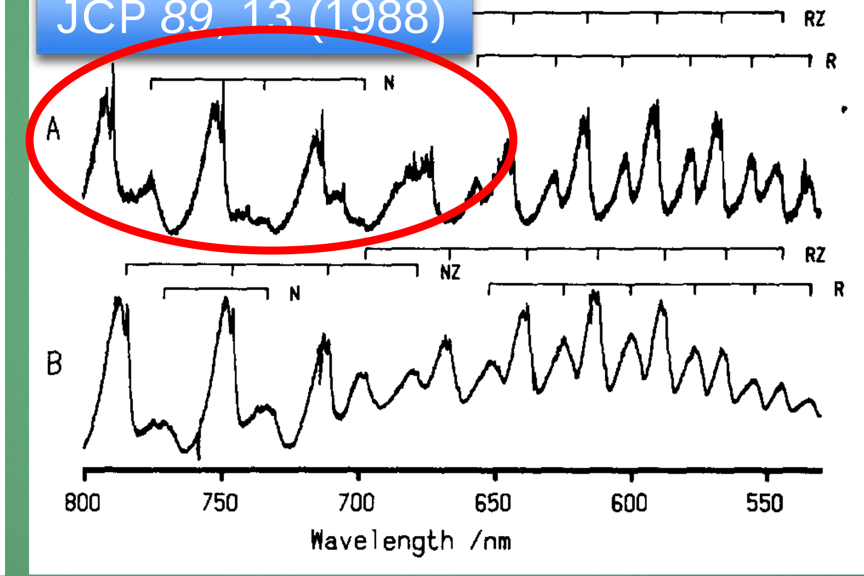

	$A'\ ^3\Delta_u \rightarrow X\ ^3\Sigma_g^-$	$c\ ^1\Sigma_u^- \rightarrow X\ ^3\Sigma_g^-$	$c\ ^1\Sigma_u^- \rightarrow a\ ^1\Delta_g$	$c\ ^1\Sigma_u^- \rightarrow a\ ^1\Delta_g$
ν_{00} /cm^{-1}	20870 ± 30	19757	15750 ± 10	15417
ω_e'' /cm^{-1}	724 ± 6	721.4	699 ± 5	698.1
$\omega_e x_e''$/cm^{-1}	2.9 ± 1.0	2.86	2.6 ± 1.0	3.04

Matrix Isolation — Inert-gas matrices

IR absorption

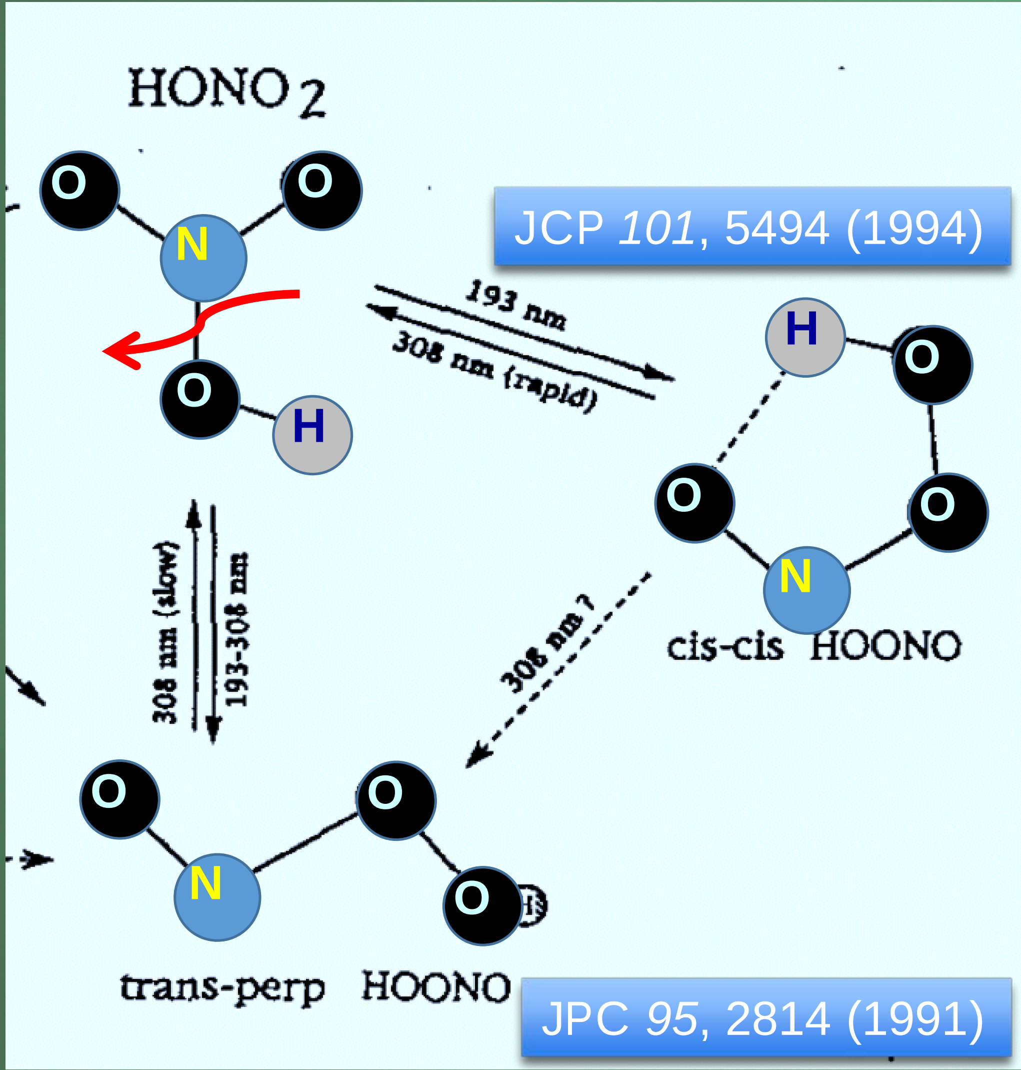

JCP *101*, 5494 (1994)

JPC *95*, 2814 (1991)

Make use of the **cage effect**

- HOONO
- KOONO — JCP *103*, 4026 (1995); CPL *242*, 147 (1995)
- *cyc*-KNO_2, KONO — JCP *104*, 935 (1996)
- OSOO — JCP *104*, 5745 (1996)
- SOO — JCP *105*, 9454 (1996)
- *cyc*-CS_2 — JACS *122*, 661 (2000)
- *cis*-, *trans*-OSNO — JCP *115*, 10694 (2001)
- HSCO — JCP *120*, 5717 (2004)
- ONCO — JCP *123*, 174301 (2005)

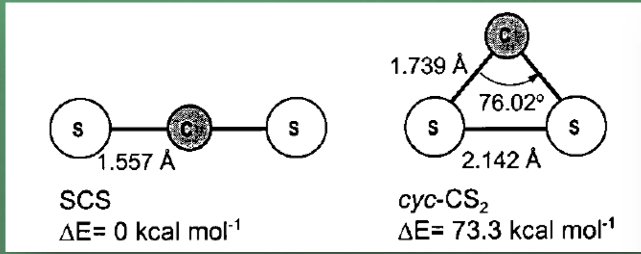

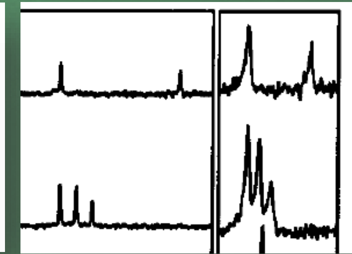

Matrix Isolation

para-H_2 matrices

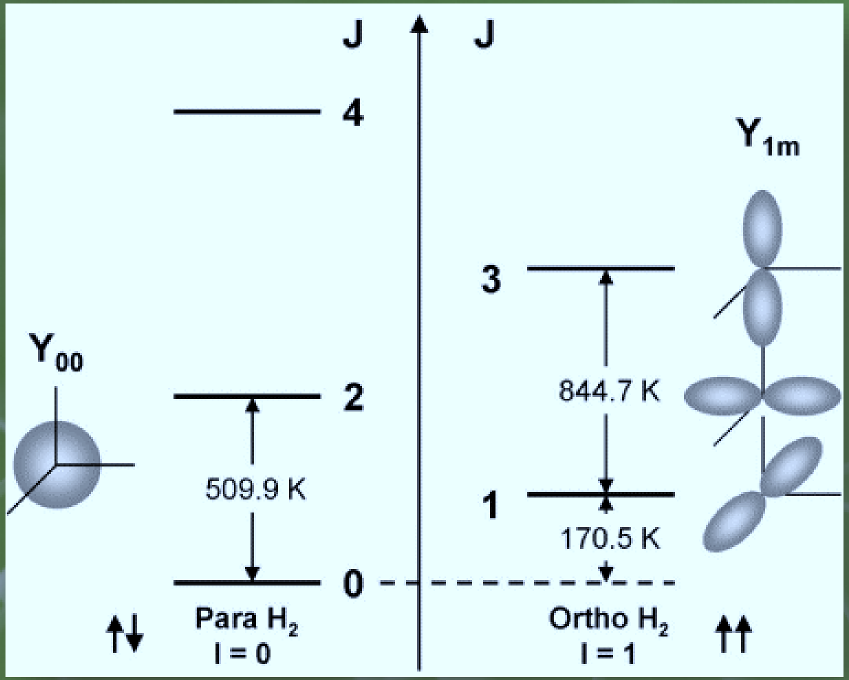

Quantum solid

large amplitude of zero-point vibration

Small interaction

- High resolution spectroscopy
- (Hindered) rotation for some molecules
- Diminished cage effect

Nuclear spin relaxation

***para*-H_2**

Nuclear spin = 0
(*antisymmetric*)

Rotational part
***J* even**
(*symmetric*)

***ortho*-H_2**

Nuclear spin = 1
(*symmetric*)

Rotational part
***J* odd**
(*antisymmetric*)

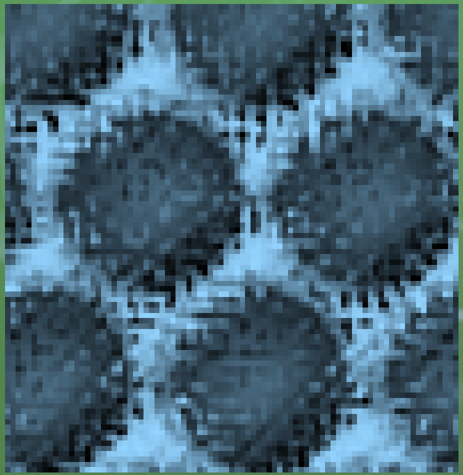

Free Radicals:

in situ photolysis

photo-induced bimolecular rxs :

atom/radical + molecules

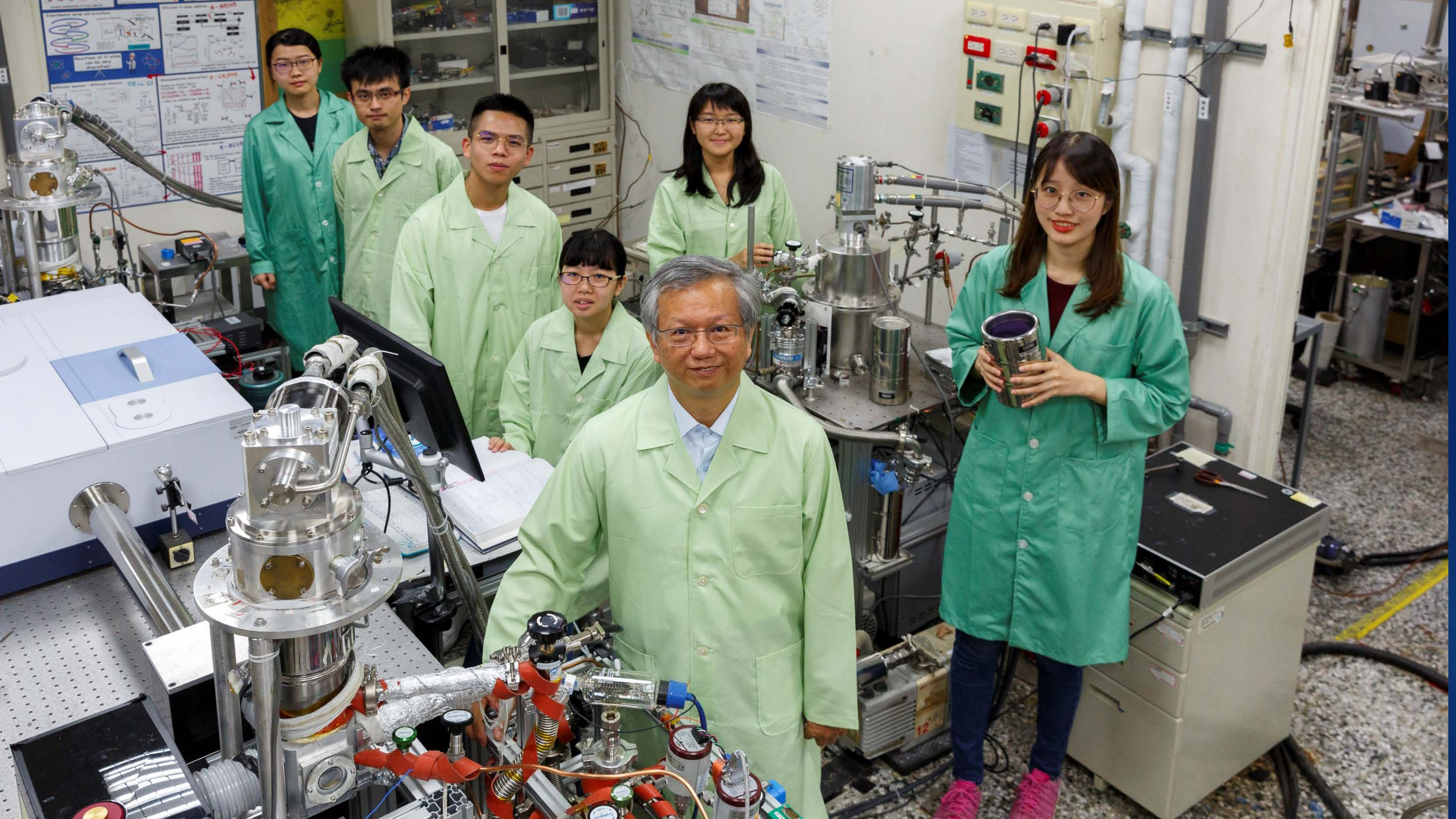

Torsional Motion of CH_3OH

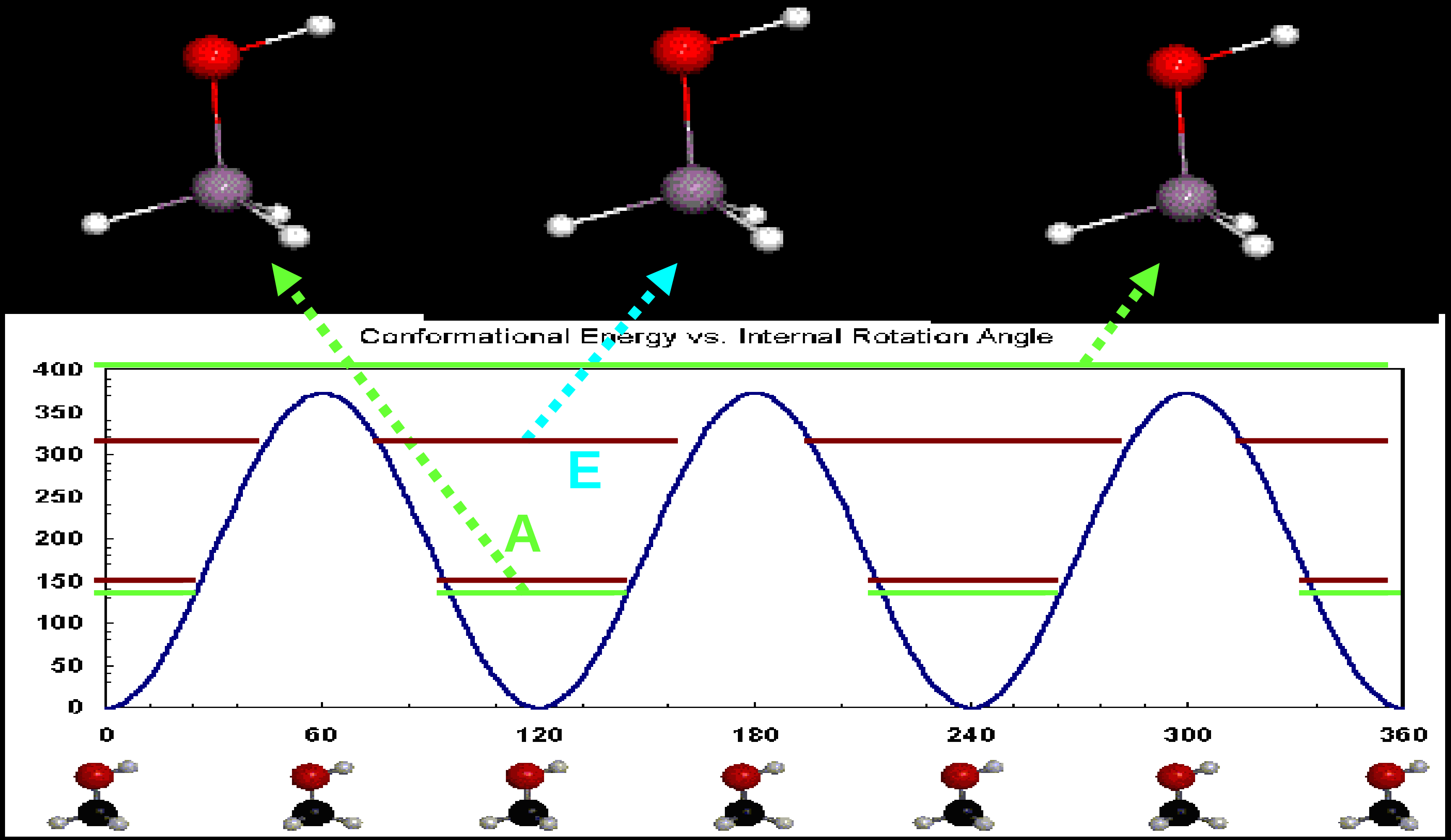

Taken from: Stephen L. Davis, George Mason University, Fairfax, VA 22030
http://classweb.gmu.edu/sdavis/research.htm

Matrix Isolation — *para*-H_2 matrices

Rotation & Nuclear Spin Relaxation

Science AAAS

Internal Rotation and Spin Conversion of CH_3OH in Solid para-Hydrogen

Yuan-Pern Lee,[1,2*] Yu-Jong Wu,[3] R. M. Lees,[4] Li-Hong Xu,[4] Jon T. Hougen[5]

VOL 311 20 JANUARY 2006 365


Jon Hougen

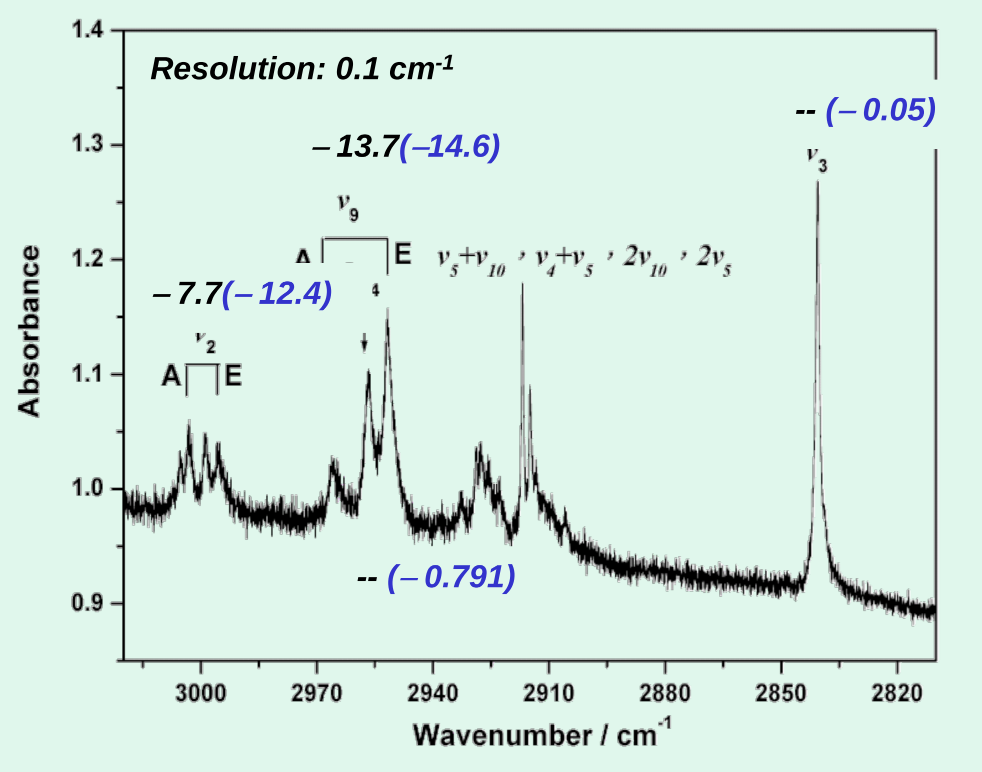

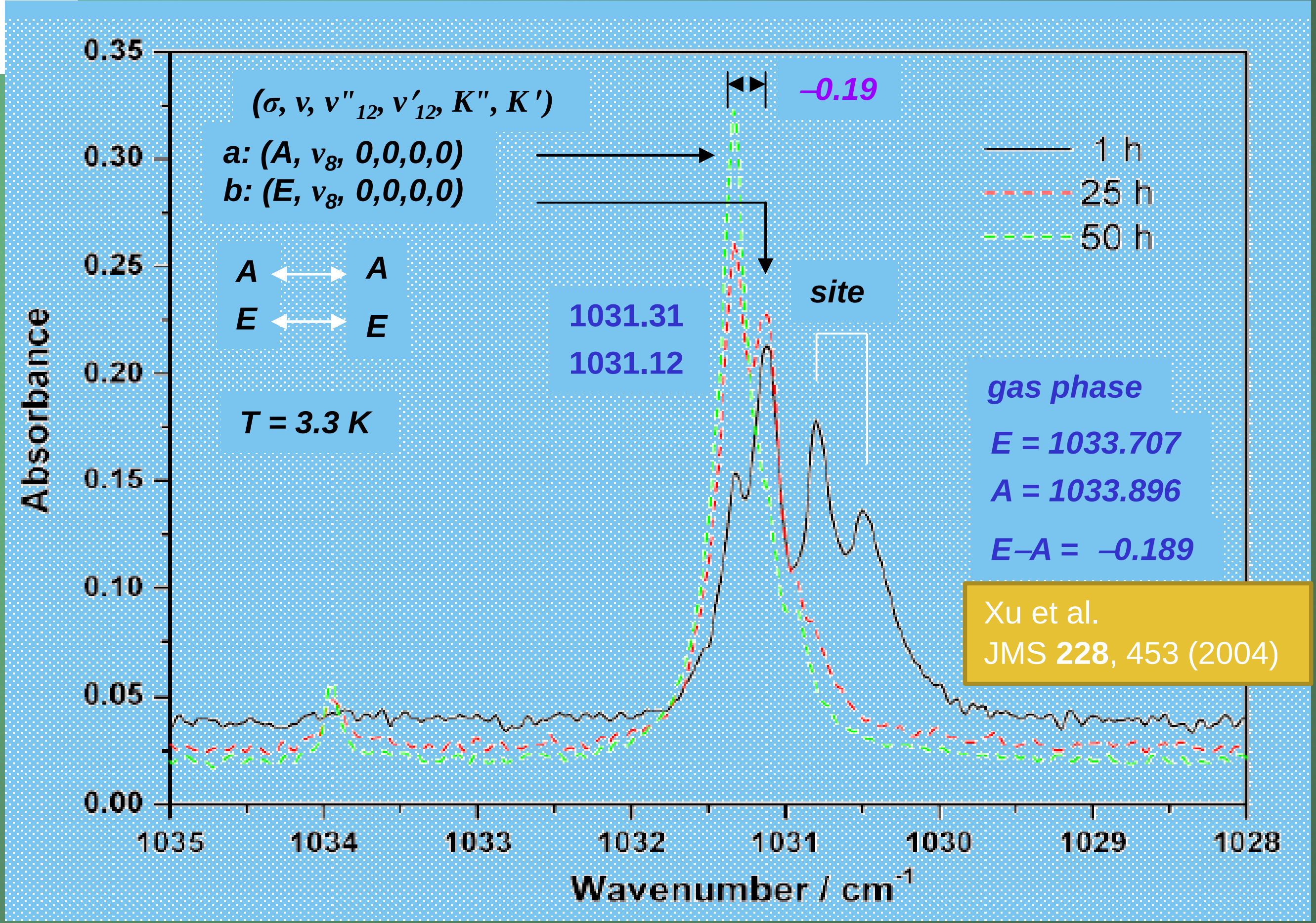

Matrix Isolation — *para*-H_2 matrices

Spinning Rotation of CH_3F

JCP *129*, 104502 (2008)

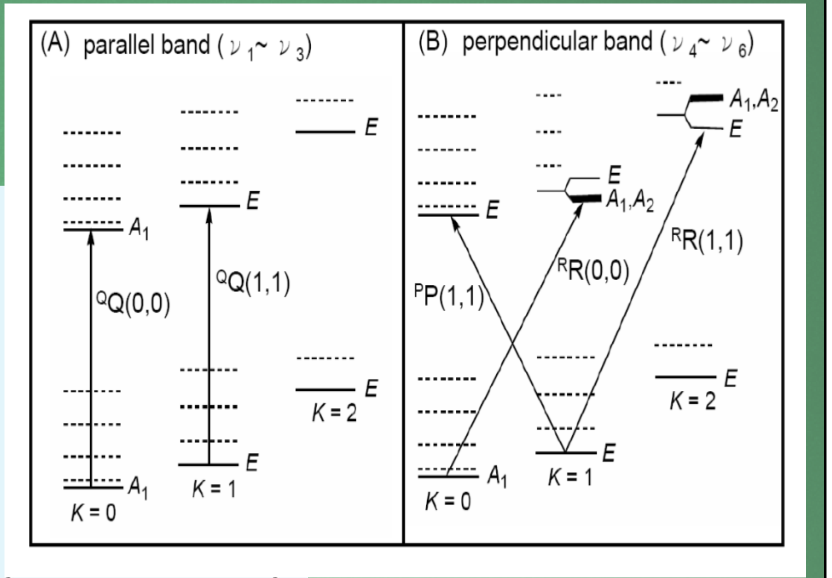

$$E = \nu_o + AK^2 - 2A\zeta Kl$$

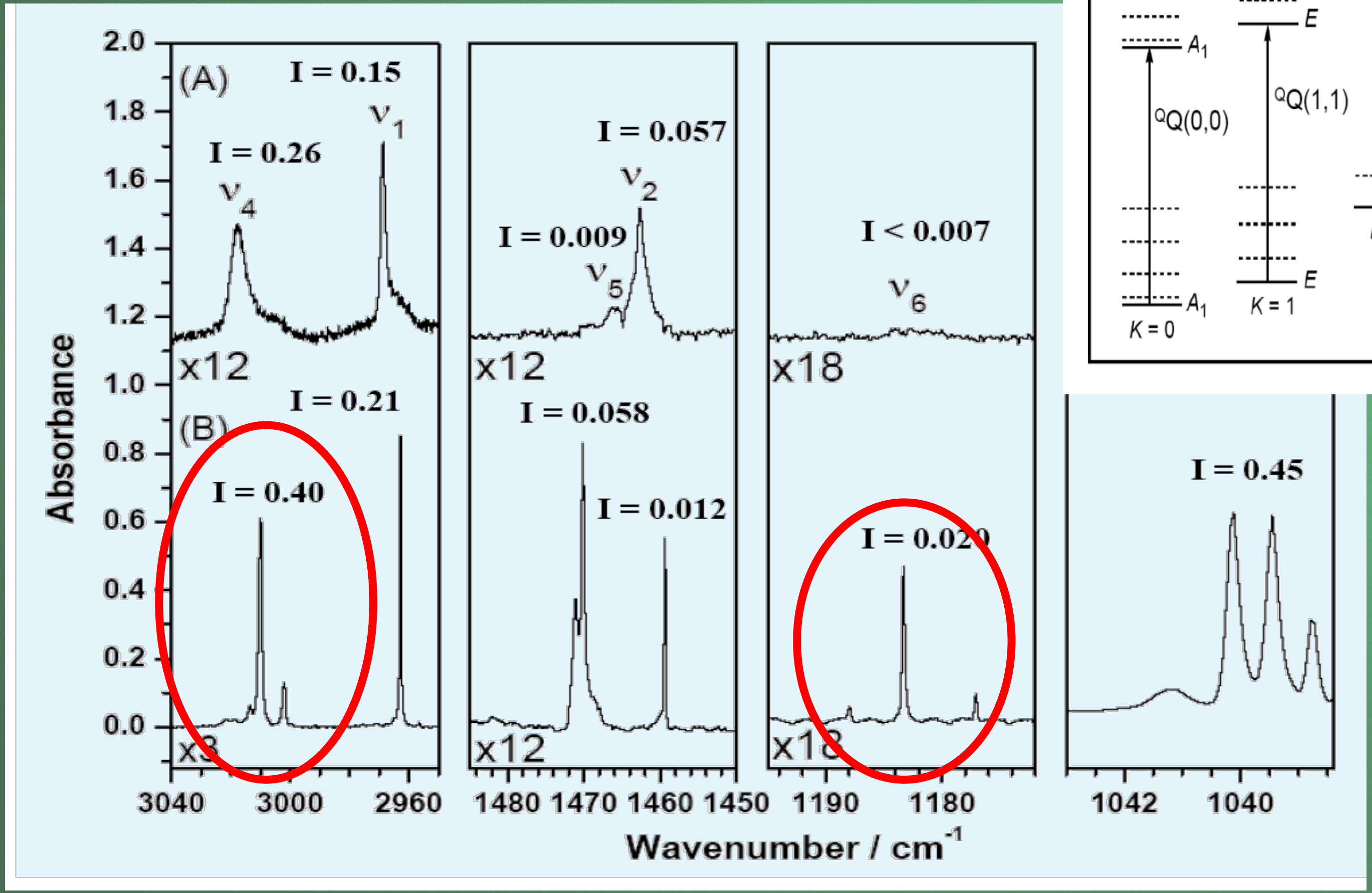

3 October 2008, Science

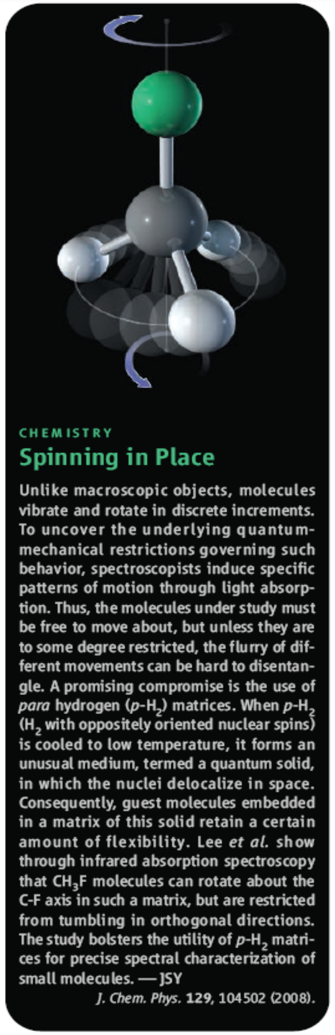

EDITORS' CHOICE

EDITED BY GILBERT CHIN AND JAKE YESTON

CHEMISTRY

Spinning in Place

Unlike macroscopic objects, molecules vibrate and rotate in discrete increments. To uncover the underlying quantum-mechanical restrictions governing such behavior, spectroscopists induce specific patterns of motion through light absorption. Thus, the molecules under study must be free to move about, but unless they are to some degree restricted, the flurry of different movements can be hard to disentangle. A promising compromise is the use of *para* hydrogen (*p*-H_2) matrices. When *p*-H_2 (H_2 with oppositely oriented nuclear spins) is cooled to low temperature, it forms an unusual medium, termed a quantum solid, in which the nuclei delocalize in space. Consequently, guest molecules embedded in a matrix of this solid retain a certain amount of flexibility. Lee *et al.* show through infrared absorption spectroscopy that CH_3F molecules can rotate about the C-F axis in such a matrix, but are restricted from tumbling in orthogonal directions. The study bolsters the utility of *p*-H_2 matrices for precise spectral characterization of small molecules. — JSY

J. Chem. Phys. **129**, 104502 (2008).

MICROBIOLOGY

Adapting to Drug Res

Developing a new therapy for infections is an expensive and that may give relief for less ti develop the agent. Hence, del resistance by administering d tion is a currently favored stra groups show this may not be implement wisely. By experim modeling, Hegreness *et al.* m tuitive discovery that synergis pairs, such as doxycycline and may actually accelerate the ev ance. In fact, antagonistic dru effective at forestalling resista because as one drug becomes suppressive effect on the othe unmask the potency of the se course, the precise outcome d drug ratios, doses, pharmacok modes of action.

Developing policies for the of drug combinations requires eling. Boni *et al.* compared th the standard wait-and-switch of drugs for malaria control w ous deployment of multiple dr shows that if three different drugs are offered for use at the same time within a malarious population, the clinical burden is reduced, the emergence of resistance is delayed by two- to fourfold, and the number of failed treatments is almost halved. — CA

Proc. Natl. Acad. Sci. U.S.A. **105**, 13977, 14216 (2008).

DEVELOPMENT

Signal Stability

Chordin and BMP signaling d trends across the *Xenopus* em between them the axis from d and destinations in between. between these and other facto plex regulatory interactions, i negative and positive feedbac predictions from some combi

*Helen Pickersgill is a locum editor in *Science*'s editorial department.

16 3 OCTOBER 2008 VOL 322 SCIEN

Published by AA

Matrix Isolation

para-H_2 matrices

Diminished Cage Effect

In situ photolysis: *The most straight-forward experiments*

CH_3S ← CH_3SSCH_3 → H_2CS + CH_3SH — JCP *133*, 164316 (2010)

CH_3O ← CH_3ONO → HNO + H_2CO — JMS *310*, 57 (2015); JCP *147*, 154305 (2017)

CH_3OSO ← CH_3OSOCl — JCP *136*, 124510 (2012)

$C_2H_3C(O)$ ← $C_2H_3C(O)Cl$ — JCP *139*, 084320 (2013)

CH_3CO ← $CH_3C(O)Cl$ — JCP *140*, 244303 (2014)

anti-, *gauche*-C_2F_4I ← CF_2ICF_2I — PCCP *20*, 12650 (2018)

n-propyl ← $CH_3CH_2CH_2I$ — JMS *363*, 111170 (2019)

i-propyl ← CH_3CHICH_3

(*Z*)-•$C_2H_3C(CH_3)I$ ← (*Z*)-$(CH_2I)HC=C(CH_3)I$ — JPCA *124*, 5887 (2020)

(*E*)-•$C_2H_3C(CH_3)I$ ← (*E*)-$(CH_2I)HC=C(CH_3)I$

Vibrations of CH_3O

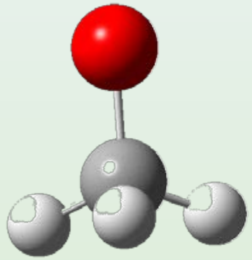

ν_1 : CH stretch

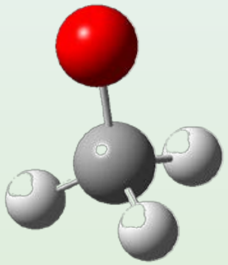

ν_2 : umbrella

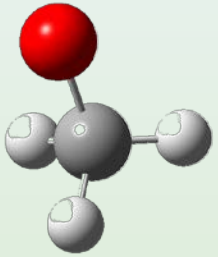

ν_3 : CO stretch

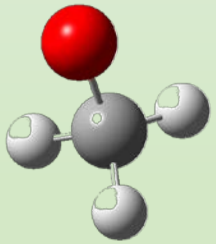

ν_4 : CH stretch

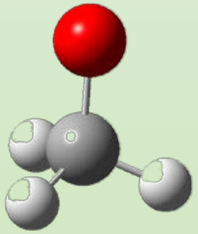

ν_5 : bend

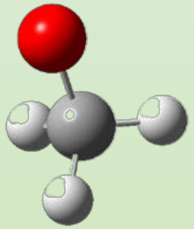

ν_6 : rocking

- Jahn-Teller Distortion
- Spin-Orbit interaction
- Ground state:

  $^2E_{1/2}$ and $^2E_{3/2}$

Degenerate modes:

4 components

No IR spectrum except the CH-stretching region (?) (Curl, JCP 2009)

Identification of Lines of CH_3O

J. Mol. Spectrosc. *310*, 57 (2015)

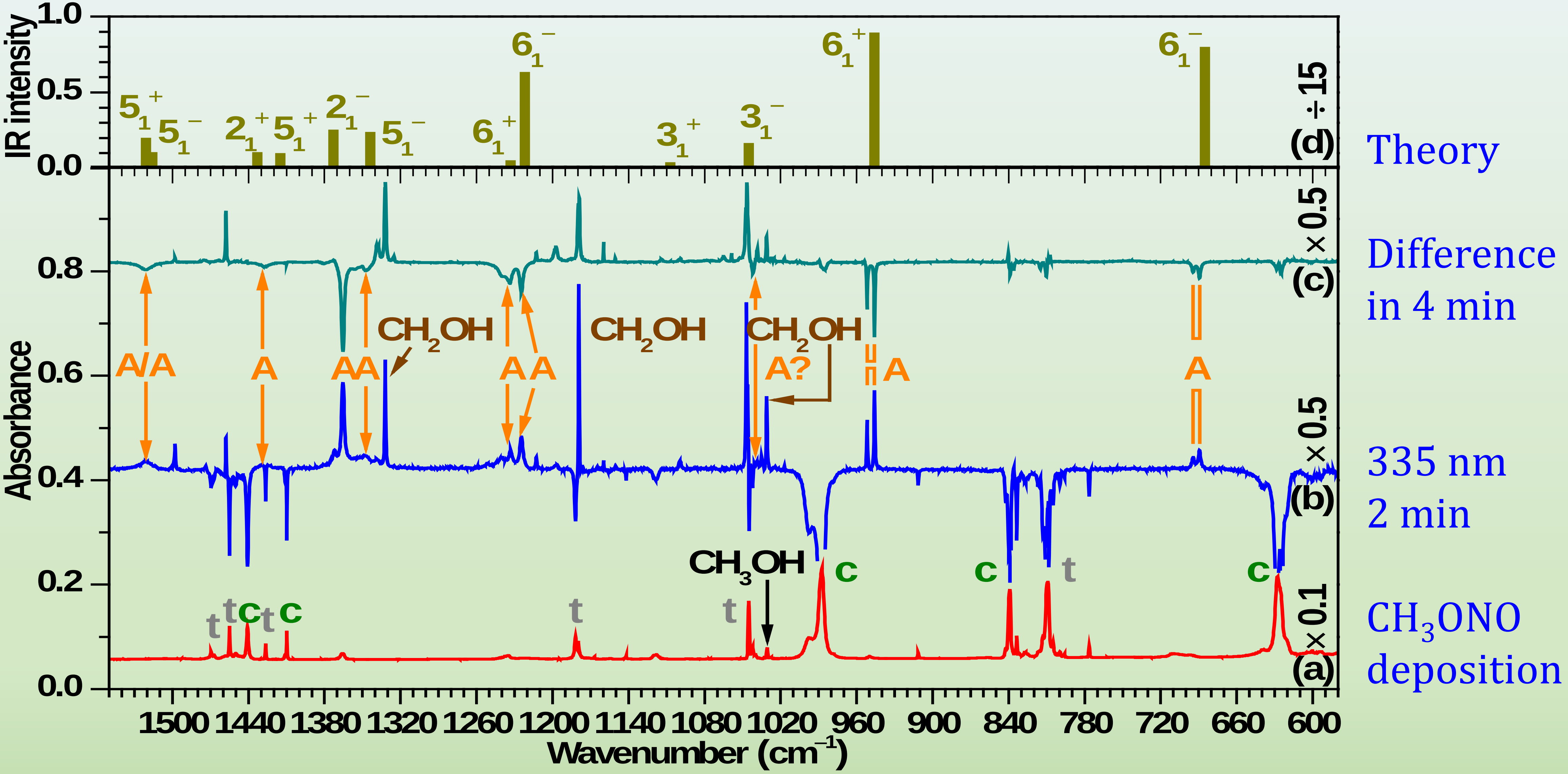

Diminished Cage Effect

Photo-induced bimolecular reactions

$CH_3 + SO_2 \rightarrow CH_3SO_2$ — JCP *134*, 124314 (2011)

$Cl + C_2H_4 \rightarrow \bullet CH_2CH_2Cl$ — PCCP *14*, 1014 (2011)

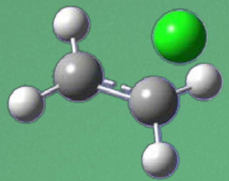

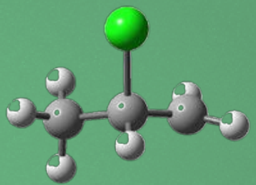

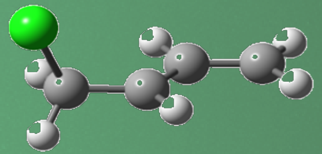

$Cl + CH_3CH{=}CH_2 \rightarrow \bullet CH_2CHClCH_3$ — JCPL *1*, 2956 (2010)

$Cl + CH_2{=}CH{-}CH{=}CH_2 \rightarrow \bullet CH_2{-}CH{=}CH{-}CH_2Cl$ — JCP *137*, 084310 (2012)

Cl + isobutene $\rightarrow \bullet C(CH_3)_2CH_2Cl$ & $\bullet CH_2C(CH_3)_2Cl$ — JCP *145*, 134302 (2016)

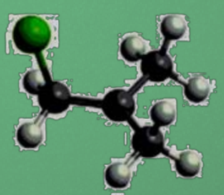

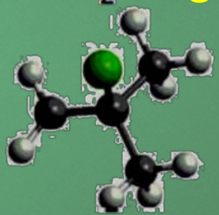

Cl + isoprene $\rightarrow$ 1- $\bullet ClC_5H_8$ & 4- $\bullet ClC_5H_8$ — JPCA *121, 8771 (2017)*

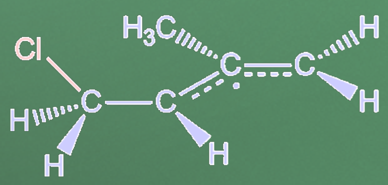

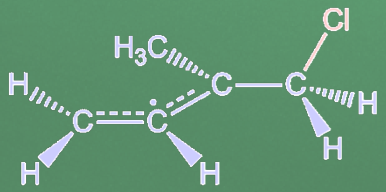

Reactions of Cl + C_6H_6 & Br + C_6H_6

- Cl + C_6H_6 → ·C_6H_6Cl (σ-complex)

J. Chem. Phys. **138**, 074310 (2013).

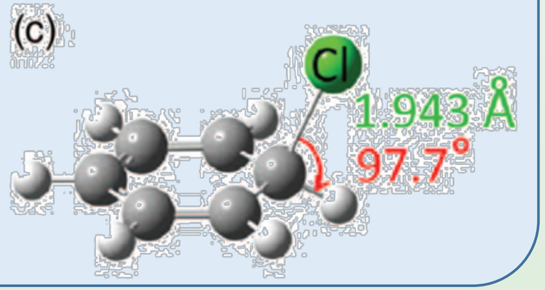

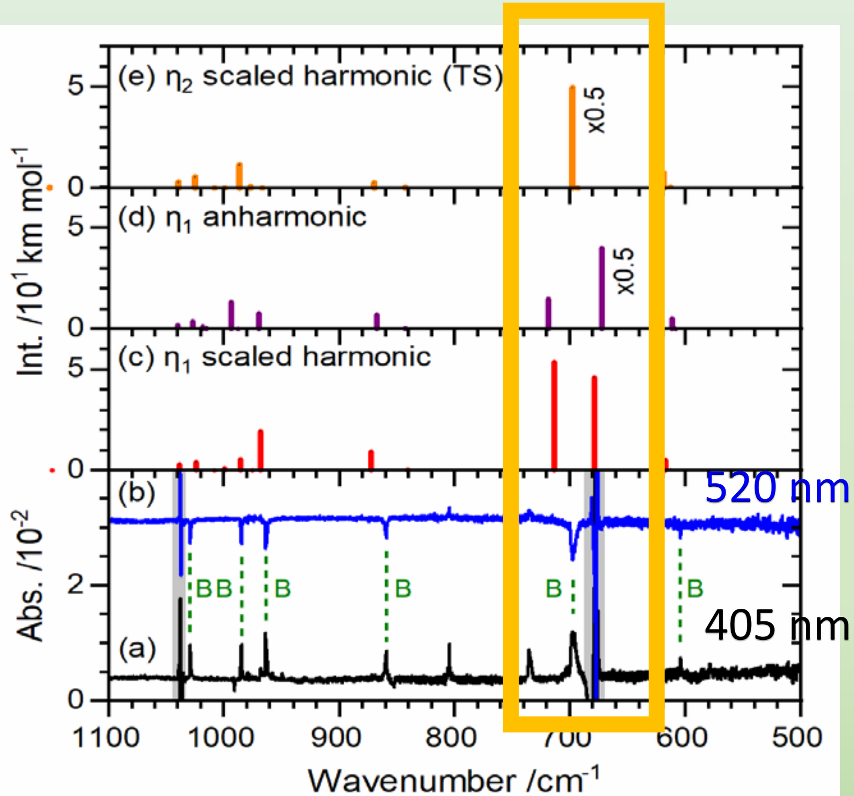

- Br + C_6H_6 → ·C_6H_6Br (η_1 π-comlex)

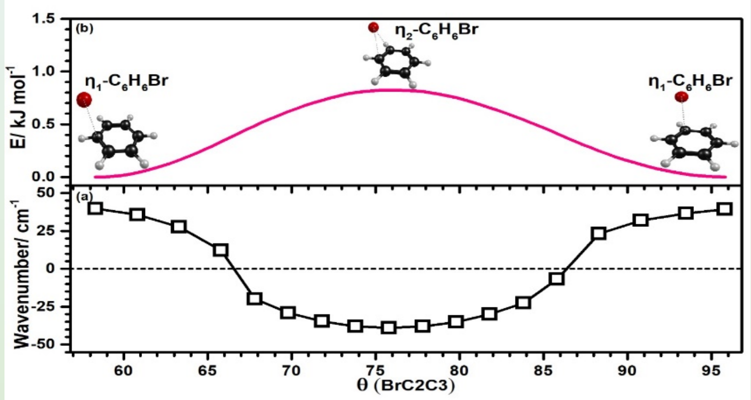

η_2

weak

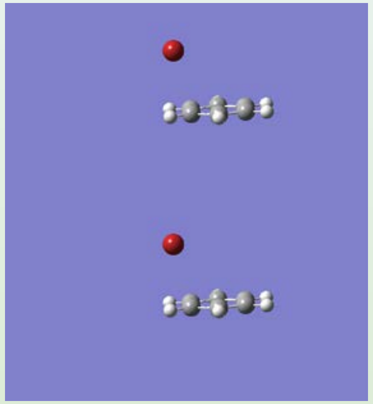

bevel-gear motion

η_1

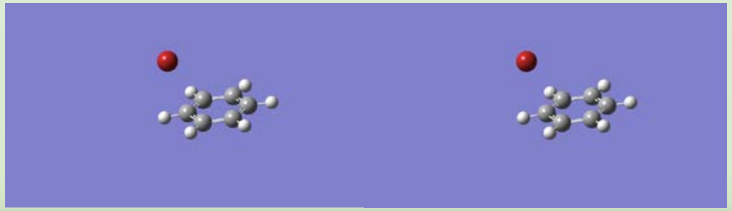

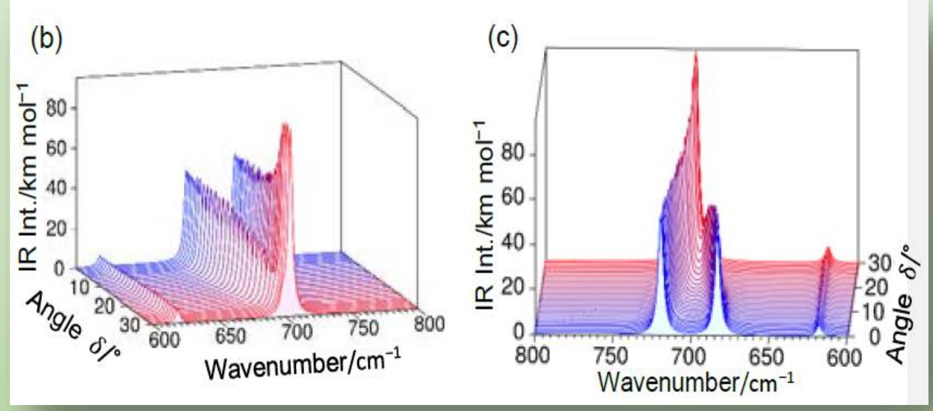

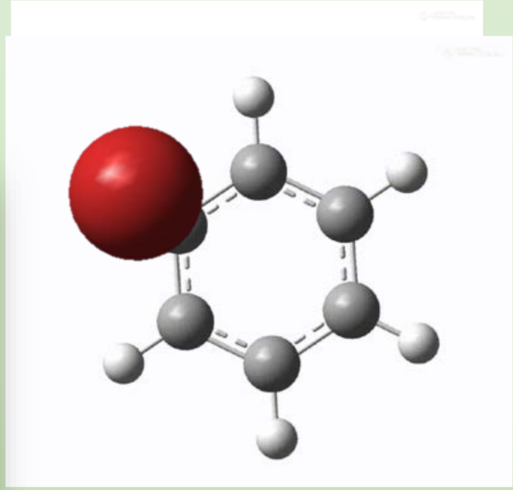

Matrix Isolation — *para*-H_2 matrices

Protonated Species

(a) During deposition

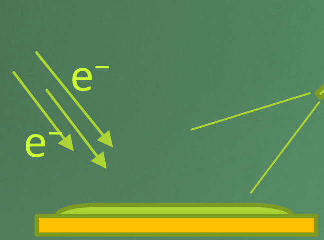

$H_2 + e^- \rightarrow H_2^+ + 2e^-$

$H_2^+ + H_2 \rightarrow H_3^+ + H$

$H_3^+ + PAH \rightarrow H^+PAH + H_2$

$H + PAH \rightarrow HPAH$

$H^+PAH + e^- \rightarrow HPAH$

(b) After long period in darkness or upon UV irradiation

$H^+PAH + e^- \rightarrow HPAH$

$H + PAH \rightarrow HPAH$

Neutral PAH: identified without E-gun
H^+PAH : appears with E-gun and decreases with time
HPAH : appears with E-gun and increases with time

After deposition

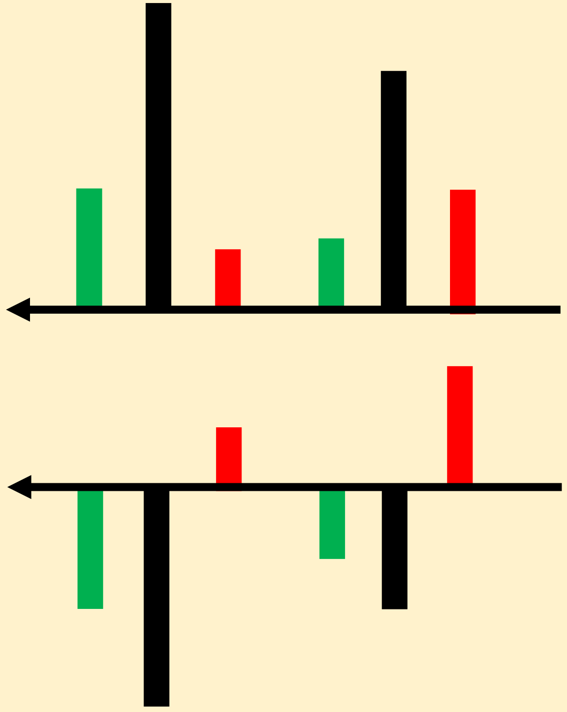

Difference after being in darkness

Matrix Isolation — *para*-H_2 matrices

Protonated Species

Proton Affinity (kJ/mol)

H_2	424
N_2	495
CO_2	548
C_6H_6	759
$C_{10}H_8$	803
$C_{24}H_{12}$	862
C_6H_5N	930

Polycyclic aromatic hydrocarbon (PAH)

- $C_6H_7^+$, $C_5H_5NH^+$ — JCP *136*, 154304 (2012); JPCA *117*, 13680 (2013)
- naphthalene, 1-, 2-$C_{10}H_9^+$ — PCCP *15*, 1907 (2013)
- pyrene, 1-$C_{16}H_{11}^+$ — JPCL *4*, 1989 (2013)
- coronene, 1-$C_{24}H_{13}^+$ — Angew. Chem. *53*, 1021 (2014)
- ovalene, 7-$C_{32}H_{15}^+$ — ApJ *825*, 96 (2016)
- *corannulene*, hub-$C_{20}H_{10}^+$ — ACSESC *2*, 1001 (2018)
- fluoranthene, 3-, 9-, 10-$C_{16}H_{11}^+$ — PCCP *21*, 1820 (2019)

Small protonated species

- KrH^+Xe, KrH^+Kr, XeH^+Xe — JPCA *119*, 2651 (2015)
- $H^+(CO_2)_2$, *t*-$HOCO^+$ — JCP *145*, 014306 (2016)
- $HOCS^+$ & $OCSH^+$ — JCP *145*, 164308 (2016)
- $HSCS^+$ — PCCP *19*, 9641 (2017)
- $H^+(CO)_2$, $N_2H^+N_2$ — JCP *153*, 084305 (2020); PCCP *19*, 20484 (2017)

Advantages

1. Negligible fragmentation
2. True IR intensity
3. Wide spectral coverage
4. Narrow linewidth with good S/N
   - isomers
5. Isotopic experiments
6. Hydrogenated species

Unidentified infrared (UIR) emission

UIR emission

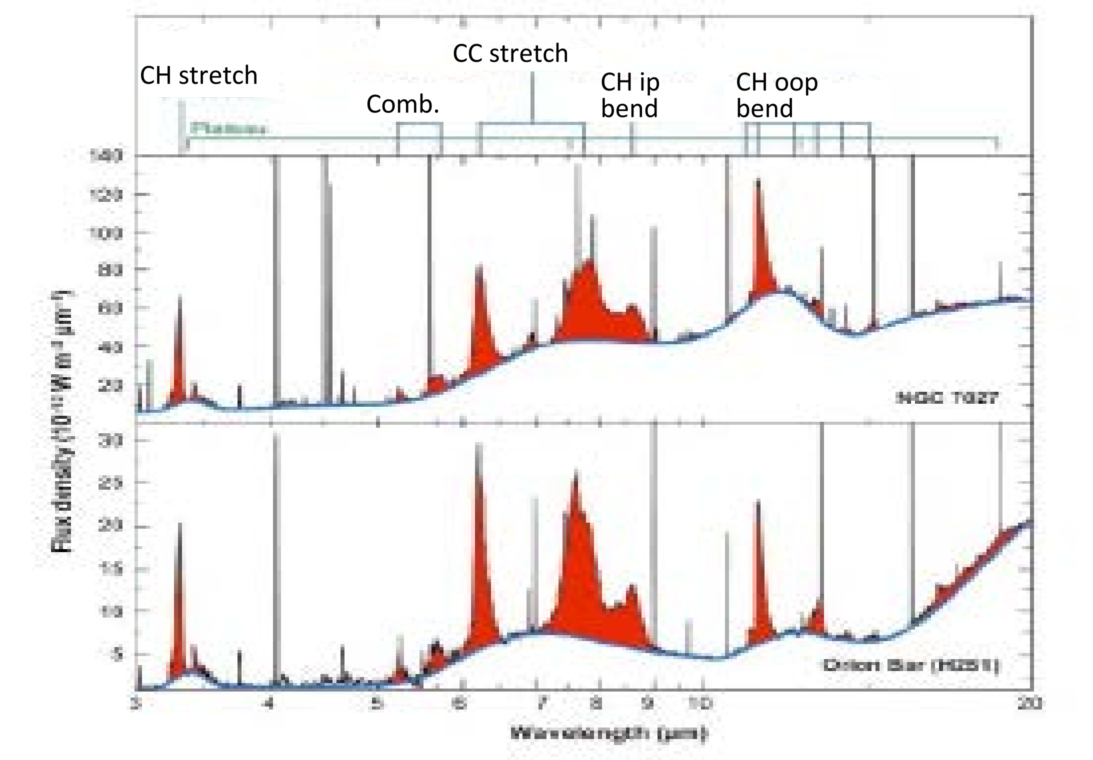

Peeters, E., Hony, S., Van Kerckhoven, C., *et al.*, 2002, A&A, 390, 1089

PAH hypothesis

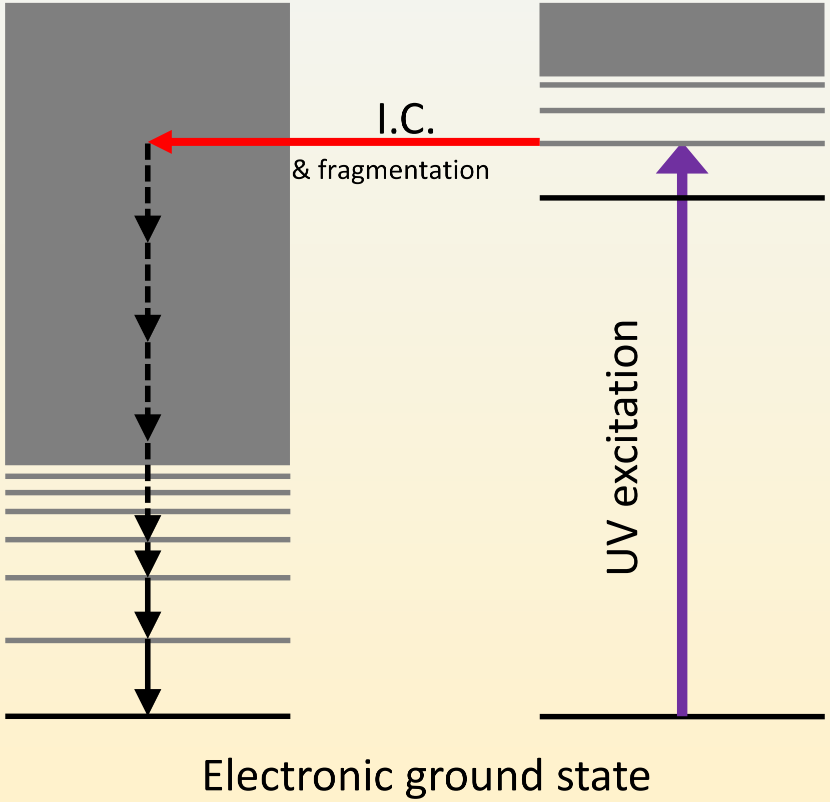

Polycyclic aromatic hydrocarbon (PAH) has been postulated to be an emitter of UIR. However, **no exact correspondences were found for neutral PAHs**.

→ ***Protonated PAH (H^{+}PAH) might be possible carriers.***

Comparison of 1-$C_{10}H_9^+$

PCCP **15**, 1907 (2013)

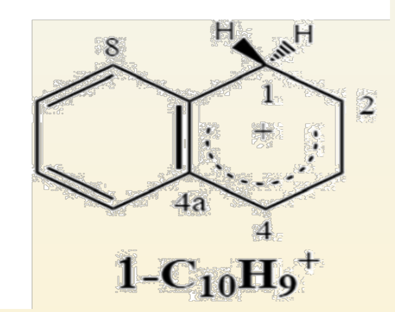

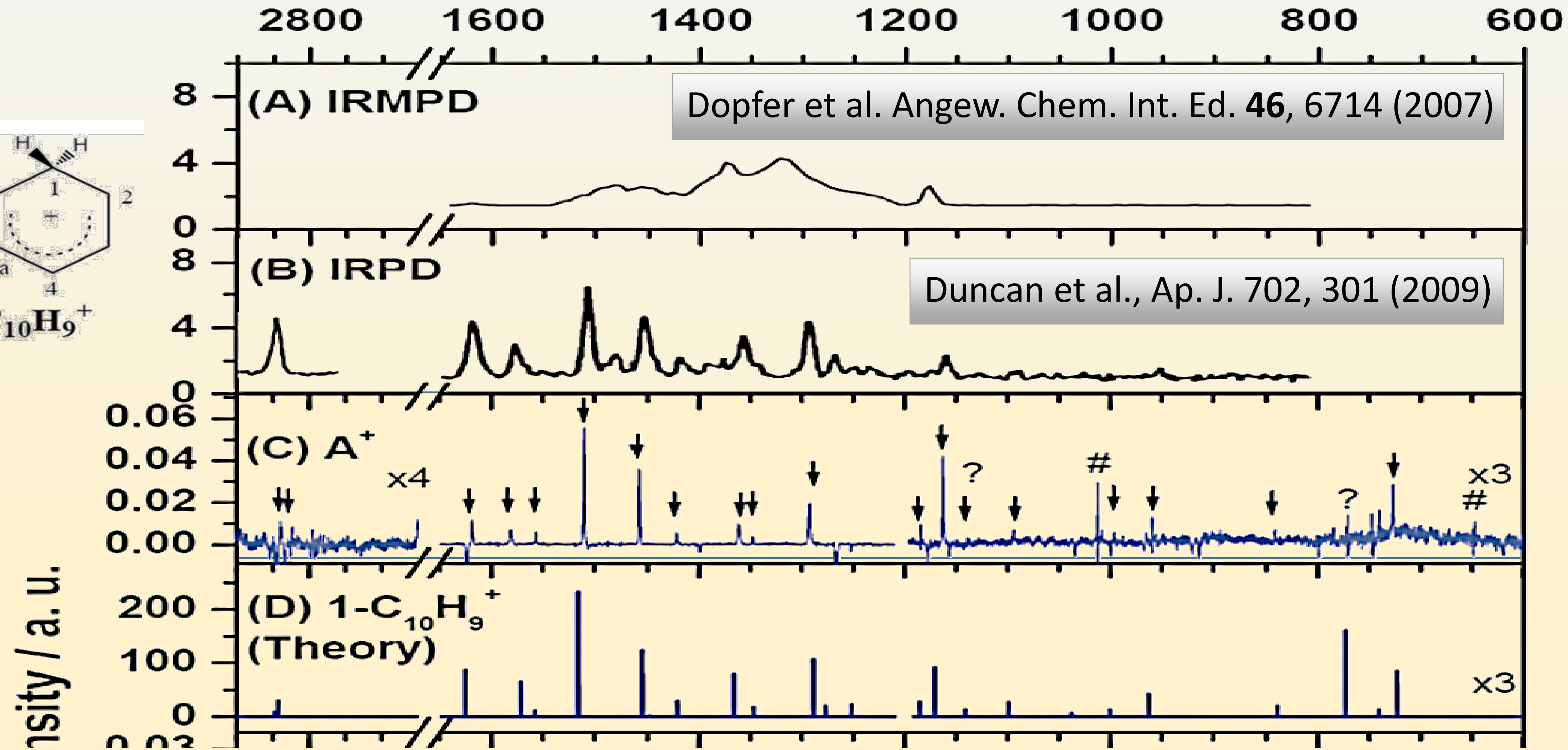

Comp

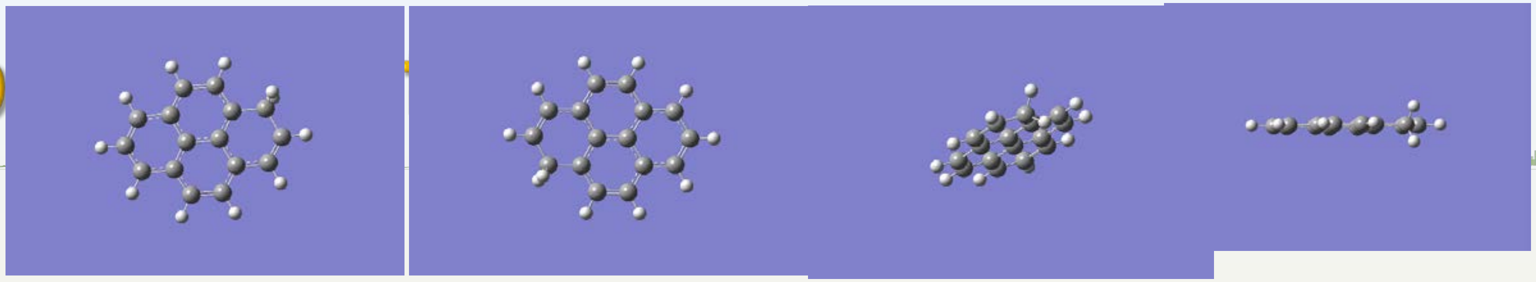

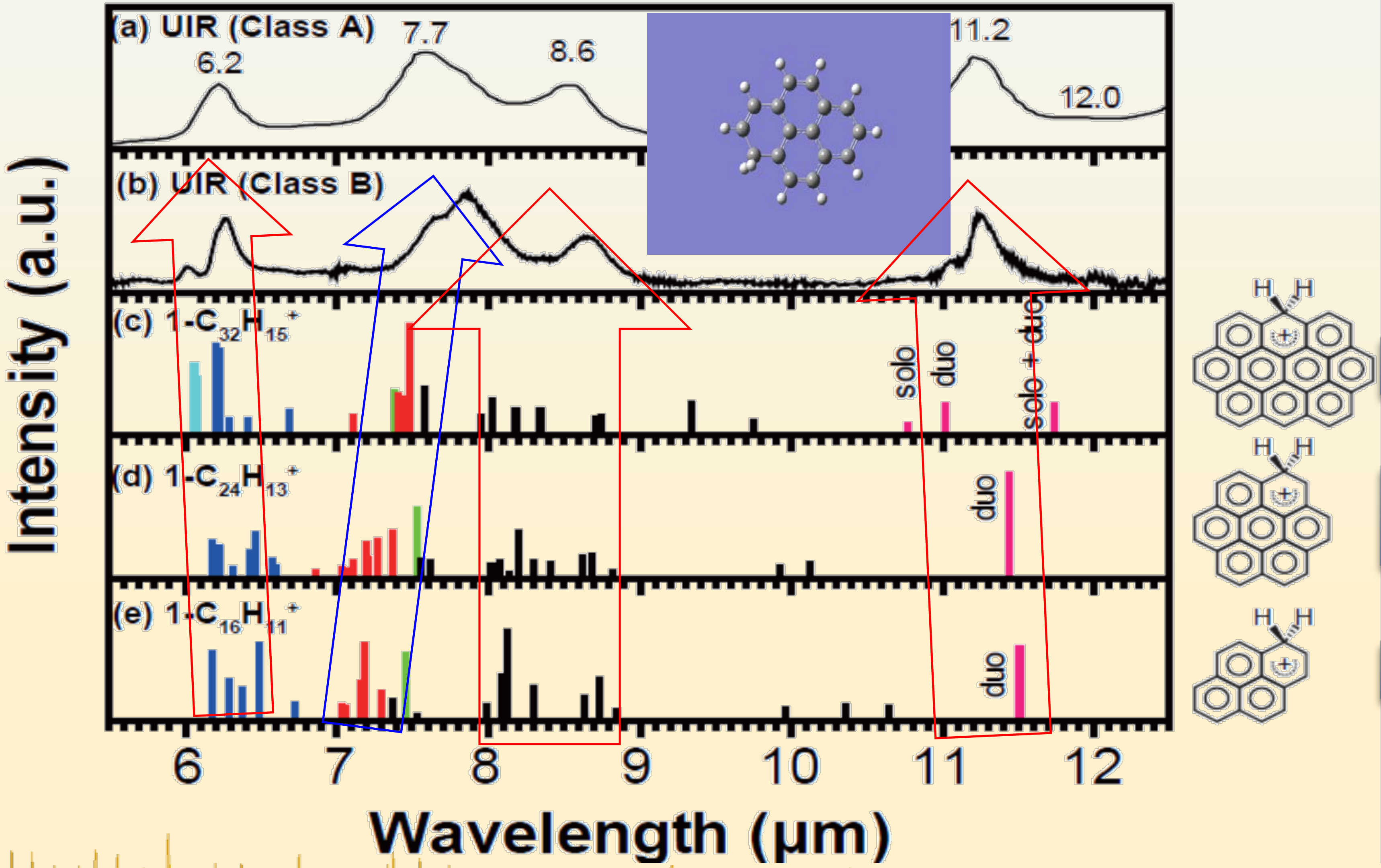

ApJ *825*, 96 (2016)

Angew. Chem. *53*, 1021 (2014)

JPCL *4*, 1989 (2013)

Matrix Isolation

para-H_2 matrices

Hydrogenated Species

Polycyclic aromatic hydrocarbon (PAH)

C_6H_7, C_5H_5NH	JCP *136*, 154304 (2012); JPCA *117*, 13680 (2013)
naphthalene, 1-, 2-$C_{10}H_9$	PCCP *15*, 1907 (2013)
pyrene, 1-$C_{16}H_{11}$	JPCL *4*, 1989 (2013)
coronene, 1-$C_{24}H_{13}$	Angew. Chem. *53*, 1021 (2014)
ovalene, 7-$C_{32}H_{15}^+$	ApJ *825*, 96 (2016)
corannulene, *rim*-$HC_{20}H_{10}$	JCP *151*, 044304 (2019)
•ONH(OH)	PCCP *19*, 16169 (2017)
trans-1-methylallyl	JCP *137*, 084310 (2012)
3-C_5H_4(OH)NH	JCP *149*, 014306 (2018)
1,1-, 1,2-dimethylallyl	JCP *149*, 204304 (2018)
ortho- and para-HC6H5NH2	JPCA *124*, 7500 (2020)
2,3-dihydropyrrol-2-yl and 2,3-dihydropyrrol-3-yl	JCP *153*, 164302 (2020)

Efficient Hydrogenation Reaction in *p*-H_2

H atoms by UV/IR irradiation of Cl_2/*p*-H_2

$Cl + H_2 (v = 1) \rightarrow HCl + H$ (D. Anderson)

(2) UV on HONO: $OH + H_2 \rightarrow H_2O + H$

(3) UV on H_2O_2: $OH + H_2 \rightarrow H_2O + H$

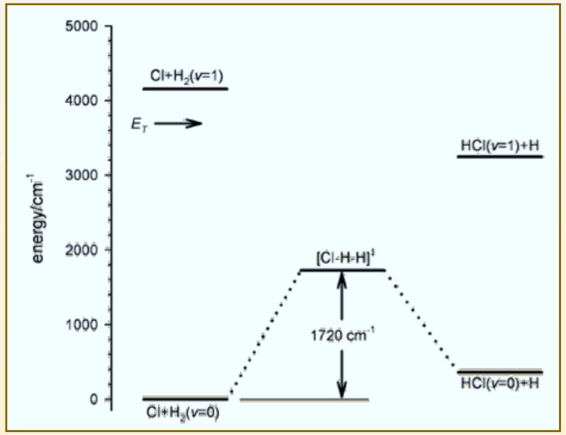

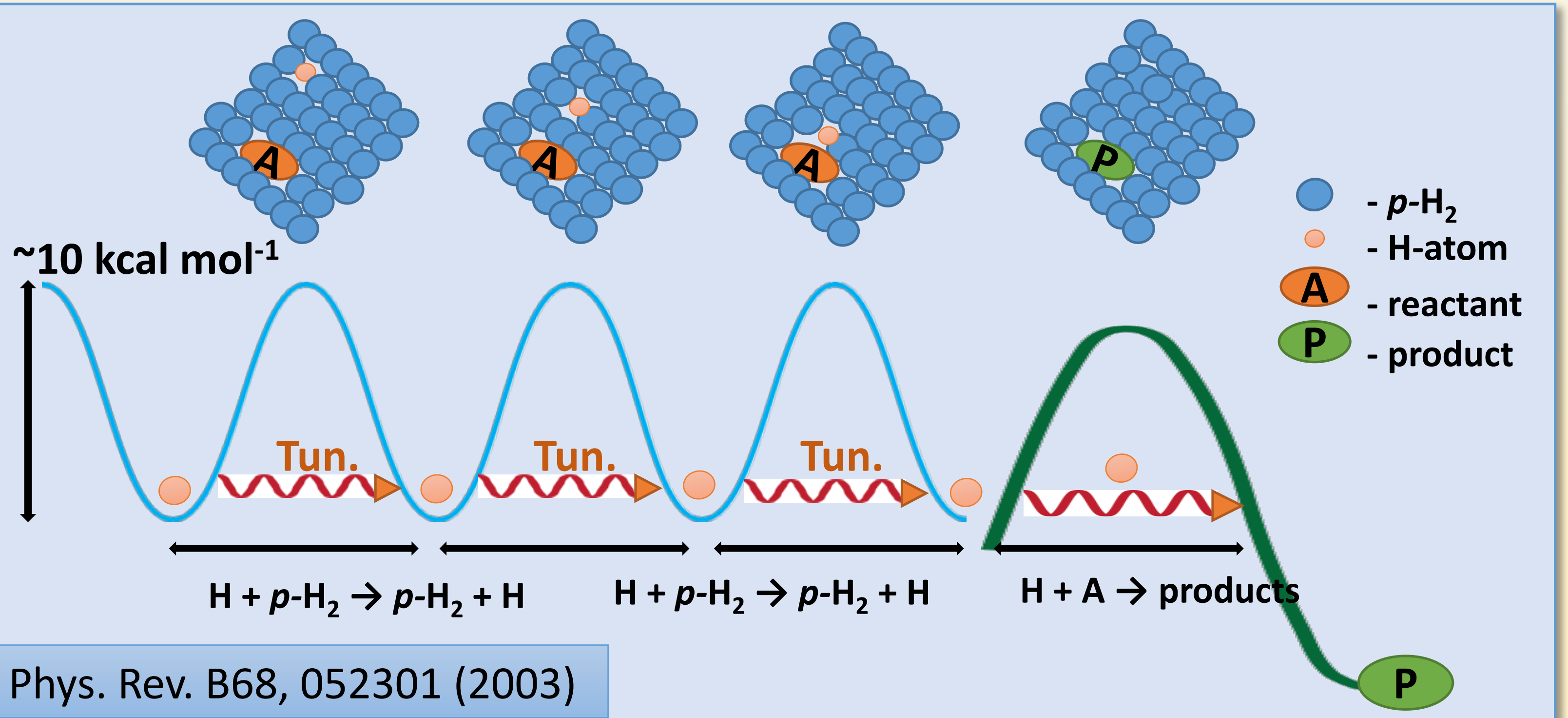

Kumada, Phys. Rev. B68, 052301 (2003)

Isoquinoline (iso-C_9H_7N)

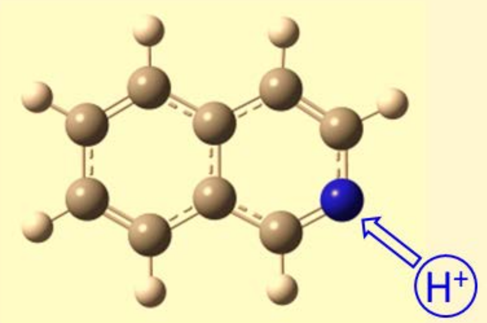

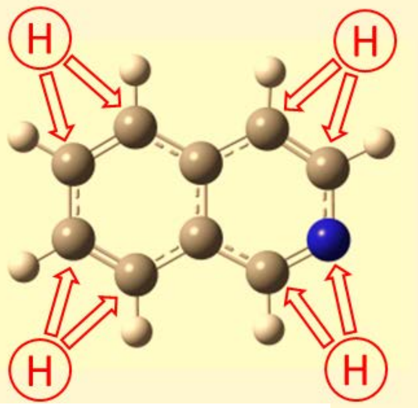

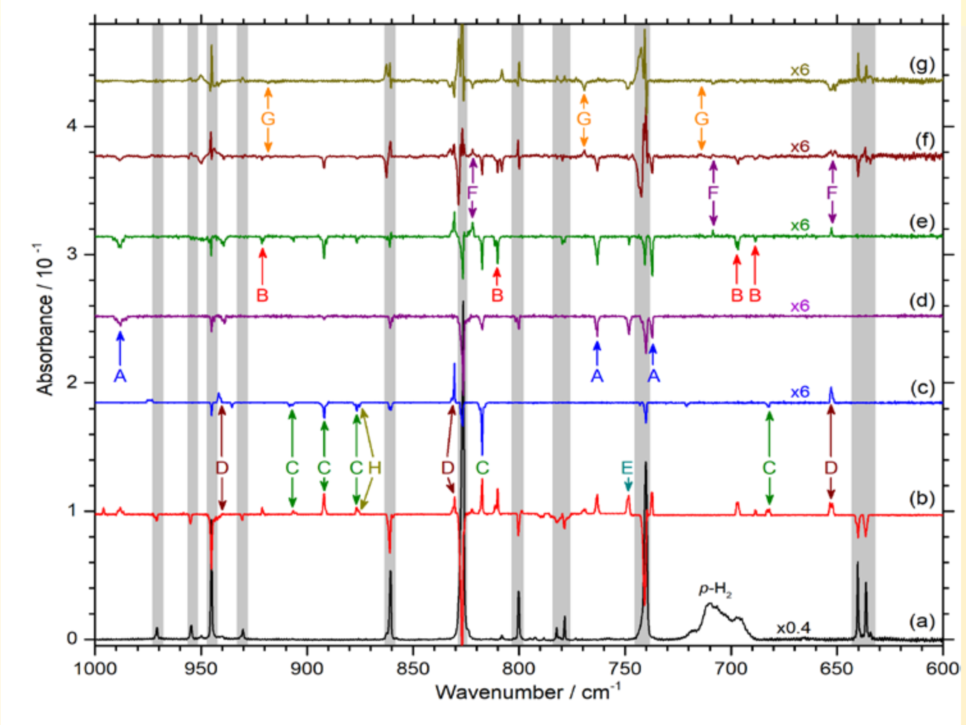

360 nm, 0.5 h

405 nm, 0.5 h

420 nm, 0.5 h

540 nm, 0.5 h

553 nm, 0.5 h

IR light, 2 h

365 nm, 1 h

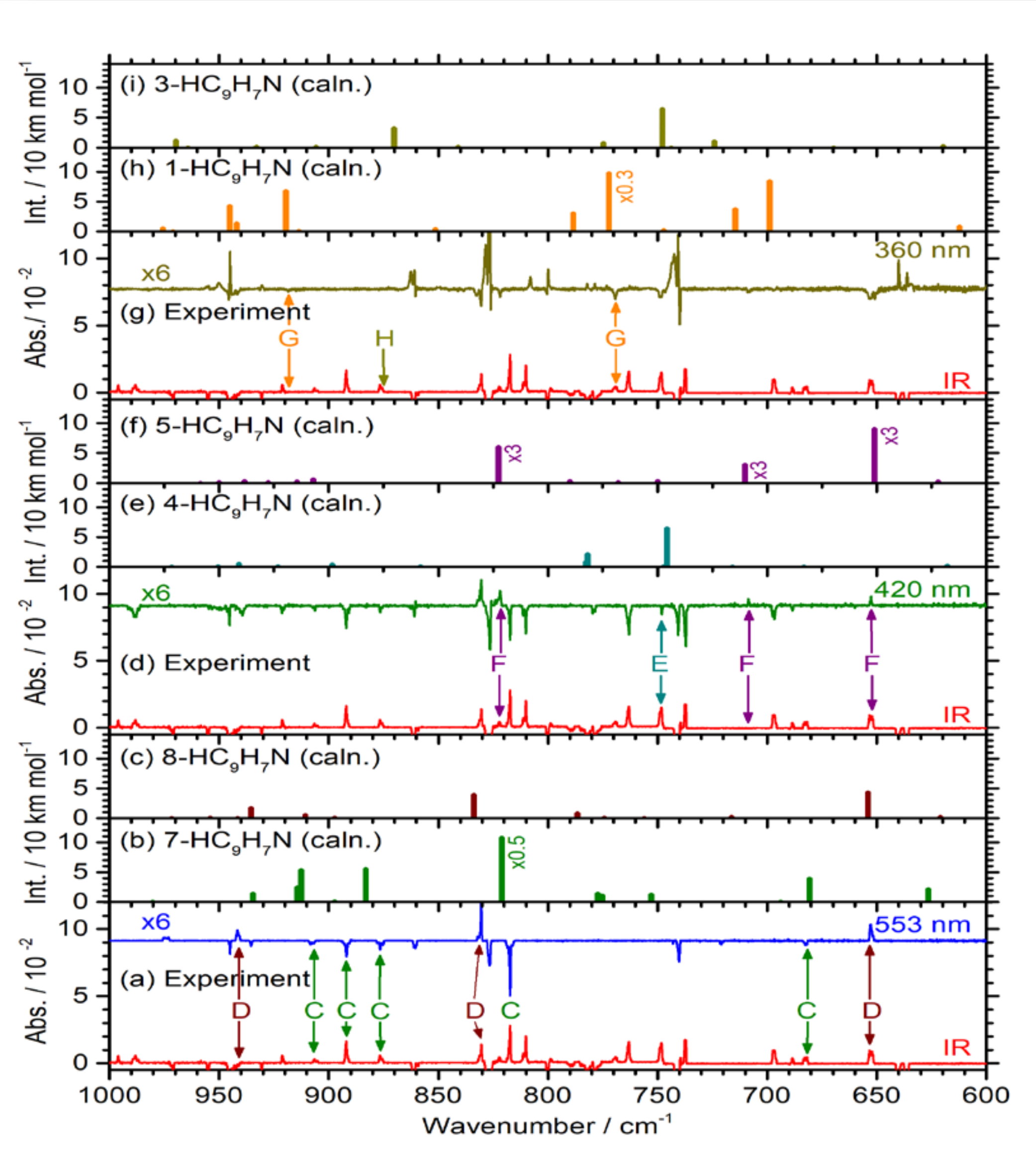

Hydrogen reactions

Complex Organic Molecules (COM) and Origin of Life

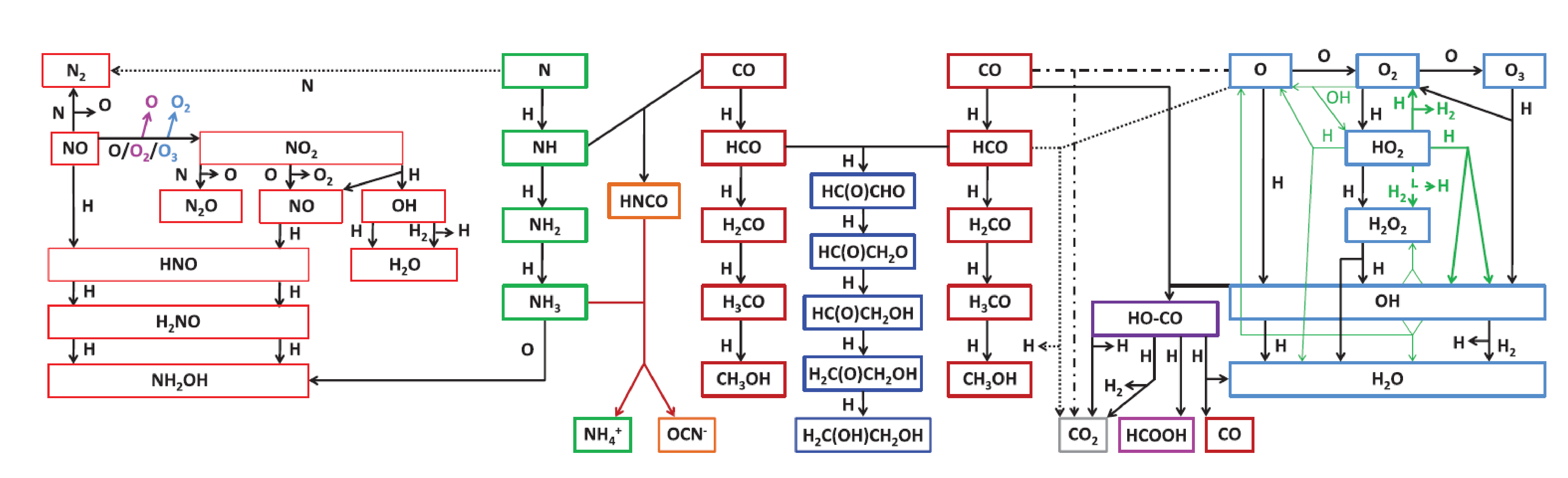

Linnartz *et al.*, Int. Rev. Phys. Chem. **34**, 205 (2015)

H-abstraction Reactions in *p*-H_2

J. Am. Chem. Soc. 141, 11614 (2019)

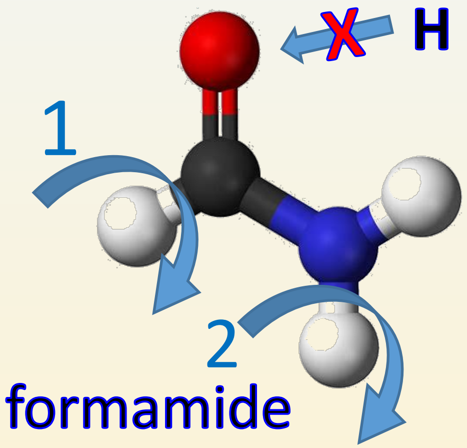

formamide

1. $[H_2NCHO]/[HNCO] << 1$
2. Catalytic conversion H to H_2

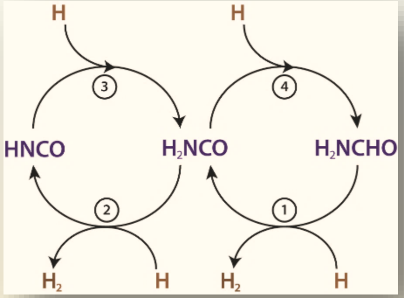

Phys. Chem. Chem. Phys. 22, 6129 (2020)

OH
NH_2
CH_3
HCO
CN

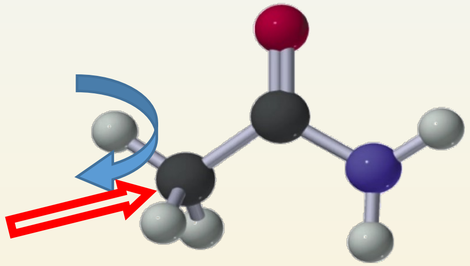

acetamide

Photolysis of $\bullet CH_2CONH_2$ forms CH_2CO
Connecting acetamide & ketene

J. Chem. Phys. 151, 234302 (2019)

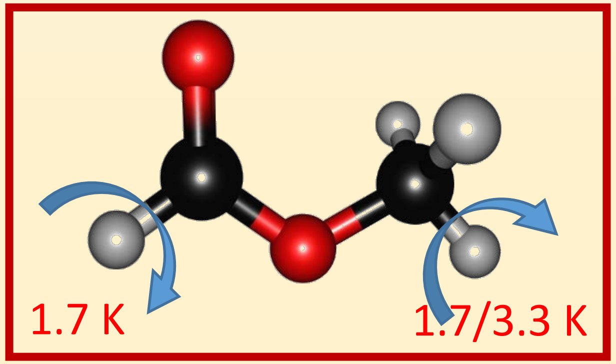

methyl formate

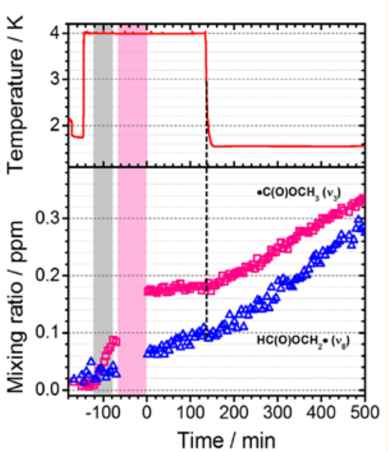

ACS Earth & Space Chem. 5, 106 (2021)

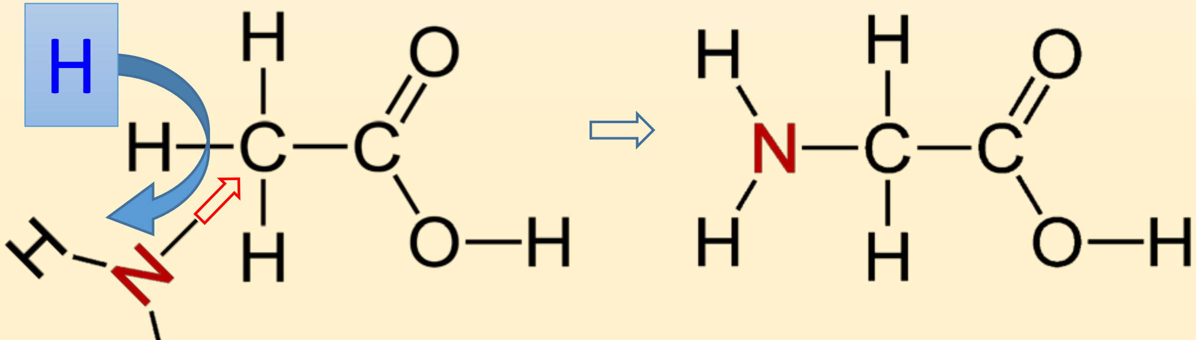

glycine

Connection between CH_3NH_2 & CH_2NH

Comm. Chem. 5, 62 (2002)

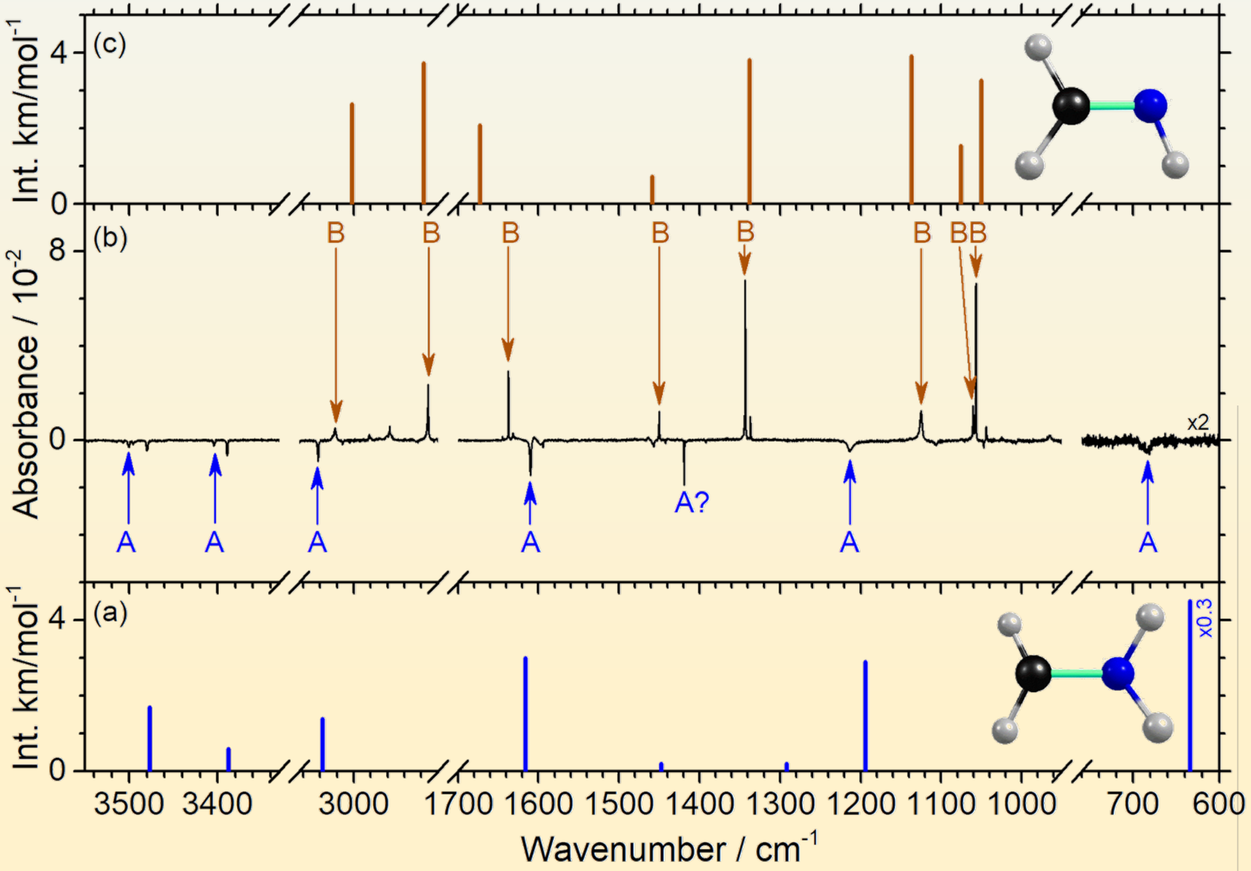

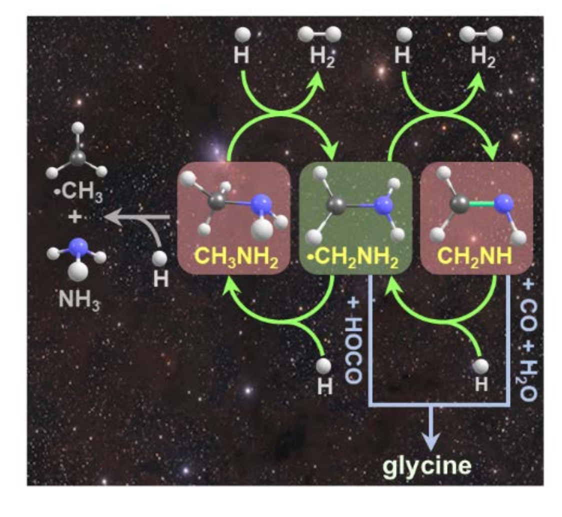

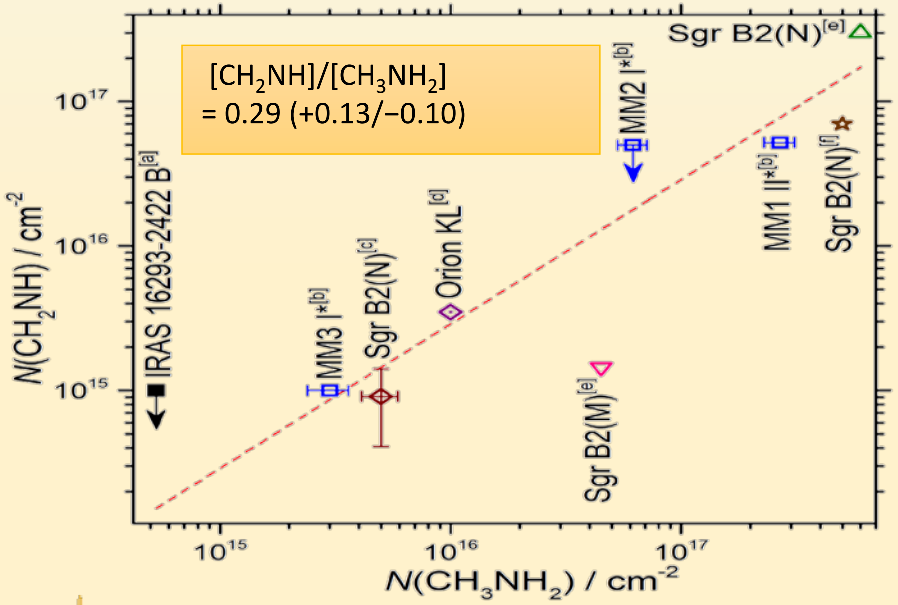

Isomerization from *trans*- to *cis*-NMF

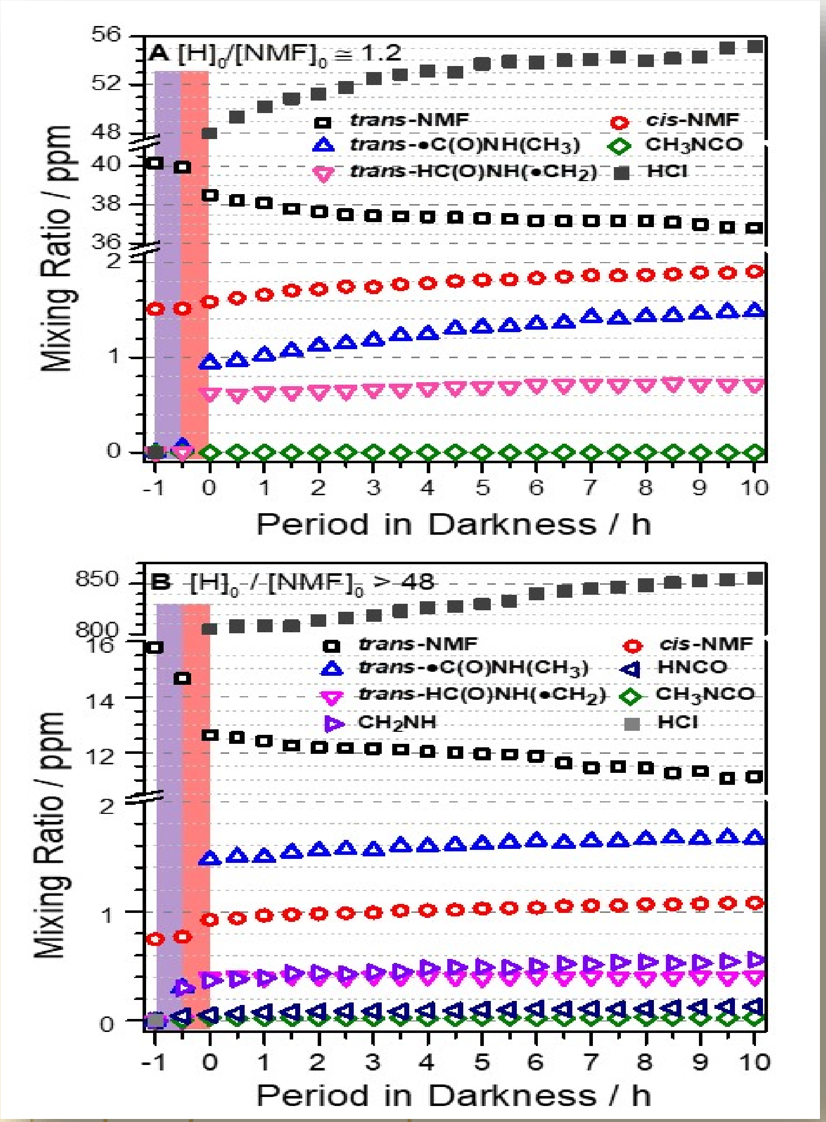

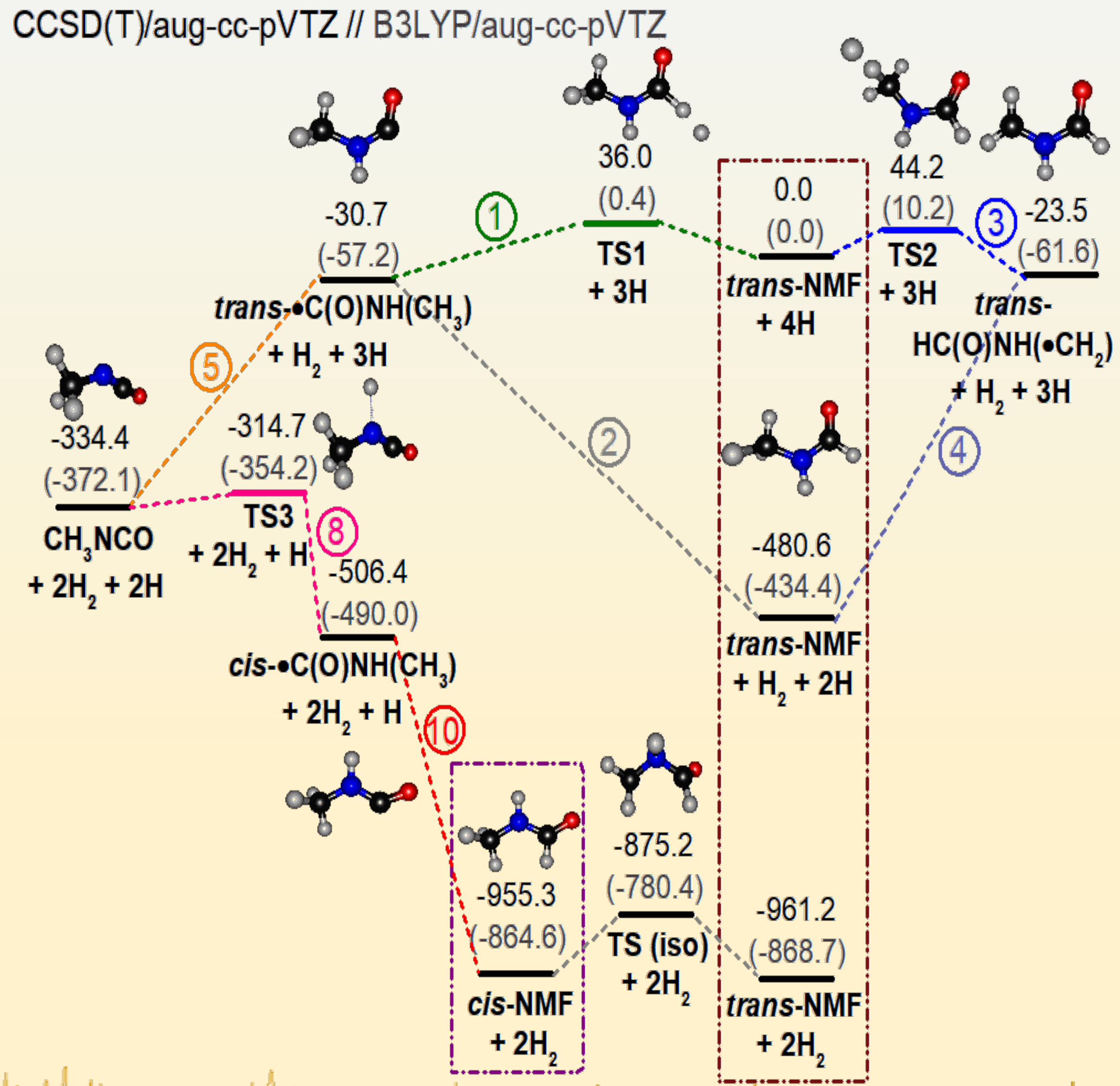

Uphill isomerization by H reactions

JACS *144*, 12339 (2022)

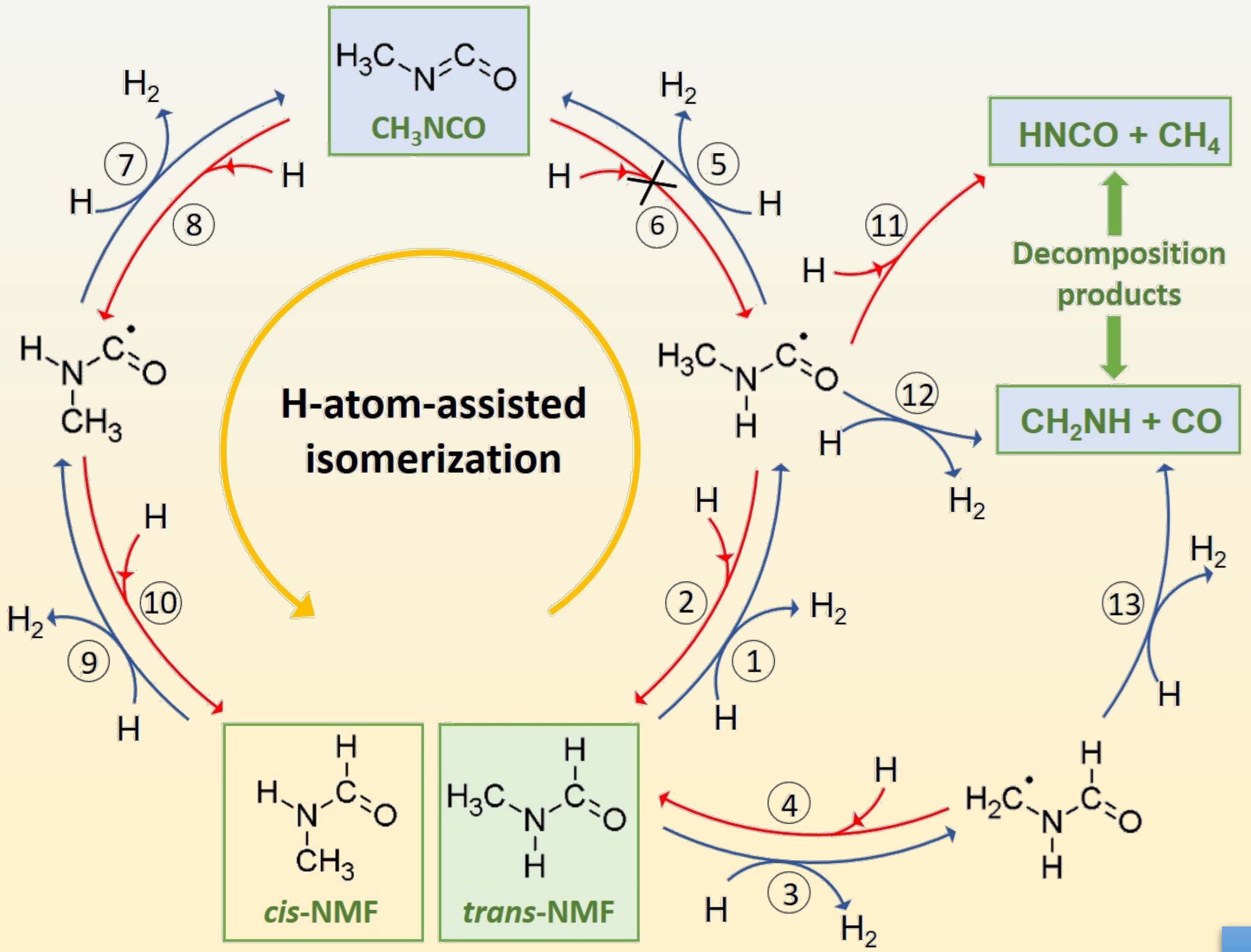

Importance of H reactions:

$H + H \rightarrow H_2$, $\Delta H = -436$ kJ mol^{-1}

- H-abstraction
- fragmentation
- Uphill isomerization

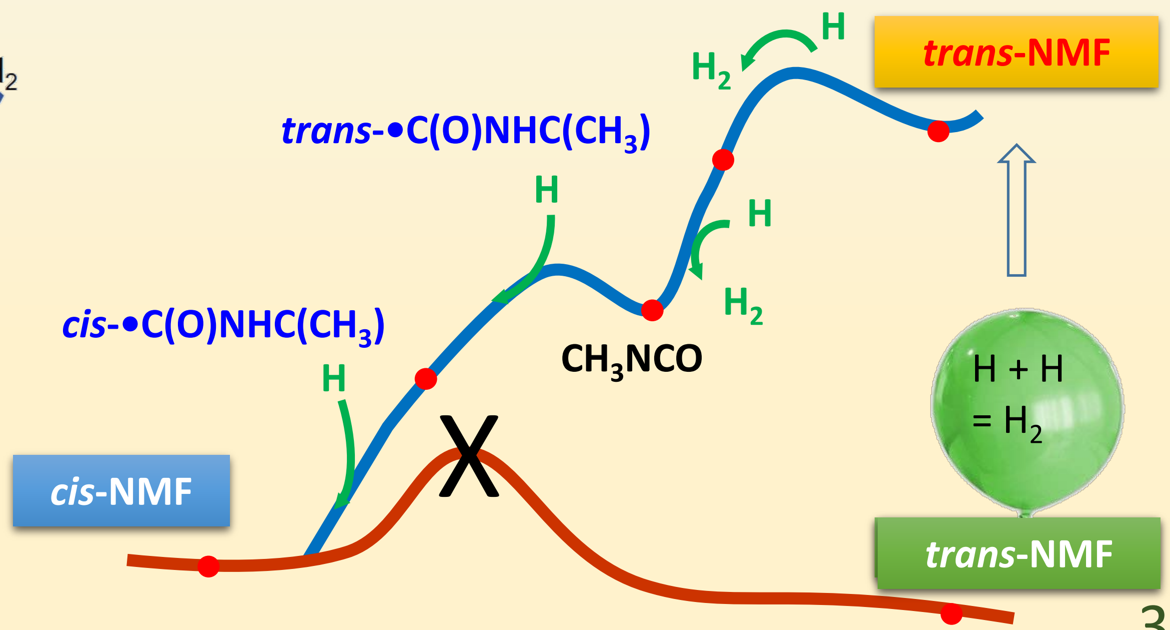

Matrix Isolation

para-H_2 matrices

Electronic transitions

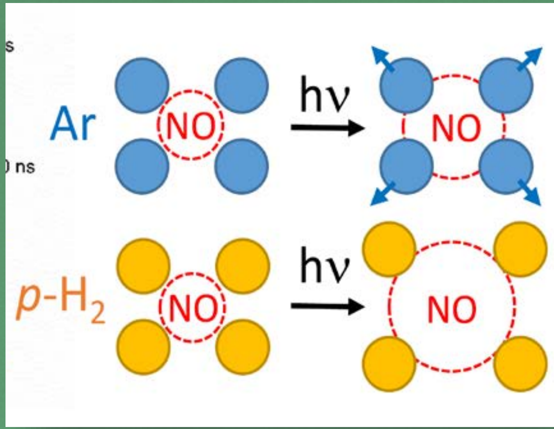

$C_{10}H_9$: 18950 cm^{-1} (gas)
18875 cm^{-1} (*p*-H_2)
Sumanene: 27943 cm^{-1} (gas)
27864 cm^{-1} (*p*-H_2)

JPCA (2022)

JCPA *126*, 5283 (2022)

JACS *144*, 12339 (2022)

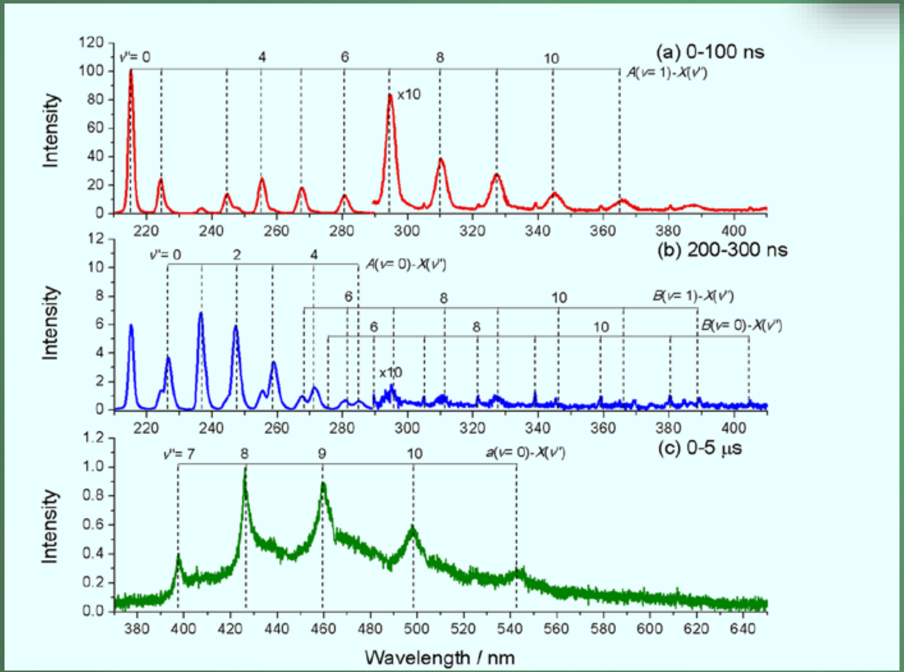

matrix	$A\ ^2\Sigma^+\ (v = 1)$ T_{00} /cm^{-1}	FWHM /cm^{-1}	$A\ ^2\Sigma^+\ (v = 0)$ T_{00} /cm^{-1}	FWHM /cm^{-1}	$B\ ^2\Pi\ (v = 0)$ T_{00} /cm^{-1}	FWHM /cm^{-1}
(gas)			44080.5		45392.1	
p-H_2	46459±20	~410	44098±40 (44105±20)	~400	45376±130 (45345±20)	~30
n-H_2			44088	427		
n-D_2				565		
Ne			45536[a]	645	45913.6	~250[a]
Ar			46377	645	45570	~170[a]
Kr			44199	645	45893	~190[a]
Xe			42828	645		

Matrix Isolation

para-H_2 matrices

Phys. Chem. Chem. Phys. **20**, 5344 (2018)

PERSPECTIVE

Check for updates

Cite this: *Phys. Chem. Chem. Phys.*, 2018, **20**, 5344

Spectroscopy of prospective interstellar ions and radicals isolated in *para*-hydrogen matrices

Masashi Tsuge,†[*a] Chih-Yu Tseng[a] and Yuan-Pern Lee[*ab]

Phys. Chem. Chem. Phys. **16**, 2200 (2014)

PERSPECTIVE

Cite this: *Phys. Chem. Chem. Phys.*, 2014, 16, 2200

Infrared spectra of free radicals and protonated species produced in *para*-hydrogen matrices

Mohammed Bahou,[a] Prasanta Das,[a] Yu-Fang Lee,[a] Yu-Jong Wu[b] and Yuan-Pern Lee[*ac]

J. Chin. Chem. Soc. **69**, 1159 (2022)

Hydrogen-atom tunneling reactions in solid *para*-hydrogen and their applications to astrochemistry

Karolina Anna Haupa[1,2] | Prasad Ramesh Joshi[1] | Yuan-Pern Lee[1,3]

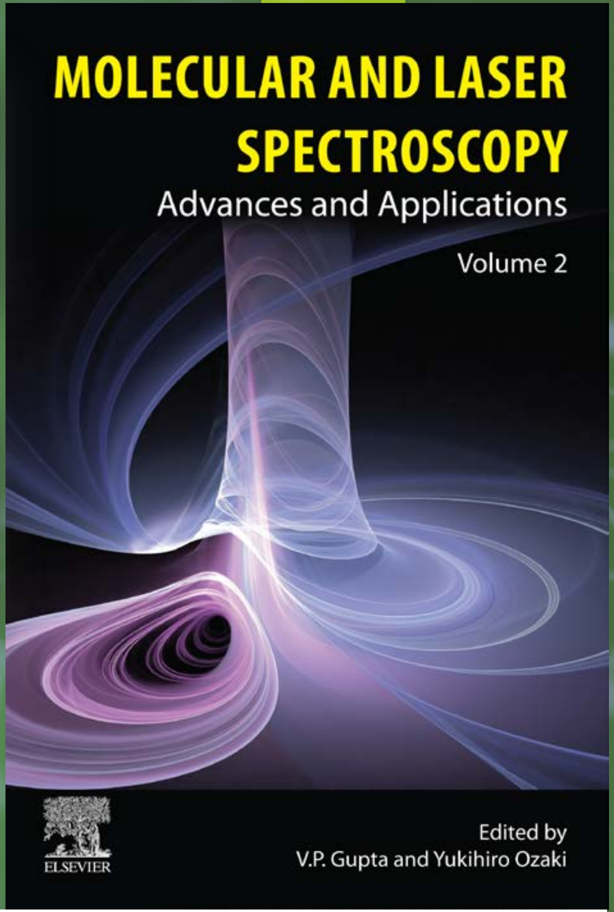

5

Spectroscopy of molecules confined in solid *para*-hydrogen

Masashi Tsuge[a,b], Yuan-Pern Lee[a,c]

Resonant Four-wave Mixing - Gas phase

Highly predissociative state

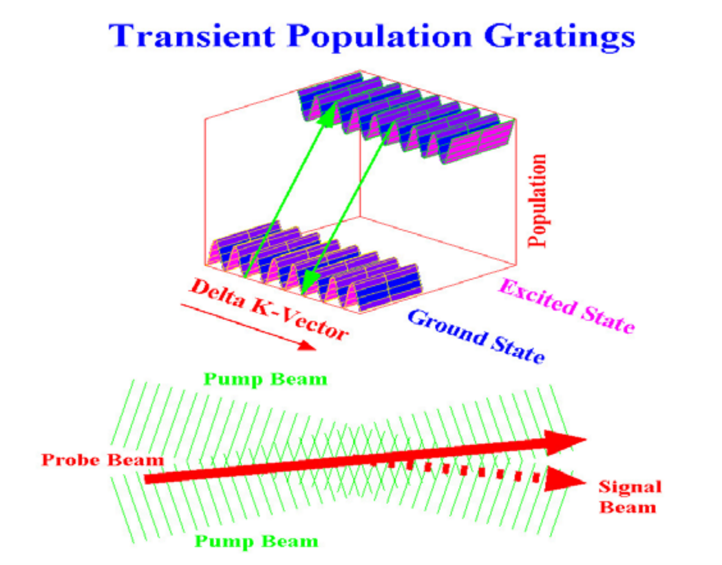

- CH in a flame — JCP *103*, 9941 (1995)
- Br_2 *B* $^3\Pi_u$-*X* $^1\Sigma_g^+$ — CPL *269*, 22 (1997)
- CH *B* $^2\Sigma^-$ — JCP *109*, 3824 (1998); CPL *297*, 300 (1998)
- CH C $^2\Sigma^-$ — JPCA *103*, 6162 (1999)
- CH *D* $^2\Sigma^-$ — JCP *111*, 4942 (1999)
- SO_2 (500) — CPL *362*, 235 (2002)
- CH_3S *A* $^2A_1$ — JCP *119*, 12335 (2003); JCP *122*, 124313 (2005)
- SO *B* $^3\Sigma^-$ — JMS *238*, 213 (2006)

David Chandler

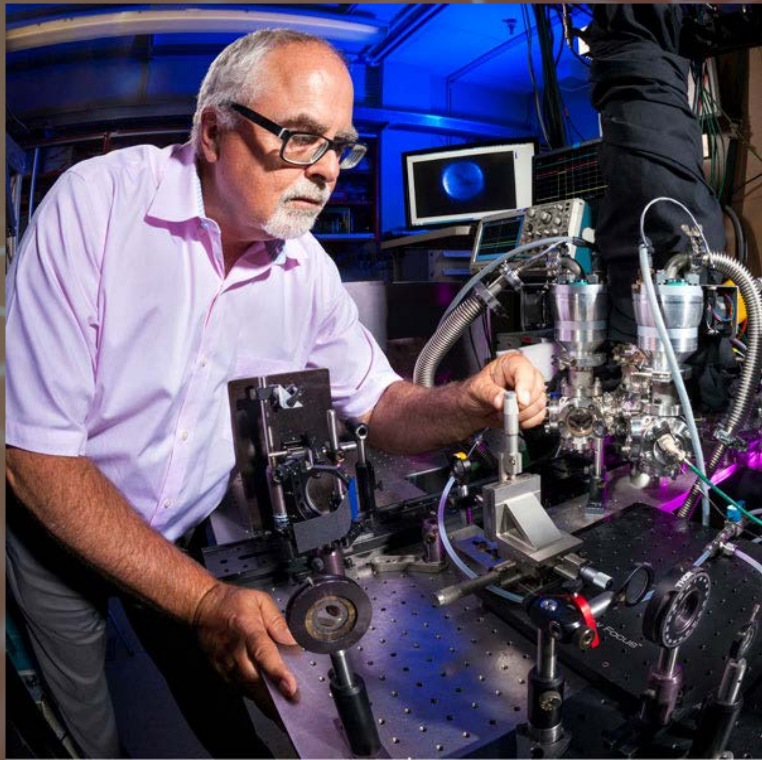

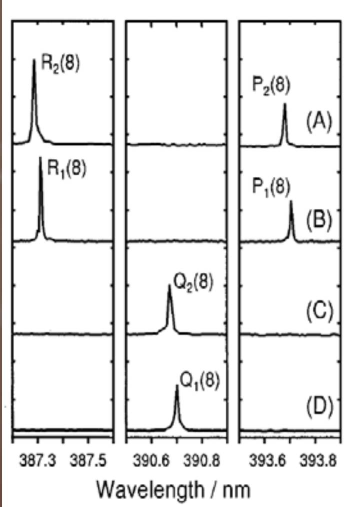

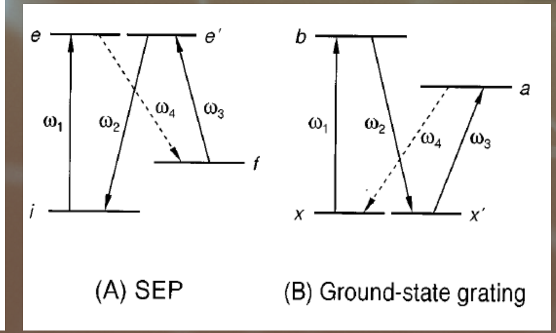

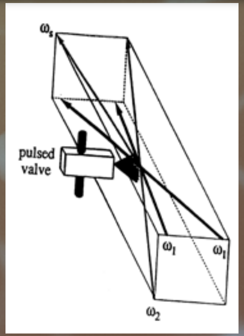

VUV absorption/Photoionization

Gas phase
Matrix

Synchrotron radiation

Astronomical species

H_2O dissociation in matrices	JCP *103*, 6404 (1995)
CH_3SO, CH_3SOH phoitoionization	JCP *105*, 7402 (1996)
C_2H_5SO ionization	JCP *107*, 8794 (1997)
HSCl, HSSSH, SSCl, HSSCl ionization	JCP *108*, 6197 (1998)
H_2O fractionation (Mars)	GRL *26*, 3657 (1999)
Deuterated ethane (Jupiter)	Astrophys. J. *551*, L93 (2001)
HCl/DCl absorption (Venus)	Astrophys. J. *559*, L179 (2001); JCP *117*, 4293 (2002)
CH_3OH & deuterated absorption	JCP *117*, 1633 (2002); JGR *107*, SIA7-1 (2002)
$H_2O/HOD/D_2O$ (with theory)	JCP *120*, 224 (2004)
NH_3 & deuterated	Astrophys. J. *647*, 1535 (2006); JCP *127*, 154311 (2007)
NH_3 fractionation (Jupiter)	Astrophys. J. *657*, L117 (2007)

Water on Mars

GRL *26*, 3657 (1999)

- D/H ratio gives the amount of water escaped

$$X(t) = X(0)[(W+L)/W]^{1-F}$$

- Dissociation of water vapor with subsequently escape of H, H_2, and O is the primary mechanism of water loss from Mars.
- Preferential escape of the light isotope could lead to the enrichment of the heavy isotope.
- *PHIFE : Photo-Induced Fractionation Effect*
- In the atmosphere of Mars, photolysis of HDO is 2-3 times less efficient than that of H_2O.
- The loss of water from Mars, based on this work, was estimated to be 50 m.

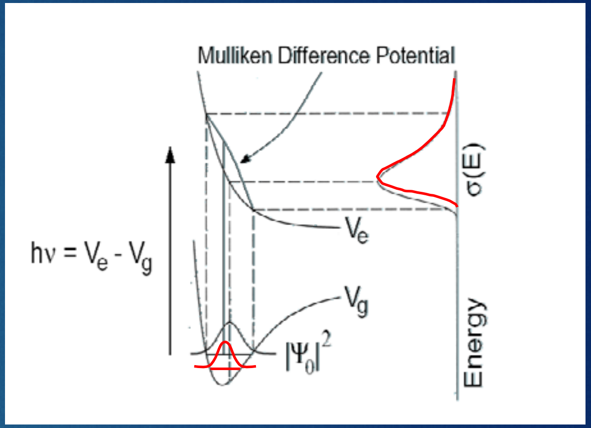

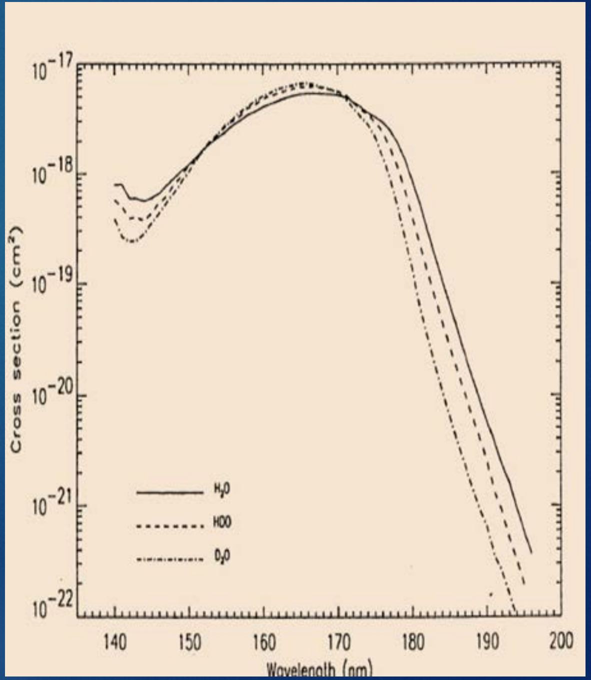

Cavity ringdown – Gas phase

Highly vibrationally excited states or weak transitions

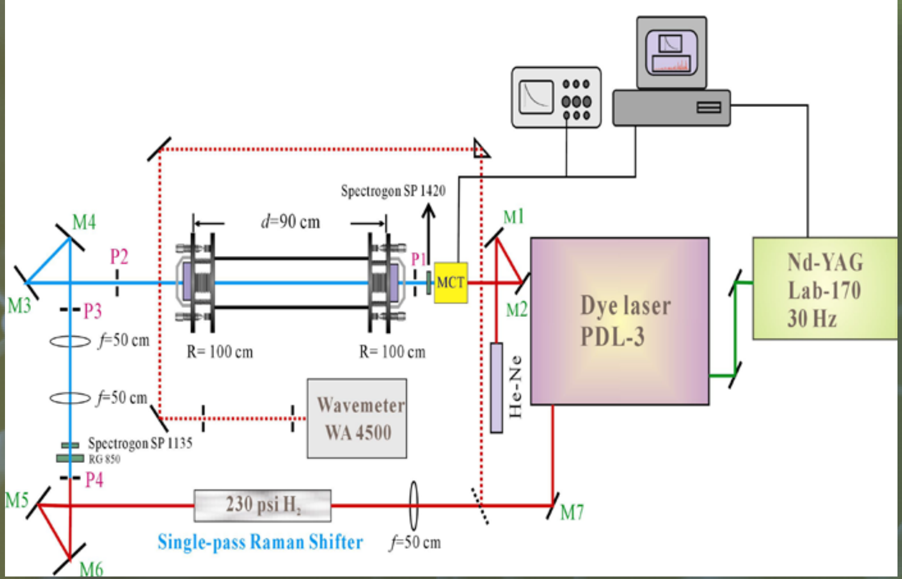

CO (5-0) — JPCA *109*, 7854 (2005)

CH_3OO/CD_3OO, $A \leftarrow X$ — JCP *127*, 044311 (2007)

C_6H_5O/C_6D_5O, $A \leftarrow X$ — JCP *129*, 154307 (2008)

S_l = 2.92x10^{-29} m (P branch only)
4.18x10^{-29} m including R branch

Richard Saykally

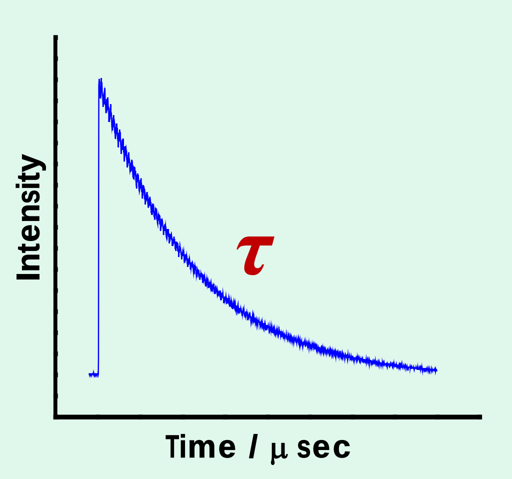

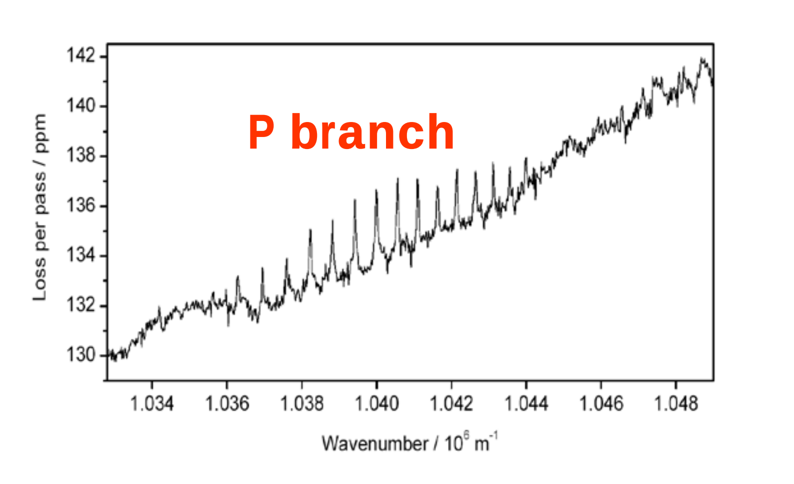

band	origin / cm-1	<v'|p(x)|0> C m	S_b / m	
0-0		$3.6632*10^{-31}$		
0-1	2143.2711	$-3.53*10^{-31}$	$1.00*10^{-19}$	
0-2	4260.0622	$2.22*10^{-32}$	$7.83*10^{-22}$	128
0-3	6350.4391	$-1.36*10^{-33}$	$4.42*10^{-24}$	177
0-4	8414.4693	$6.95*10^{-35}$	$1.53*10^{-26}$	289
0-5	10452.2222	$3.27*10^{-36}$	$4.18*10^{-29}$	366

Mass-selected IR spectrum – Gas phase

VUV ionization/IR excitation/TOF detection

$(CH_3OH)_n$	JCP *134*, 144309 (2011)
CH_3S	CPL *515*, 1 (2011)
$(CH_3SH)_n$	JCP *137*, 234307 (2012)
$(CH_3OH)_n(H_2O)$	JCP *146*, 144308 (2017)
CH_3SH autoion.	PCCP *19*, 29153 (2017)
$CH_3S\cdots CH_3SH$	JPCL *9*, 3725 (2018)
$(CH_3SH)_2^+$-X	PCCP *21*, 16055 (2019)
$(pyridine)_2$	PCCP *22*, 21520 (2020)

TOF spectrum

Action spectra

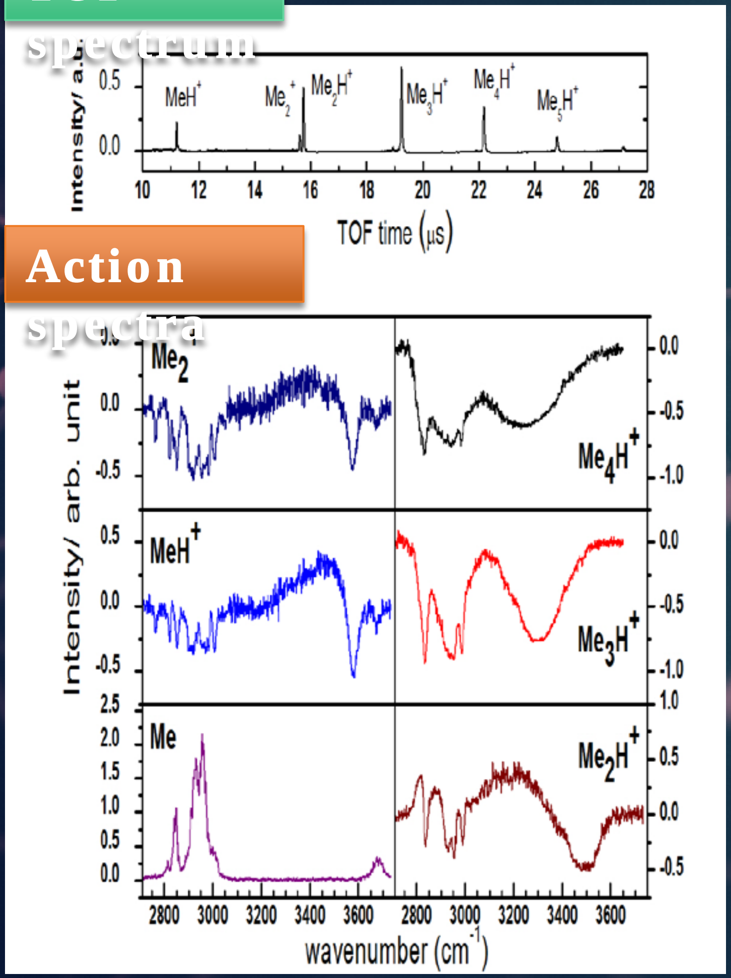

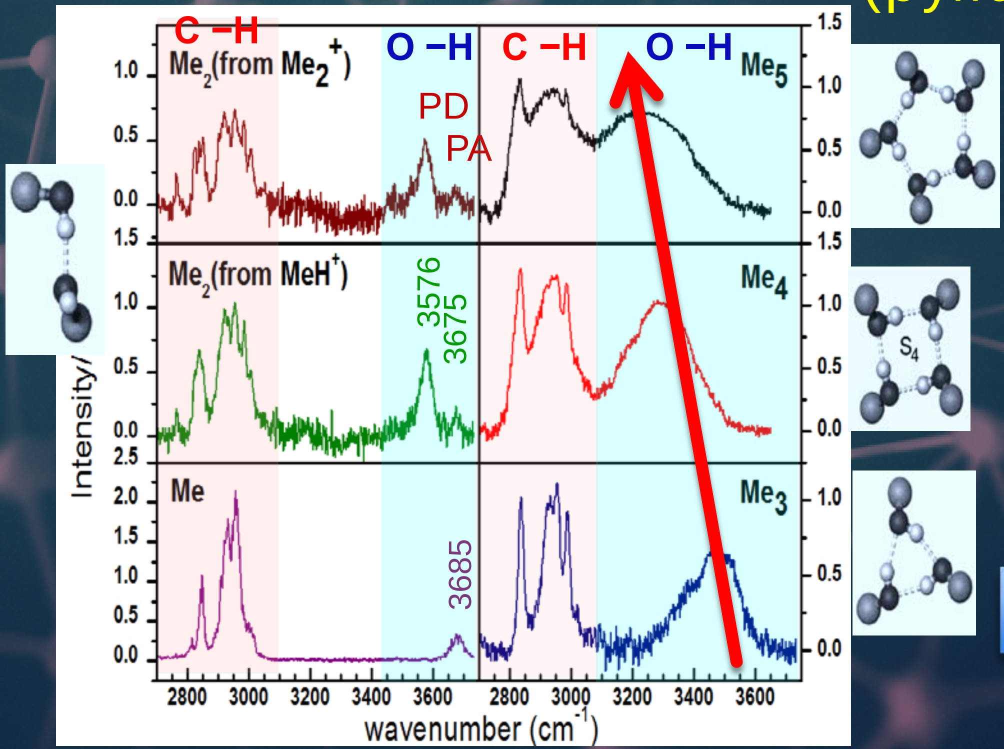

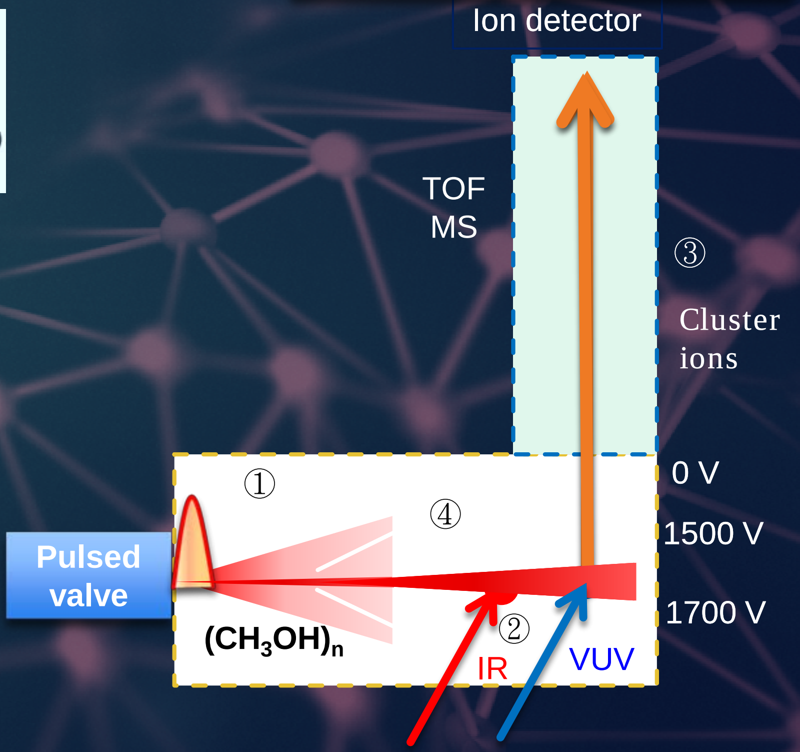

Step-scan FTIR

Gas phase

1990 — **Synchronous triggering– Bomem** — Not successful

1995 — **Step-scan (emission)– Bruker ifs66v** — NIR emission of NO from HNO_3

1999 — HF* from CH_2CF_2

1997 — **Step-scan (absorption)– Bruker ifs66v** — HCl(v) from Cl + H_2

2001 — ClCO; CH_4(v) from Cl + CH_4

2004 — **Step-scan (absorption)– Nicholet Nexus 870** — ClSO from Cl_2SO

2006 — CH_3SO_2 from CH_3 + SO_2

2013 — **Step-scan (absorption)– Bruker Vertex 80v** — CH_2OO

Fourier-Transform IR Spectrometer

(continuous scan)

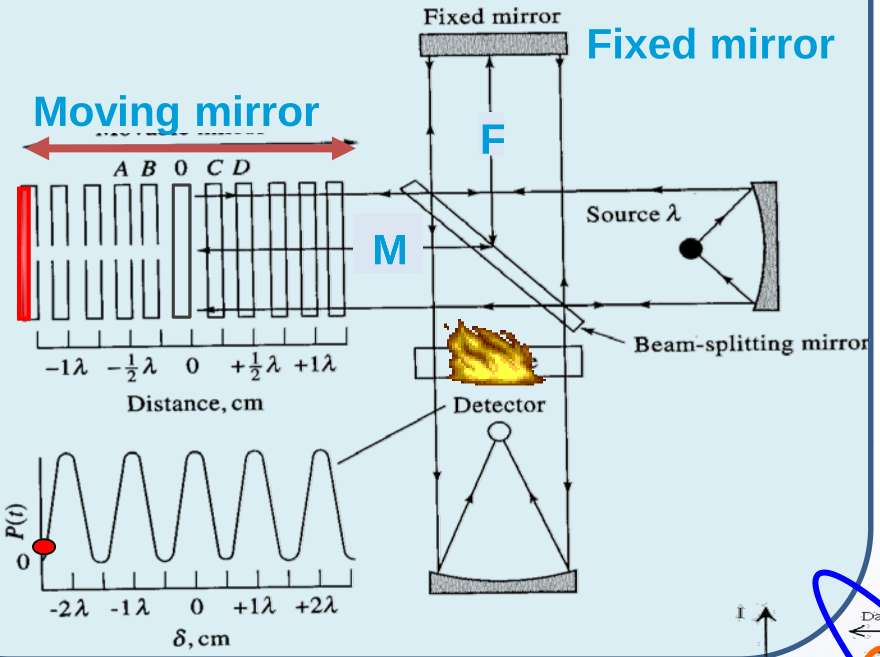

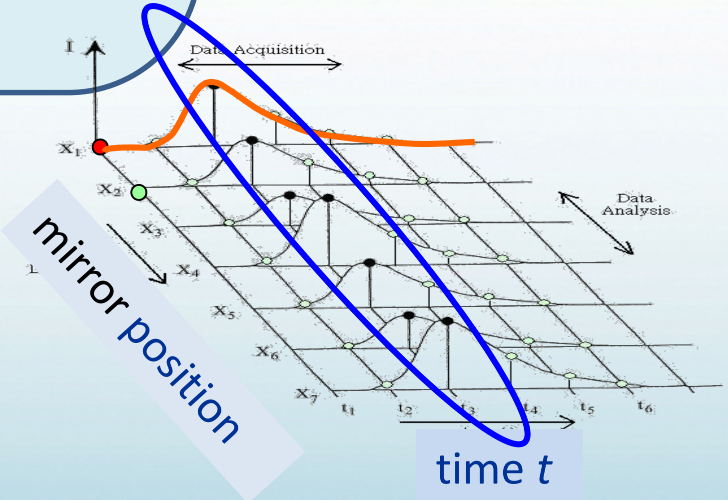

(step scan)

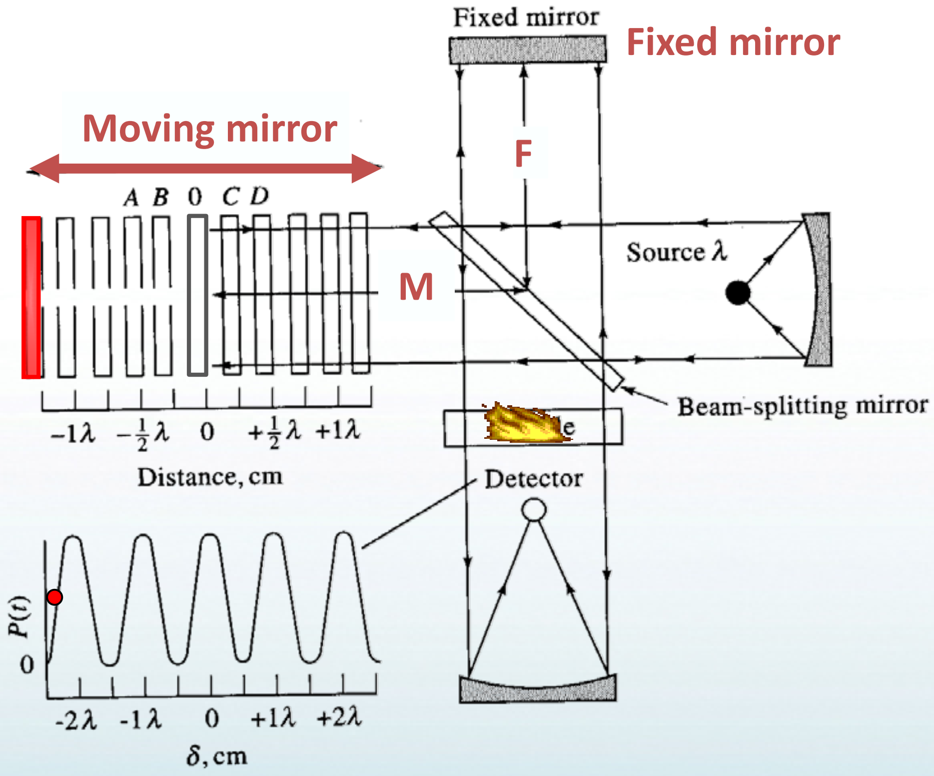

Photolysis of HNO_3 at 193 nm

JCP *103*, 4879 (1995)

NO D $^2\Sigma^+$ – A $^2\Sigma^+$ emission

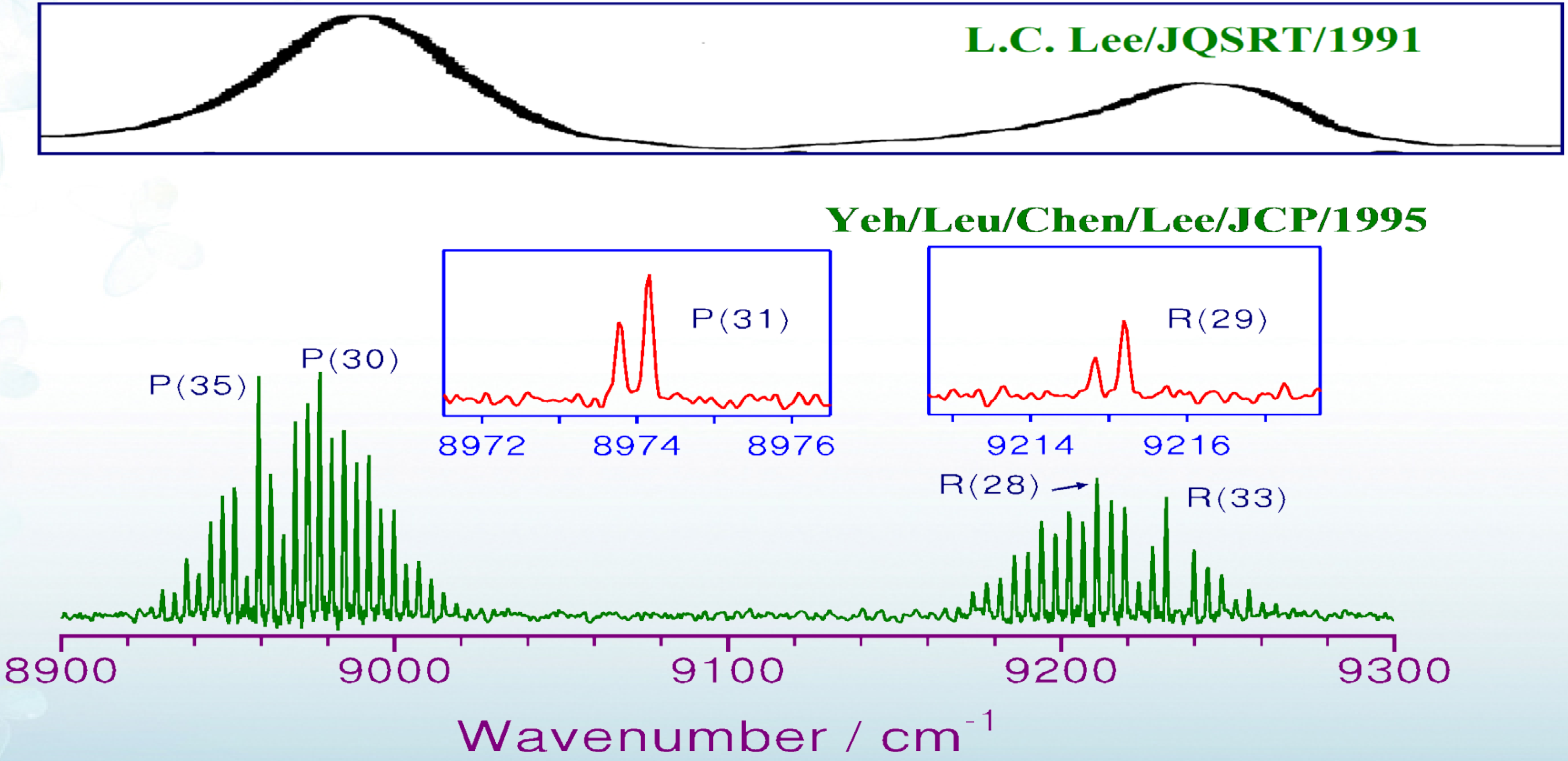

HCl Emission from CH_2CHCl + 193 nm

$CH_2CHCl \rightarrow :CCH_2 + HCl$ (3-center)

$\rightarrow HCCH + HCl$ (4-center)

Molecular beam: YT Lee, JCP *108*, 5414 (1998)

HCl is highly excited. IP (HCl) = 12.75 eV

Observed threshold : 10.5 ± 0.30 eV

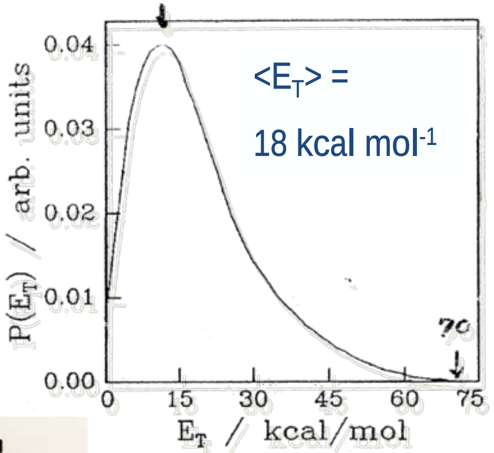

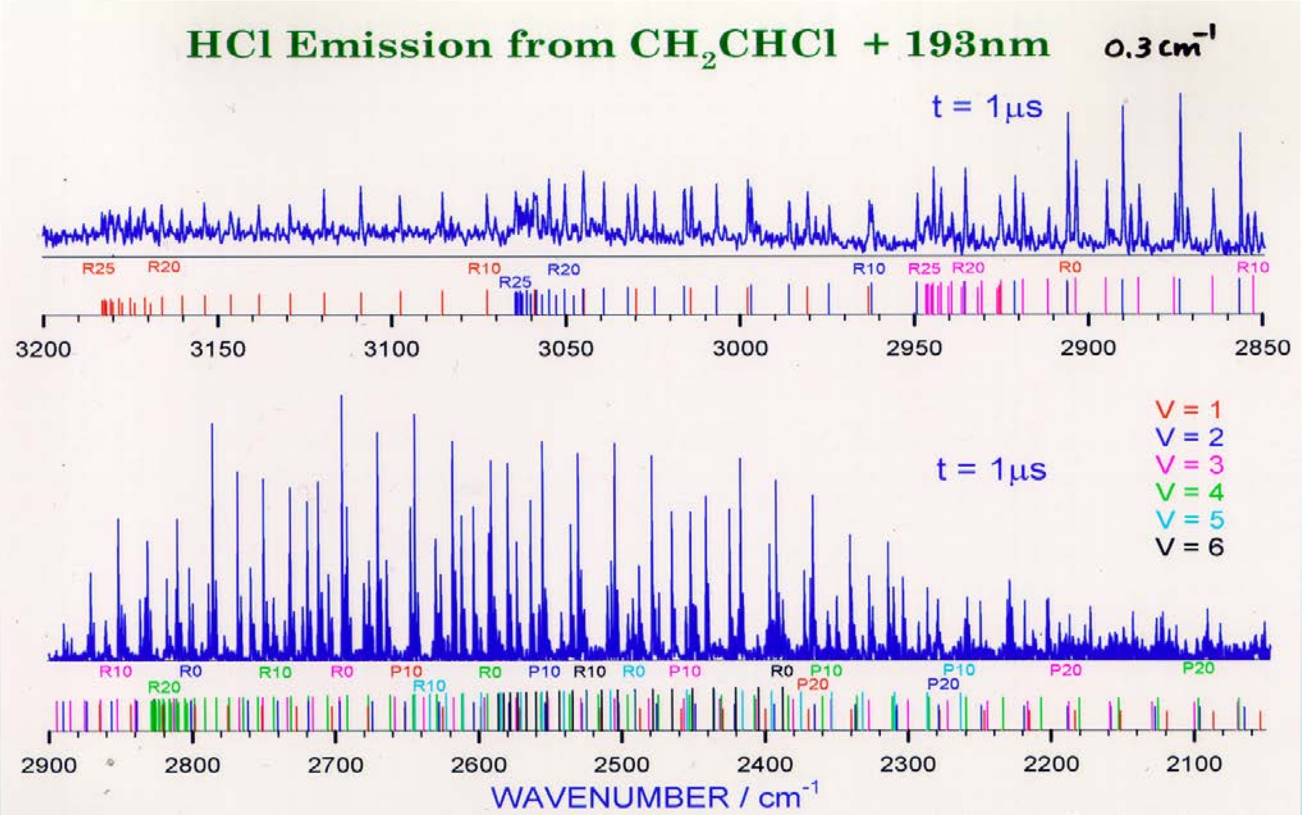

high *J*
$T_{rot} \cong$ 10,000 K
nearly statistical
$T_{vib} \cong$ 16,000 K
near statistical

low J
$T_{rot} \cong$ 500 K
impulse model
peaked at v = 2
non-statistical

JCP *114*, 160 (2001)

Rotational distributions of HCl from CH_2CHCl + 193nm

CH_2CHCl (110 mTorr) / Ar (240 mTorr) , 0-1 μs

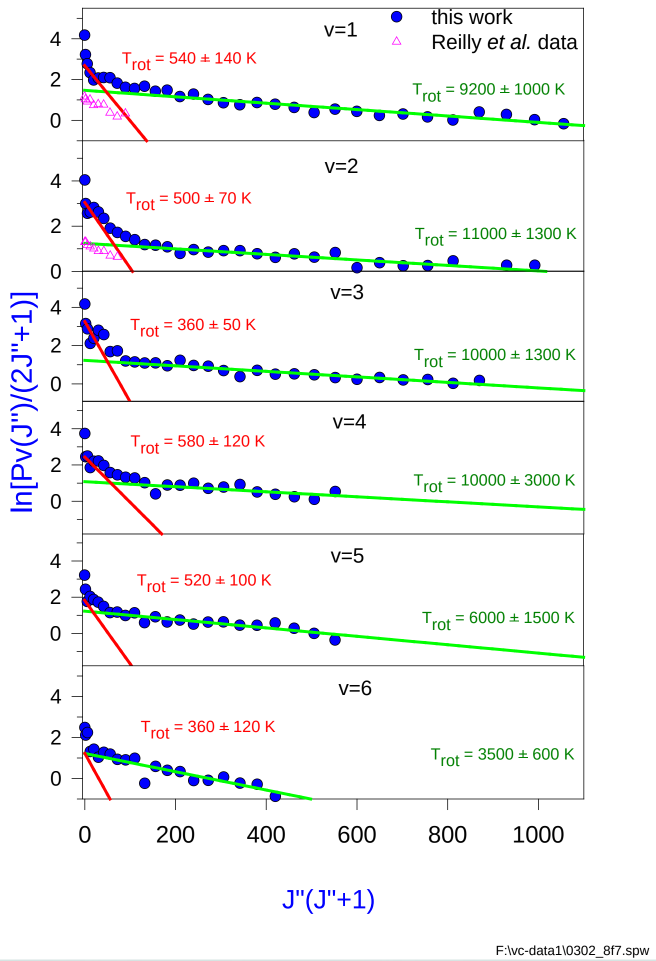

Step-scan Fourier-transform IR Absorption

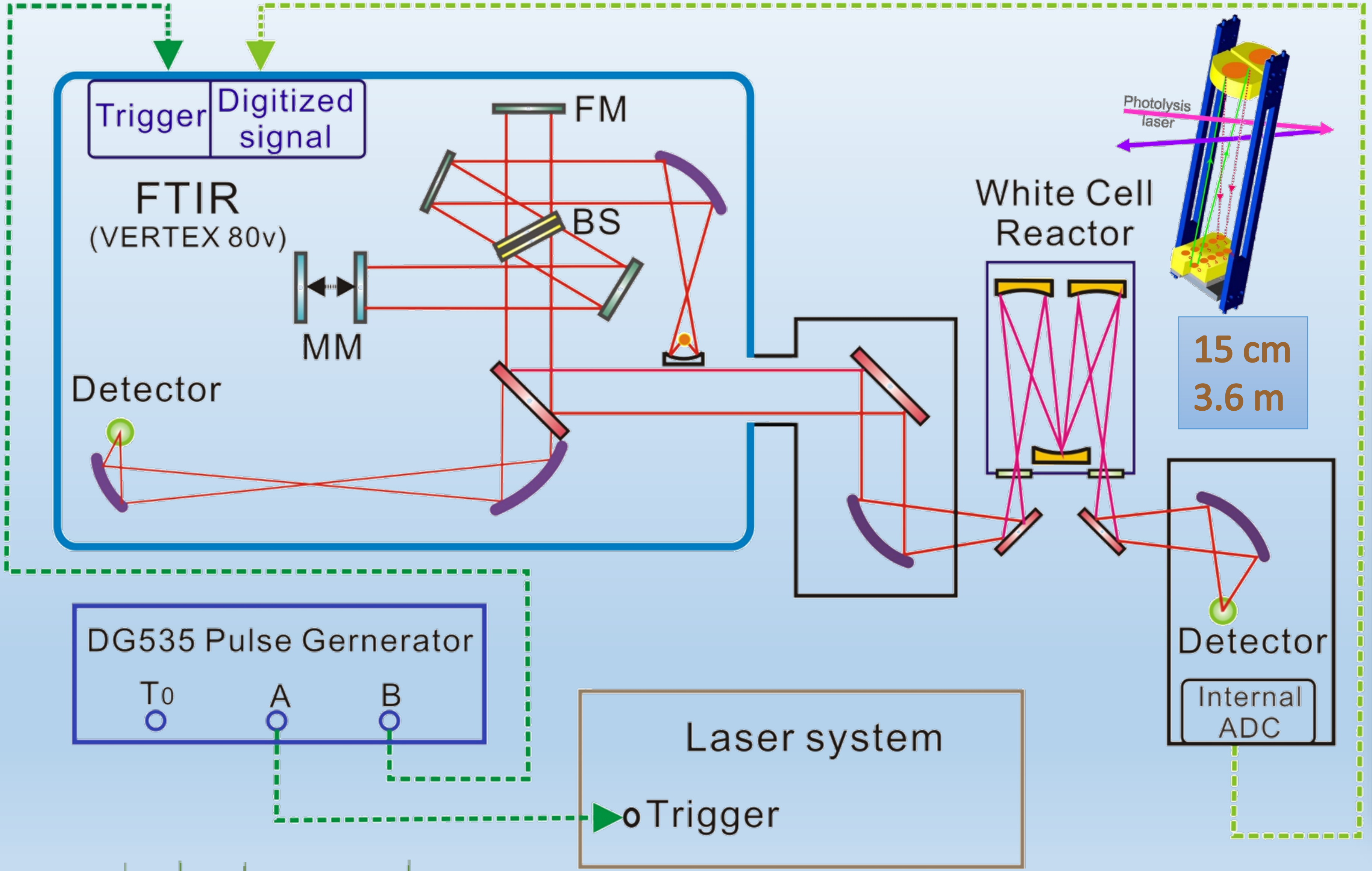

AC/DC Detection

25 ns / 1–5 μs
0.15 / 0.5–1.0 cm $^{-1}$

15 cm
3.6 m

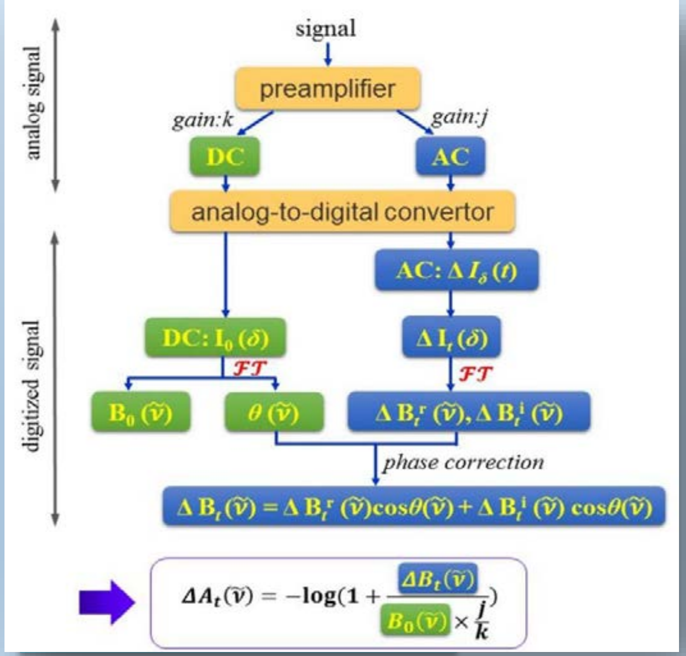

Second-Generation TR-FTIR

2.5 ns / 12.5 μs
0.075 cm^{-1}

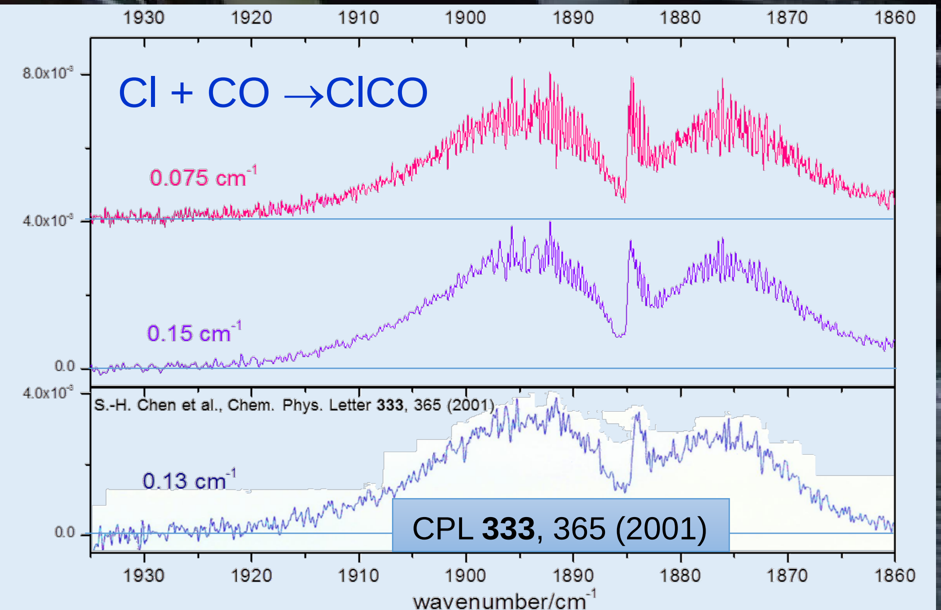

Step-scan FTIR

Gas phase

Absorption of Transient Species

ClCO	CPL *333*, 365 (2001)
ClSO	JCP *120*, 3179 (2004)
ClCS	JCP *126*, 134310 (2007)
CH_3SO_2	JCP 124, 244301(2006)
CH_3SOO, CH_3SO	JCP *133*, 184303 (2010)
CH_3OSO	JCP *825*, 094304 (2011)
$C_6H_5SO_2$	JCP *126*, 134311 (2007)
CH_3OO	JCP *127*, 234318 (2007)
c-, *t*-$CH_3C(O)OO$	JCP *132*, 114303 (2010)
C_6H_5CO	JPCA *116*, 6366 (2012)
$C_6H_5C(O)OO$	JCP *135*, 224302 (2011)
c-, *t*-ClCOOH	JCP *130*, 174304 (2009)

Photolysis at 248 nm of CH_3SSCH_3/O_2 (1/700, total 220 Torr) at 260 K

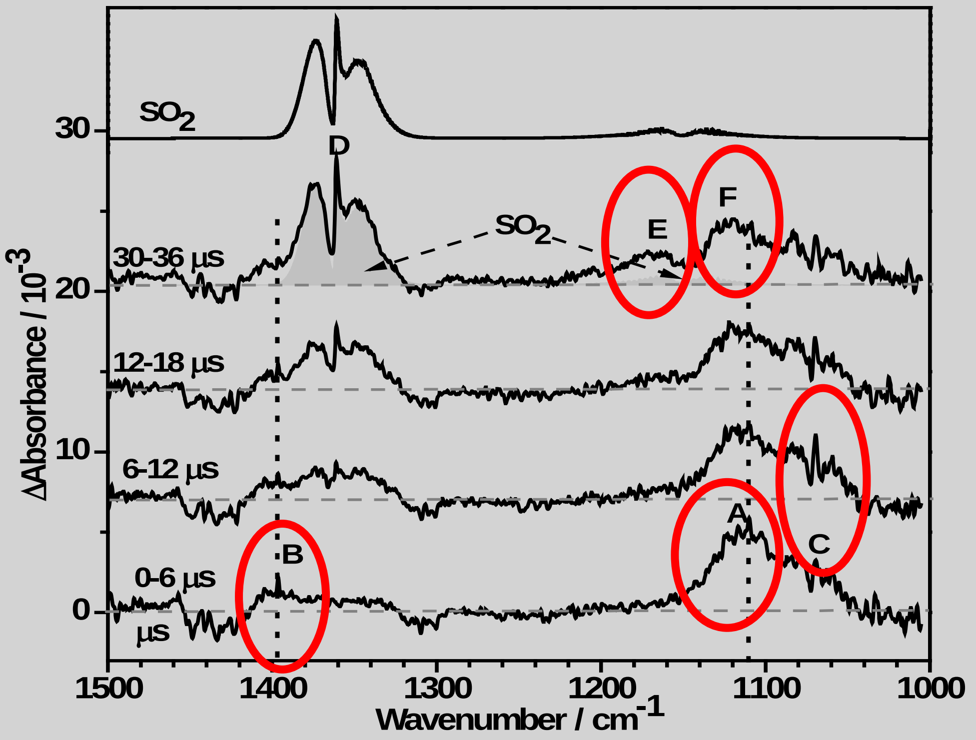

A (1110 cm^{-1}), B (1397 cm^{-1}): *syn*-CH_3SOO

C (1071 cm^{-1}): CH_3SO

E (1170 cm^{-1}): $CH_3S(O)OSCH_3$

F (1120 cm^{-1}): $CH_3S(O)S(O)CH_3$

Importance of Criegee Intermediates

- **Criegee mechanism**

important for the removal of unsaturated hydrocarbons and for the production of OH in the atmosphere

R. Criegee, Rec. Chem. Prog. **18**, 111 (1957)

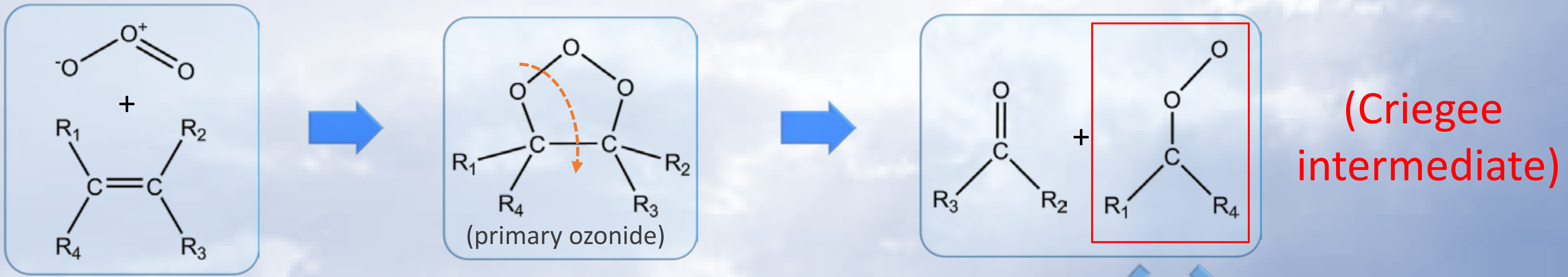

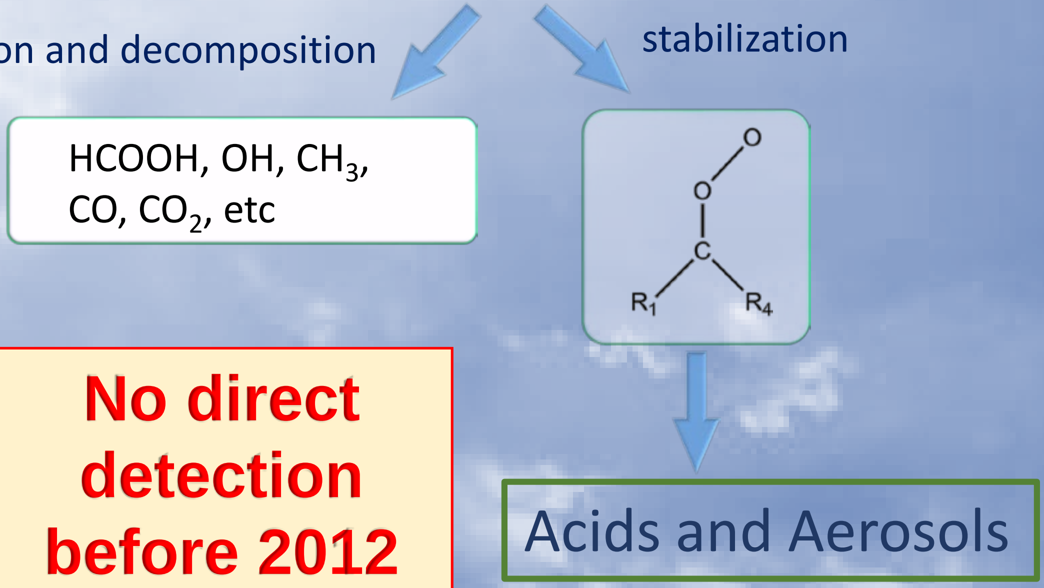

- **Decomposition of CH_2OO**

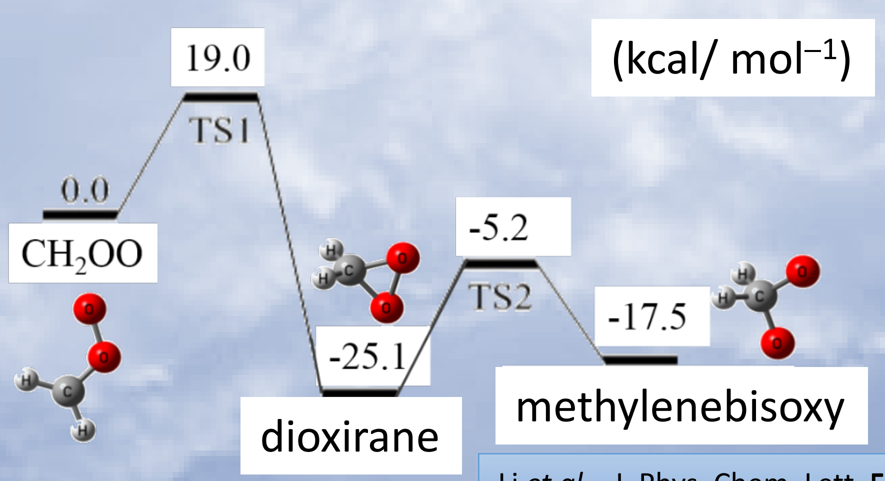

Li *et al.*, J. Phys. Chem. Lett. **5**, 13 (2014)

No direct detection before 2012

Infrared Spectrum of CH_2OO

12 APRIL 2013 VOL 340 **SCIENCE**

$CH_2I_2 + h\nu \rightarrow CH_2I + I$,
$CH_2I + O_2 \rightarrow CH_2O_2 + I$

Welz et al.
Science 335, 204 (2012)
Detection by MASS

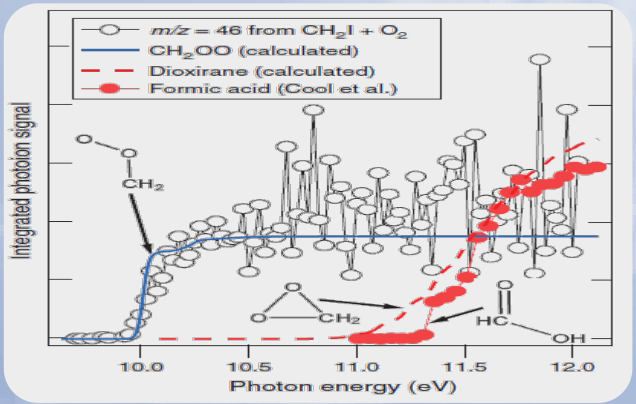

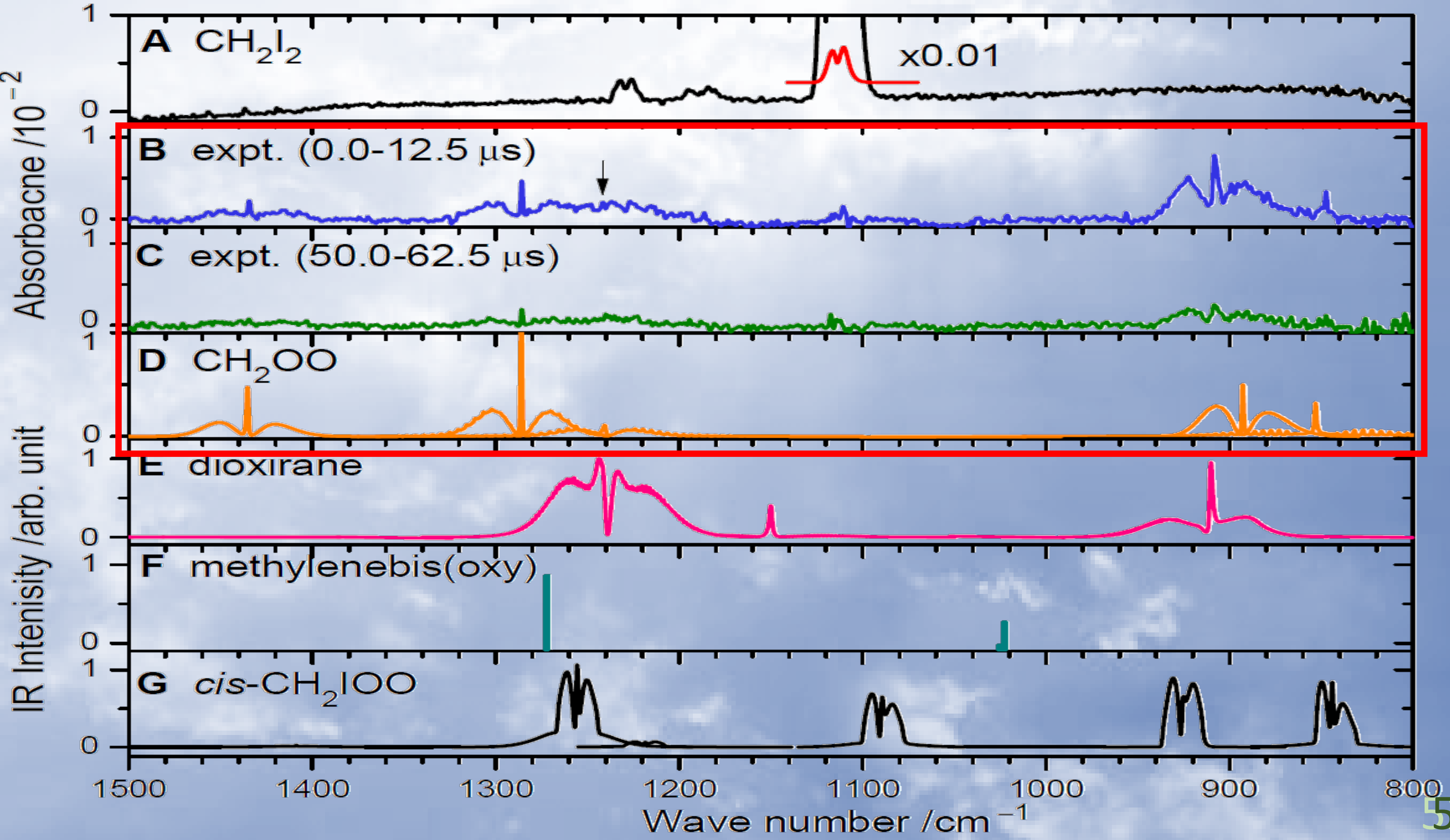

Comparison of Experiments with Calculations

mode	sym.	experiment	NEVPT2/aVDZ harmonic	NEVPT2/aVDZ anharmonic	CAS(14,12) /VDZ	CCSD(T) /aVTZ	description[a]
ν_1	A'		3370 (5)[b]	3149	3215	3290	*a*-CH str.
ν_2	A'		3197 (1)	3030	3065	3137	*s*-CH str.
ν_3	A'	1435(33)[c]	1500 (52)	1458	1465	1483	CH_2 scissor /CO str.
ν_4	A'	1286 (42)	1338 (100)	1302	1269	1306	CO str. /CH_2 scissor
ν_5	A'	1241 (39)	1235 (33)	1220	1233	1231	CH_2 rock
ν_6	A'	908 (100)	916 (100)	892	849	935	OO str.
ν_7	A'		536 (1)	530	537	529	COO deform
ν_8	A''	848 (24)	856 (31	[illegible]	[illegible]	862	CH_2 wag
ν_9	A''		620 (2)	[illegible]	[illegible]	632	CH_2 twist
reference		this work	this work	this work	16	13	

Zwitterion

Dimer of CH_2OO – *Zwitterionic Character*

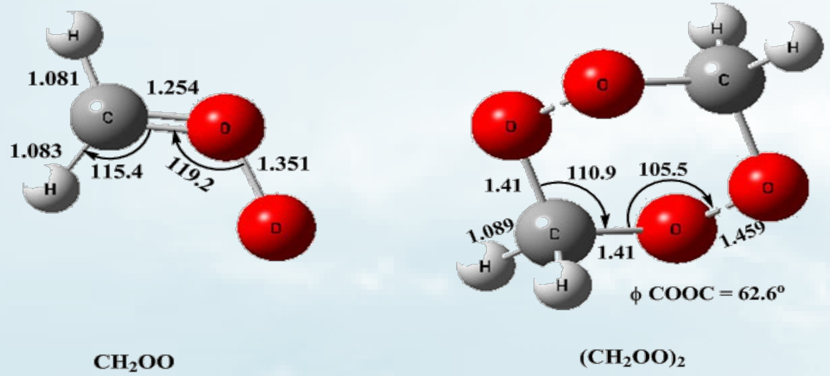

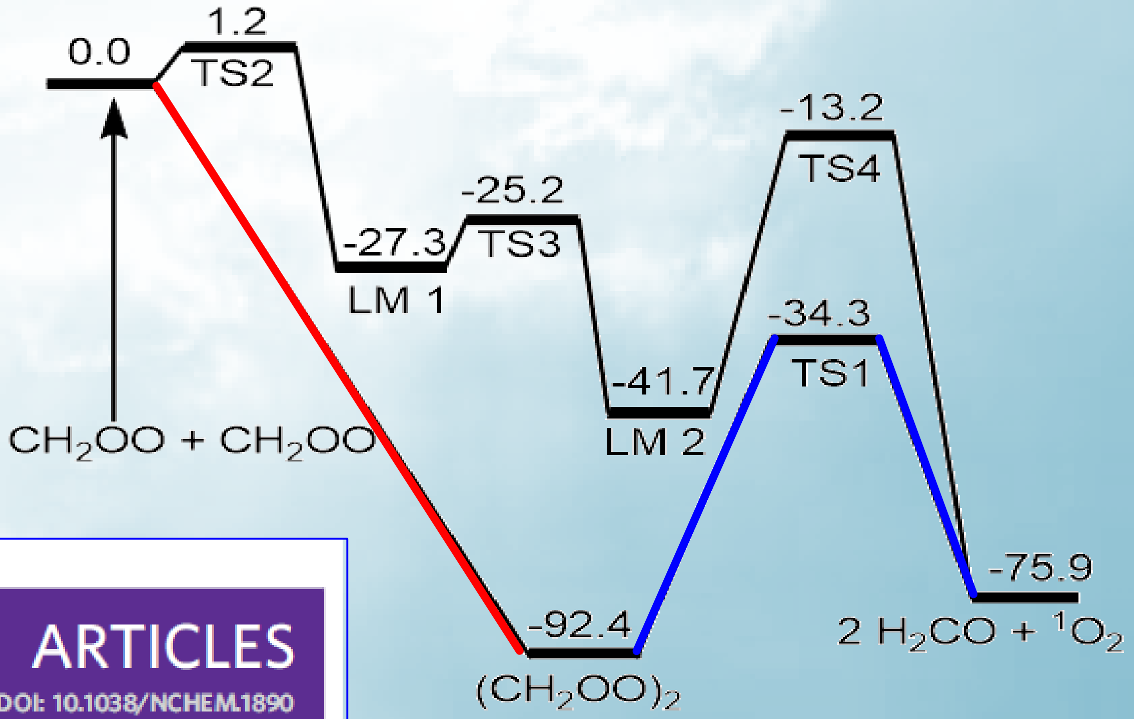

nature chemistry
ARTICLES
PUBLISHED ONLINE: 23 MARCH 2014 | DOI: 10.1038/NCHEM.1890

Extremely rapid self-reaction of the simplest Criegee intermediate CH_2OO and its implications in atmospheric chemistry

Yu-Te Su[1], Hui-Yu Lin[1], Raghunath Putikam[1], Hiroyuki Matsui[1], M. C. Lin[1]* and Yuan-Pern Lee[1,2]*

Nat. Chem. 6, 477 (2014)

Spectra of ICH_2OO Adduct

JPCL 6, 4610 (2015)

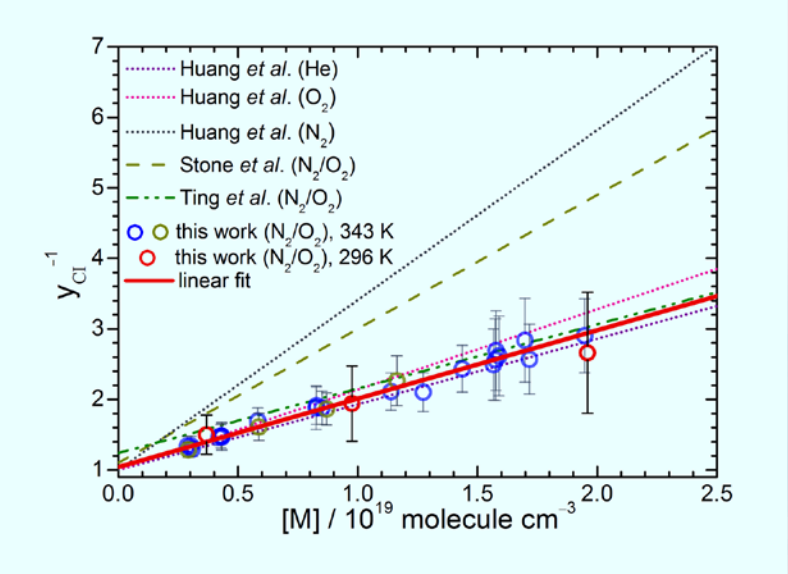

gauch-ICH_2OO *anti*-ICH_2OO

P (*anti*-ICH_2OO) = 13 %

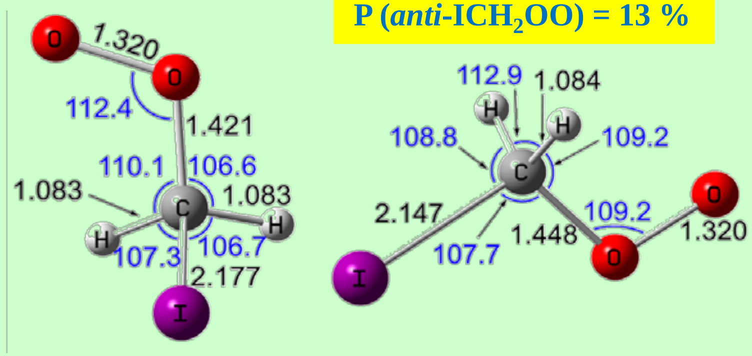

δ (ICOO) = –87.6
δ (HCOO) = 31.7
Δ E = 0 kJ mol^{-1}

δ (ICOO) = 180
δ (HCOO) = 62.0
Δ E = 3.8 kJ mol^{-1}

$CH_2I_2/O_2/N_2$ (0.06/16/94)@308 nm

average **12** spectra

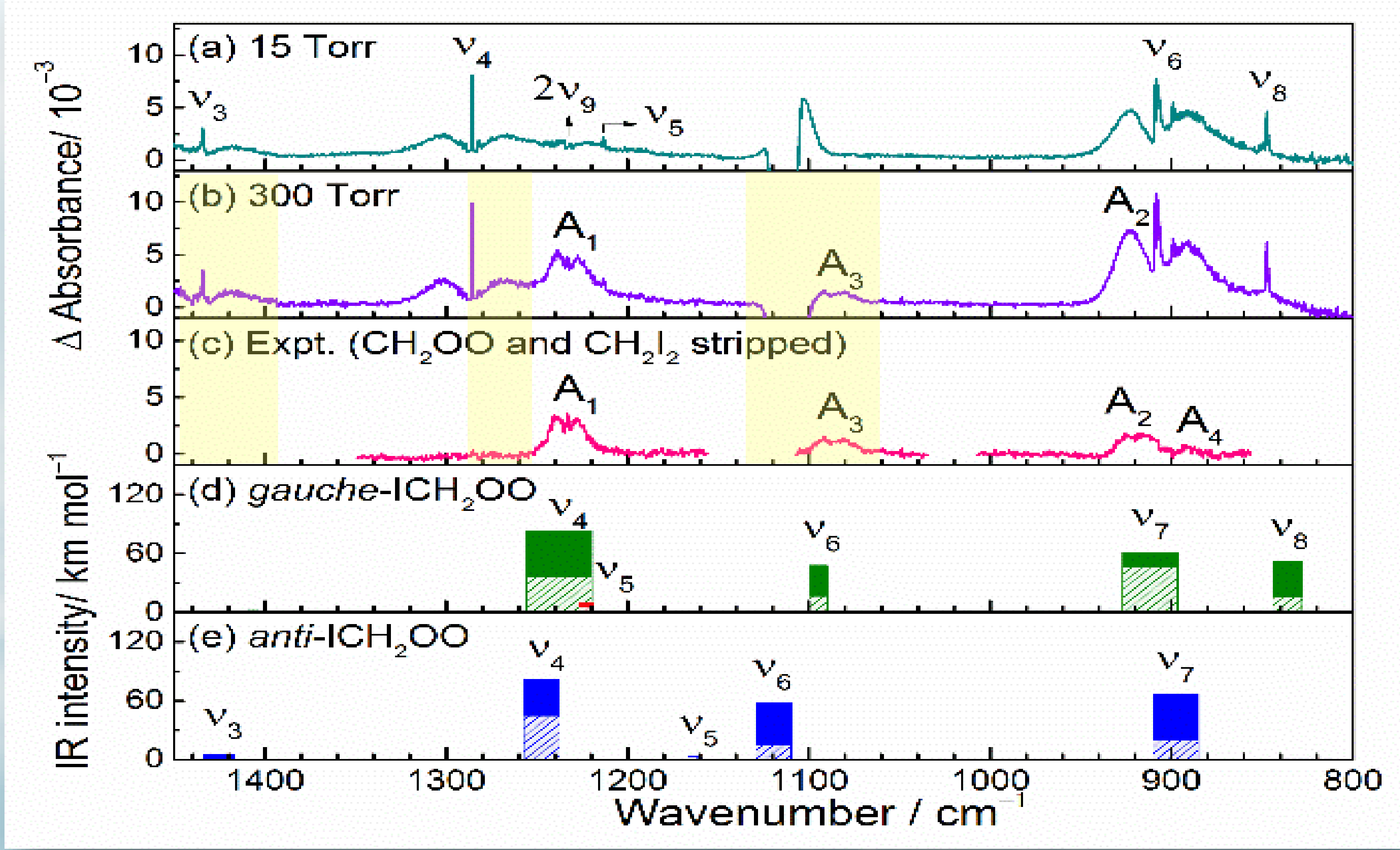

NEVPT2/aVDZ B3LYP/aug-cc-pVTZ-pp

Larger Criegee Intermediates

nature COMMUNICATIONS

Nat. Comm. *6*, 7012 (2015)

syn-CH_3CHOO

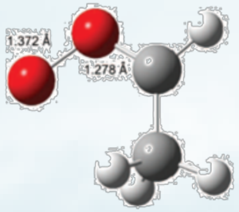

anti-CH_3CHOO

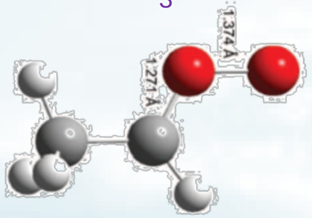

- Two conformers
- Torsion
  – low-frequency mode
  – hot bands

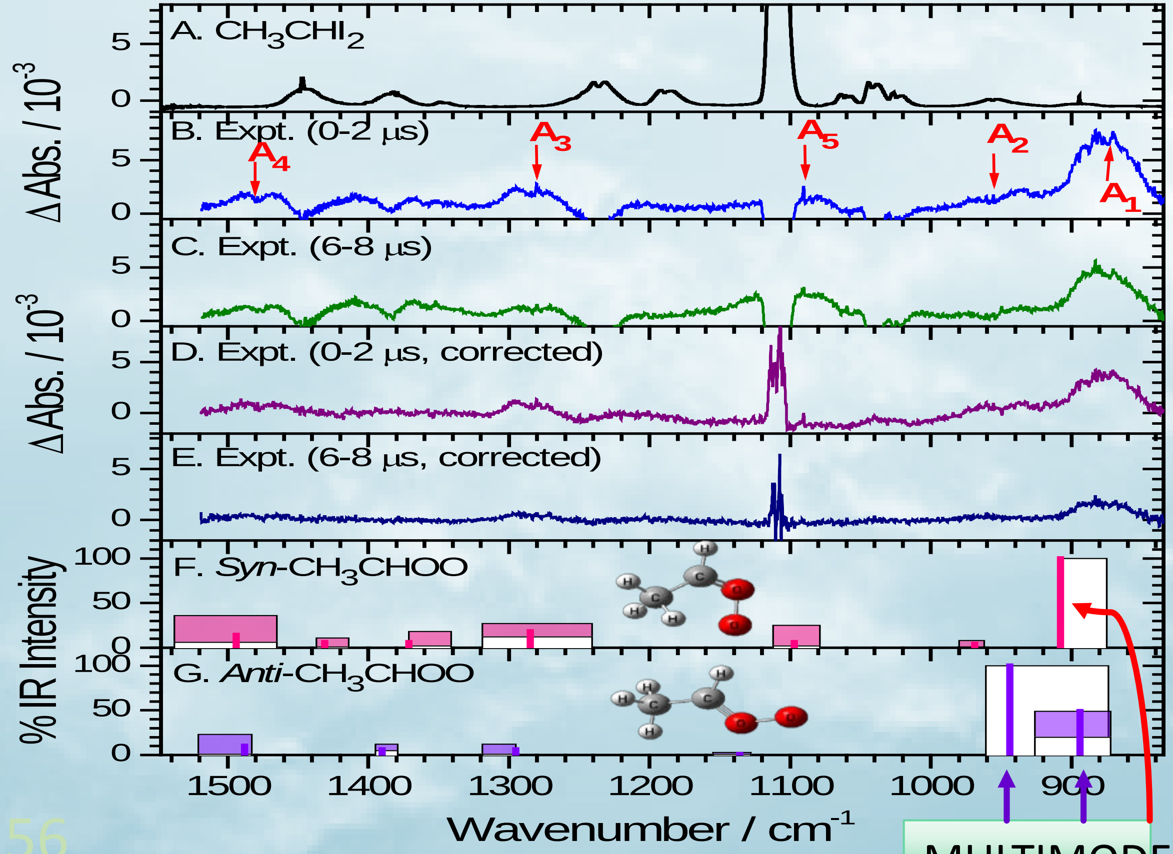

MULTIMODE

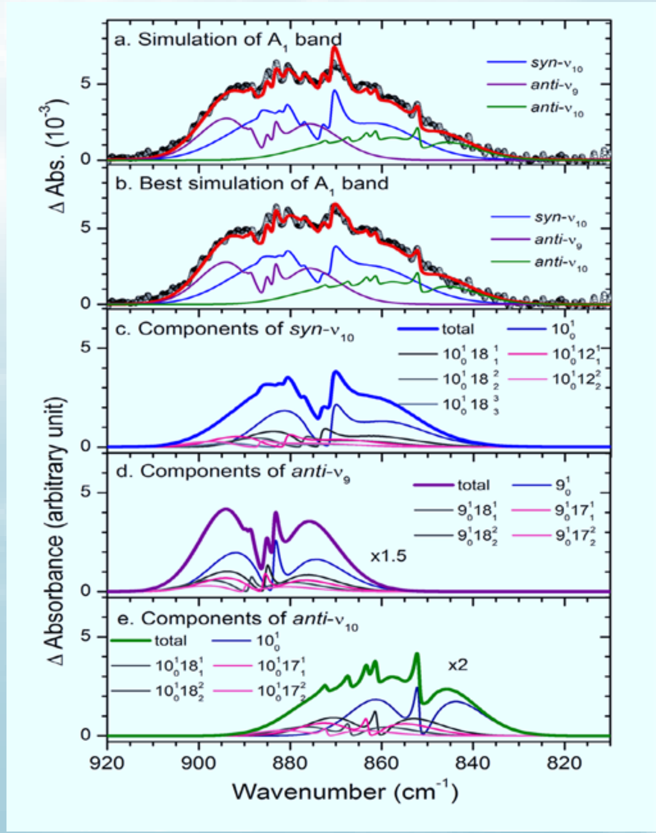

Added NO/NO_2

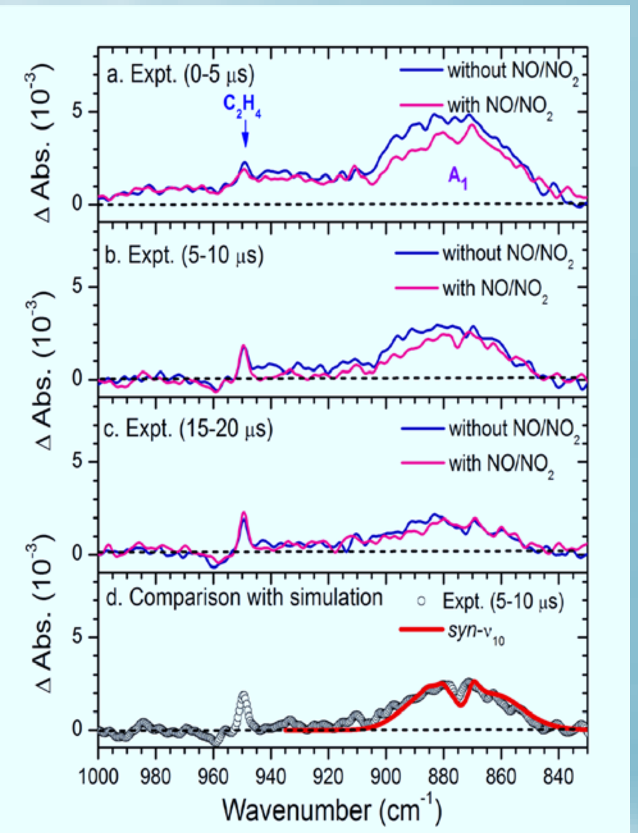

Ozonolysis of Isoprene

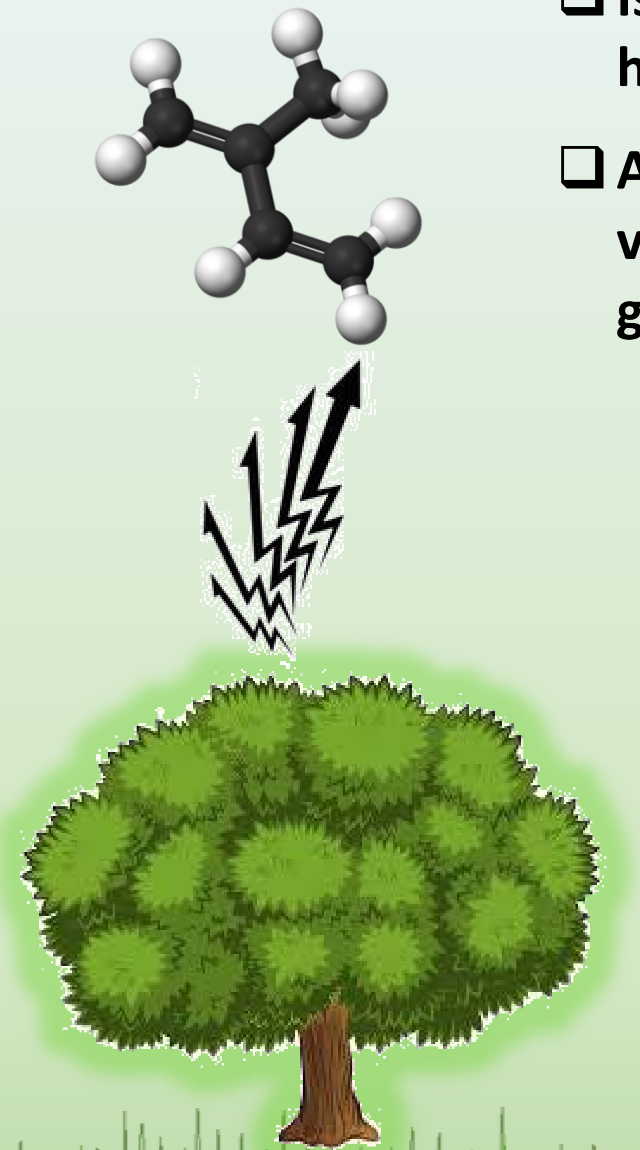

- ❑ Isoprene is the most abundant non-methane hydrocarbon emitted into the atmosphere.
- ❑ Approximately 500–750 Tg of isoprene are emitted by vegetation each year, with roughly 10% removed globally by reactions with ozone.

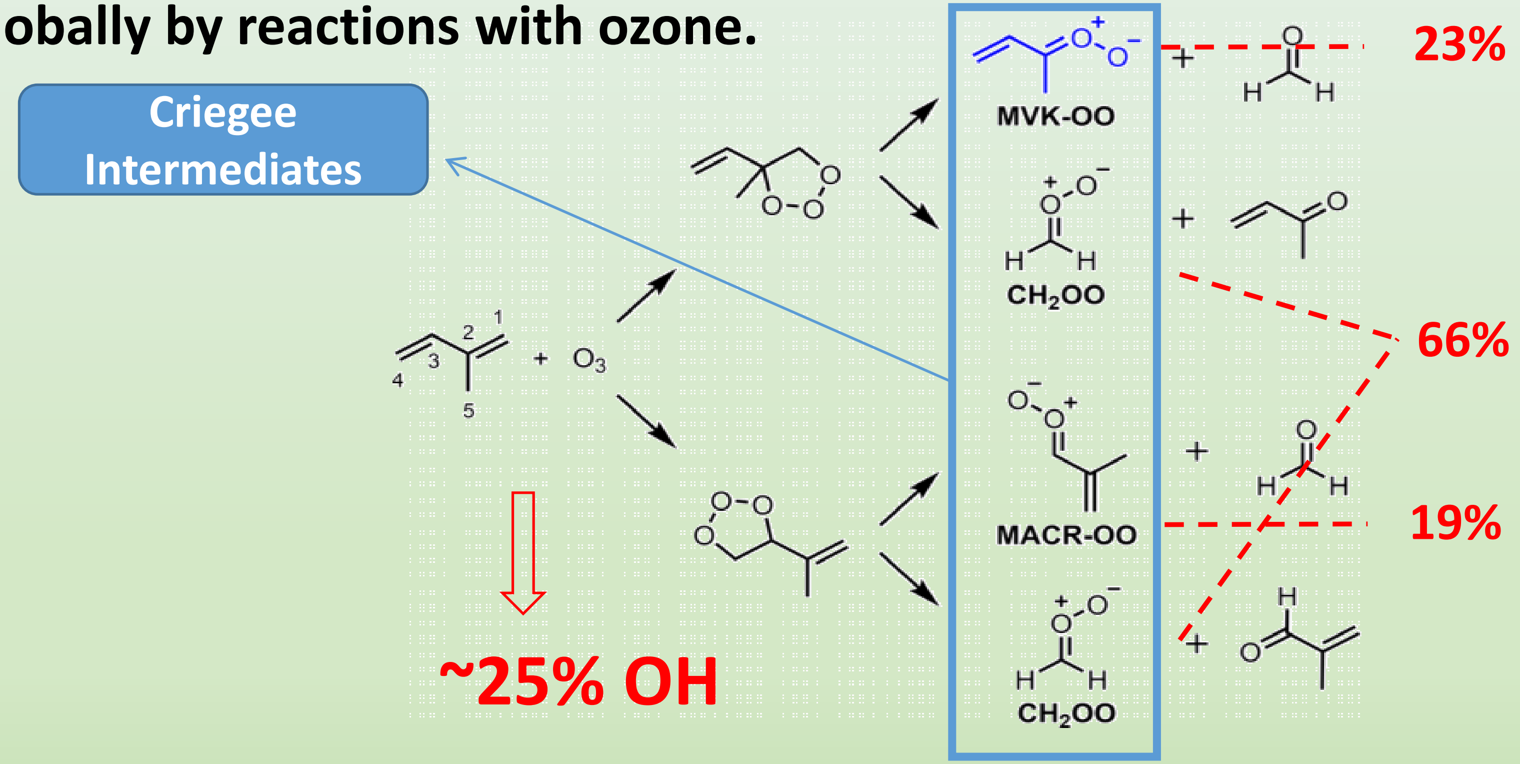

Porterfield *et al.* PCCP, **20**, 16828 (2018); **Barber** *et al.* JACS, **140**, 10866 (2018)

IR Spectra of MVKO

C.-A Chung and Y.-P. Lee, Commun. Chem. **4**, 8 (2021)

- Fission of the terminal allylic C–I bond rather than the central vinylic C–I bond.
- With O_2 at 35 Torr, the Criegee intermediate *syn-trans*-MVKO was observed; the *syn-cis*-MVKO might contribute slightly to the observed spectrum.
- With O_2 at 80–347 Torr, the reaction adduct 3-iodo-but-1-en-3-yl peroxy [$C_2H_3C(CH_3)IOO$] radical was observed.

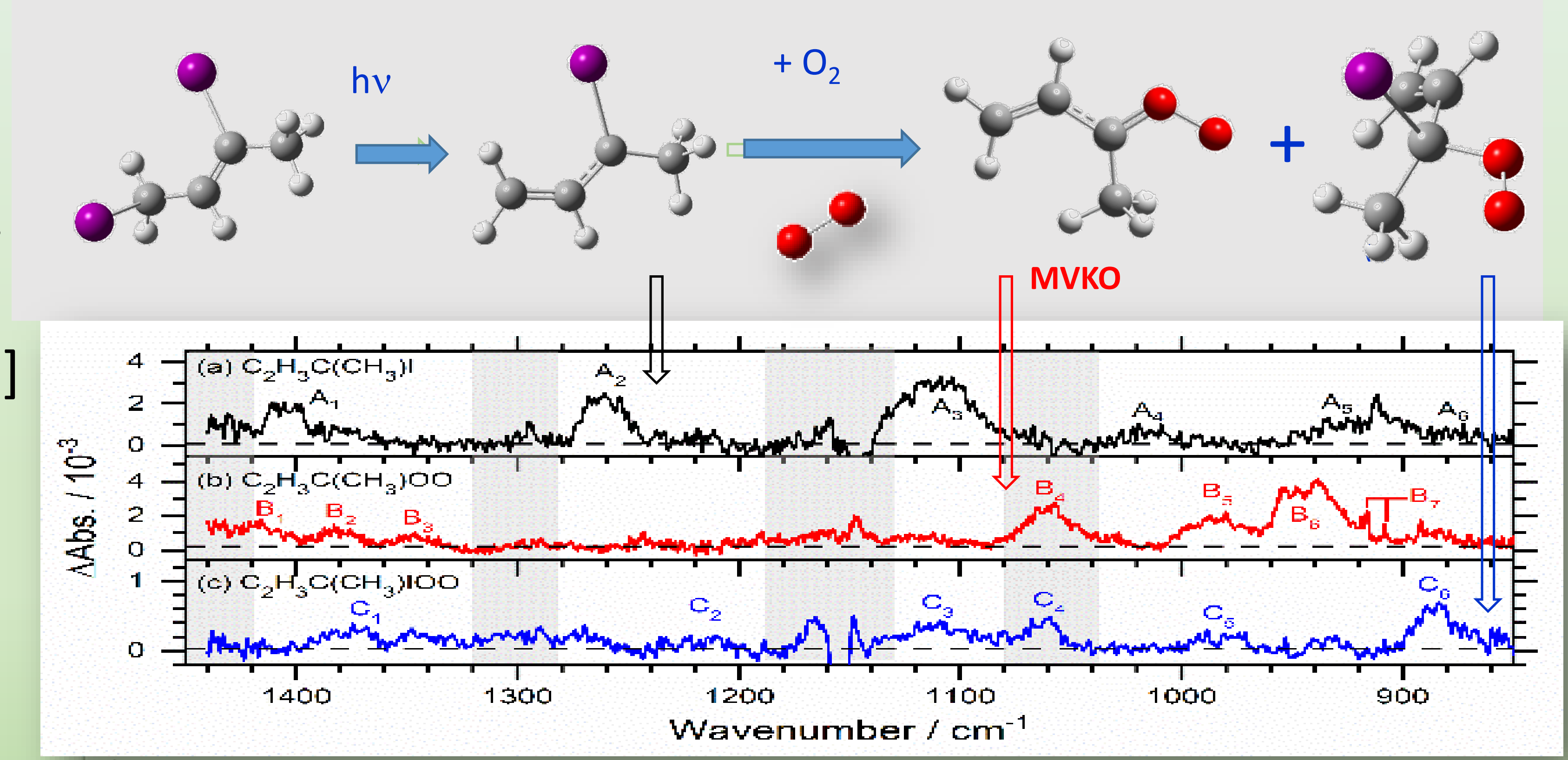

MACRO in the Laboratory

- In laboratory studies, MACRO has been produced in the photolysis of 1,3-diiodo--2-methyl-prop-1-ene, $CH_2IC(CH_3)CHI$, in the presence of O_2.

kcal mol^{-1}

- Proposed reaction scheme: $CH_2C(CH_3)CHI_2$

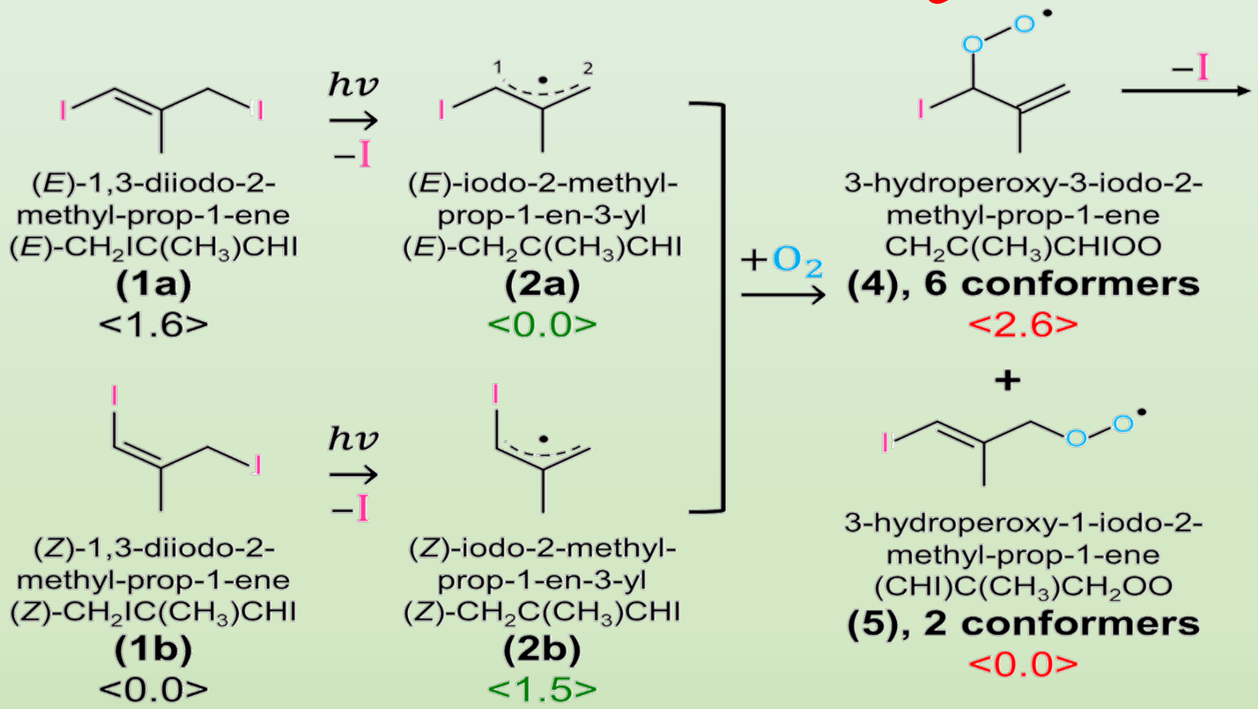

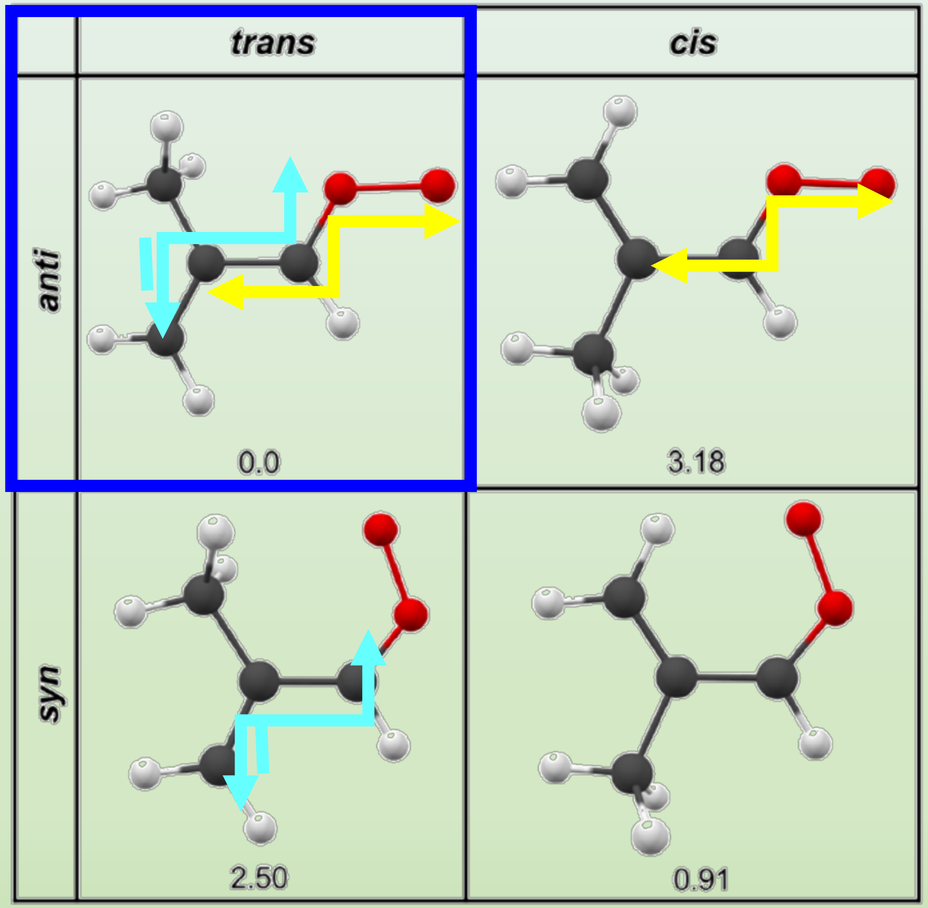

- Mechanism requires verification

Vansco *et al.* JACS, **141**, 15058 (2019)

Summary of IR Spectra of MACI

Cai, Su & Lee, Commun. Chem. **5**, 26 (2022)

- Fission of the allylic C–I bond rather than the central vinylic C–I bond.
- With O_2 at 20 Torr, the Criegee intermediate *anti-trans*-MACRO was observed; the *syn-cis*-MACRO might contribute slightly to the observed spectrum.
- With O_2 at 86–346 Torr, the reaction adduct 3-hydroperoxy-3-iodo-2-methyl-prop-1-ene [$CH_2C(CH_3)CHIOO$] & 3-hydroperoxy-1-iodo-2-methyl-prop-1-ene [$(CHI)C(CH_3)CH_2OO$] were observed.

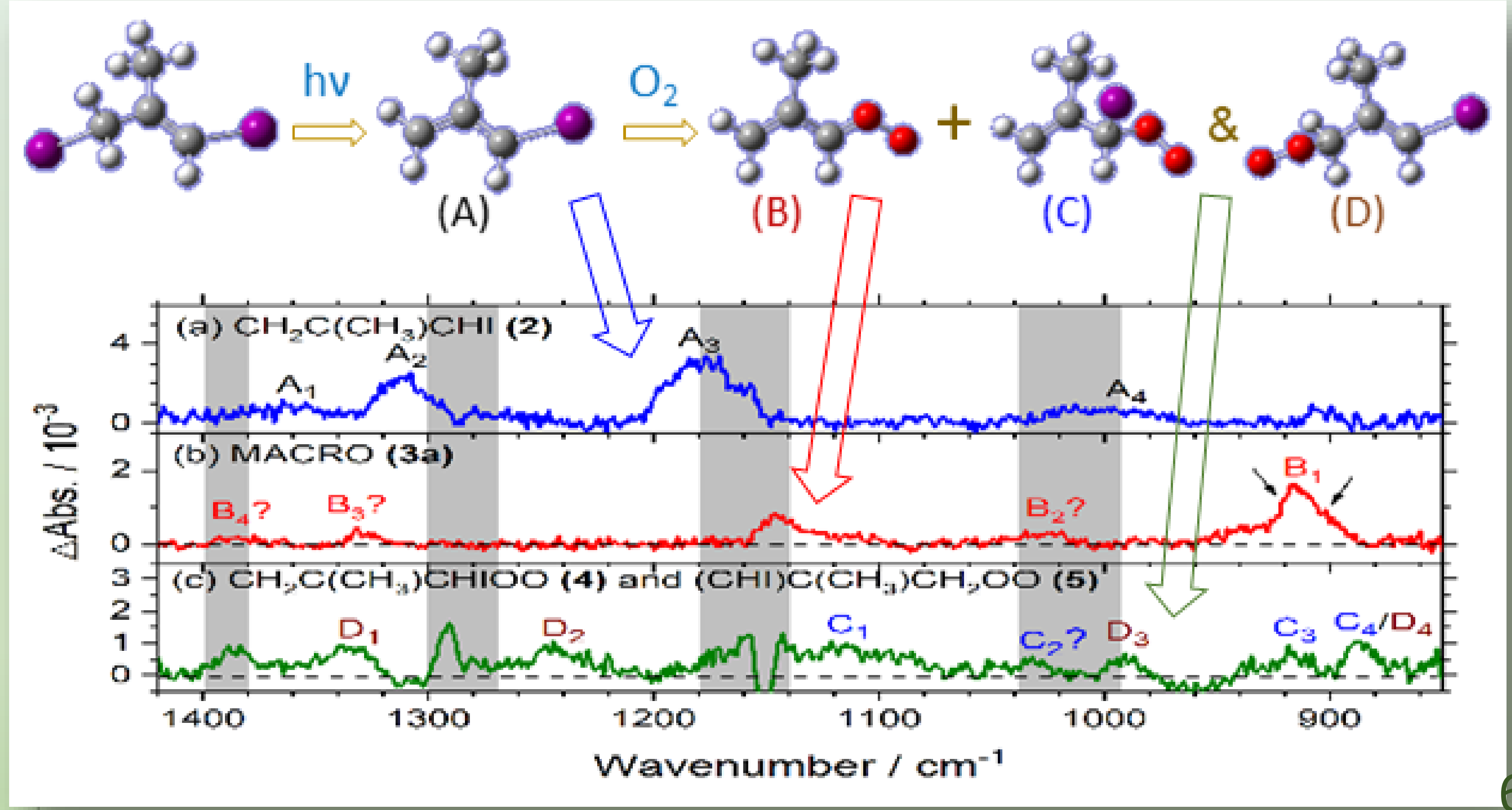

Resonance Stabilization of MVKO & MACRO

	anti-trans- MACRO	*syn-trans-* MVKO[a]	*syn-* CH_3CHOO[b]	*anti-* CH_3CHOO[b]	$(CH_3)_2COO$[c]
r(O–O) /Å	1.365	1.353	1.380	1.381	1.380
r(C–O) /Å	1.266	1.297	1.284	1.279	1.270
ν(OO) /cm^{-1}	917	948	871	884	887

[a] Bond distances predicted with the CCSD(T)/cc-pVTZ method; *J. Phys. Chem. A.* **2020.** [b] Bond distances predicted with the NEVPT2(8,8)/aug-cc-pVDZ method; *Nat. Comm.* **2015**, *6*, 7012. [c] Bond distances predicted with the B3LYP/aug-cc-pVTZ method; *J. Chem. Phys.* **2016**, *145*, 154303.

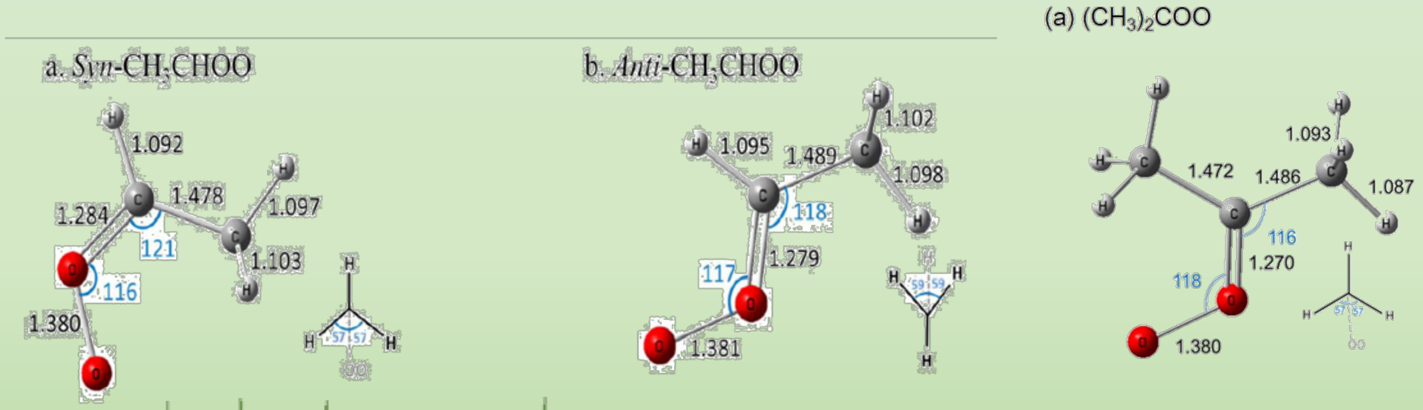

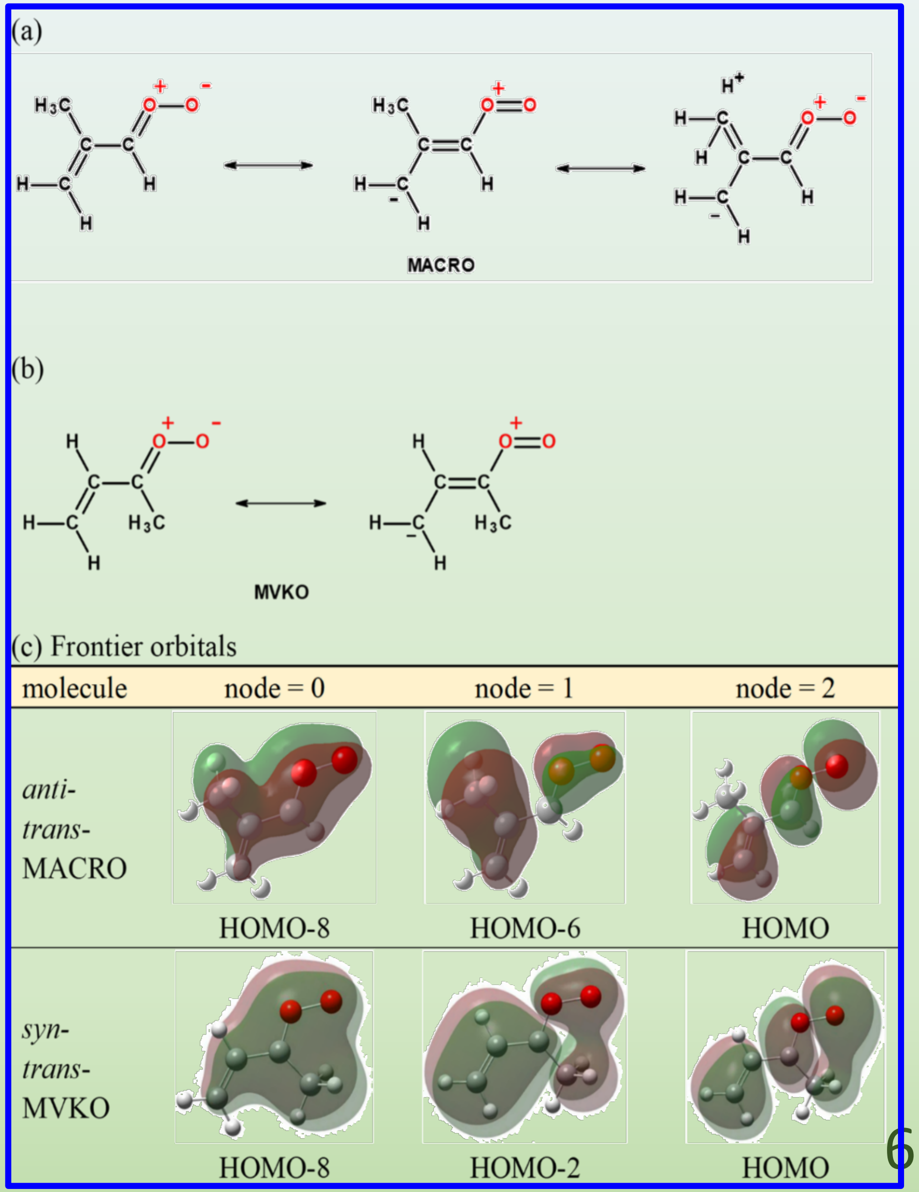

Step-scan FTIR

Gas phase

Reactions of Criegee Intermediates

$CH_2OO + SO_2$	JCP *148*, 064301(2018)
CH_2OO + HC(O)OH	PCCP *21*, 21445 (2019)
$CH_2I + O_2$	PCCP *22*, 17540 (2020)
CH_2OO + HCl	PCCP *23*, 11082 (2021)
$CH_3CHI + O_2$	JPCA *125*, 8373 (2021)
$CH_2OO + CH_3C(O)OH$	PCCP *24*, 18568 (2022)
$CH_2OO + HNO_3$	JPCA *126*, 5738 (2022)

1. Reaction of $CH_2OO + CH_3C(O)OH$

conformation-dependent reactivity

PCCP *24*, 18568 (2022)

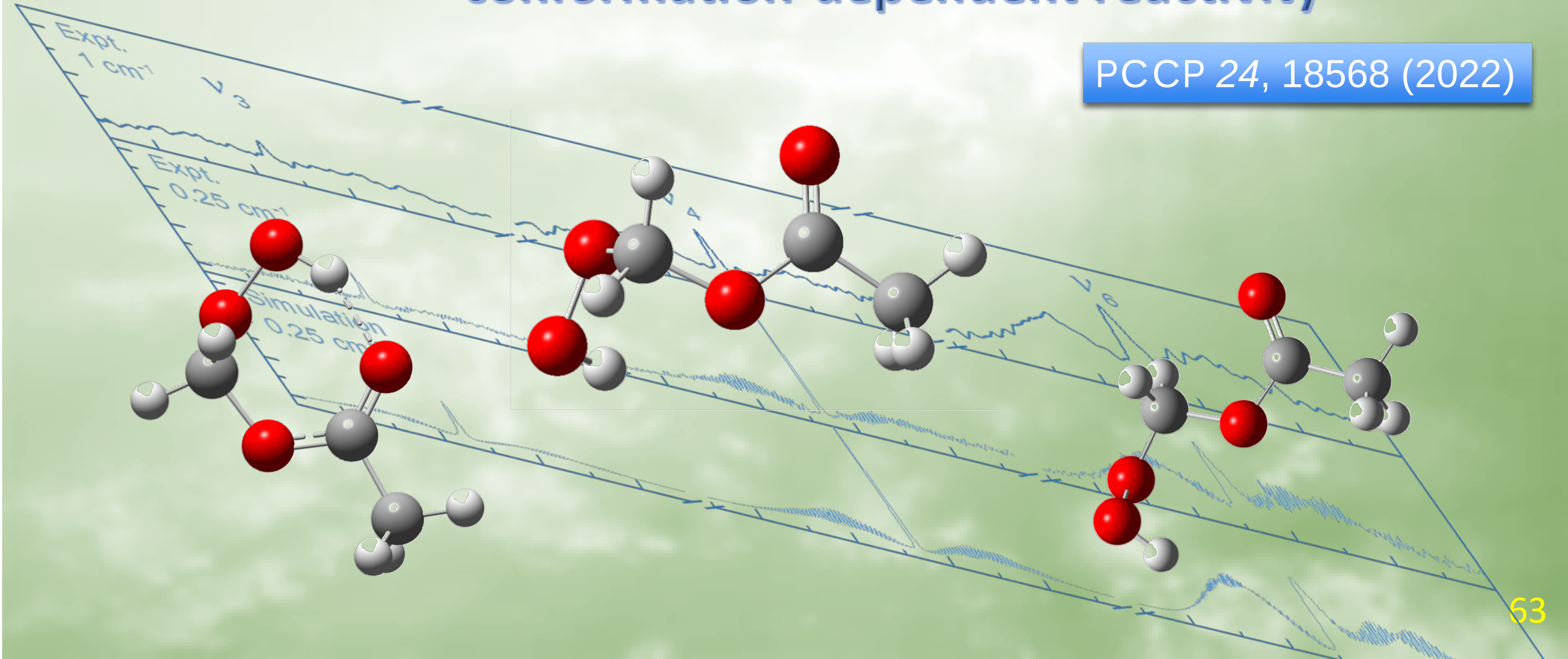

PES of the reaction $CH_2OO + CH_3COOH$

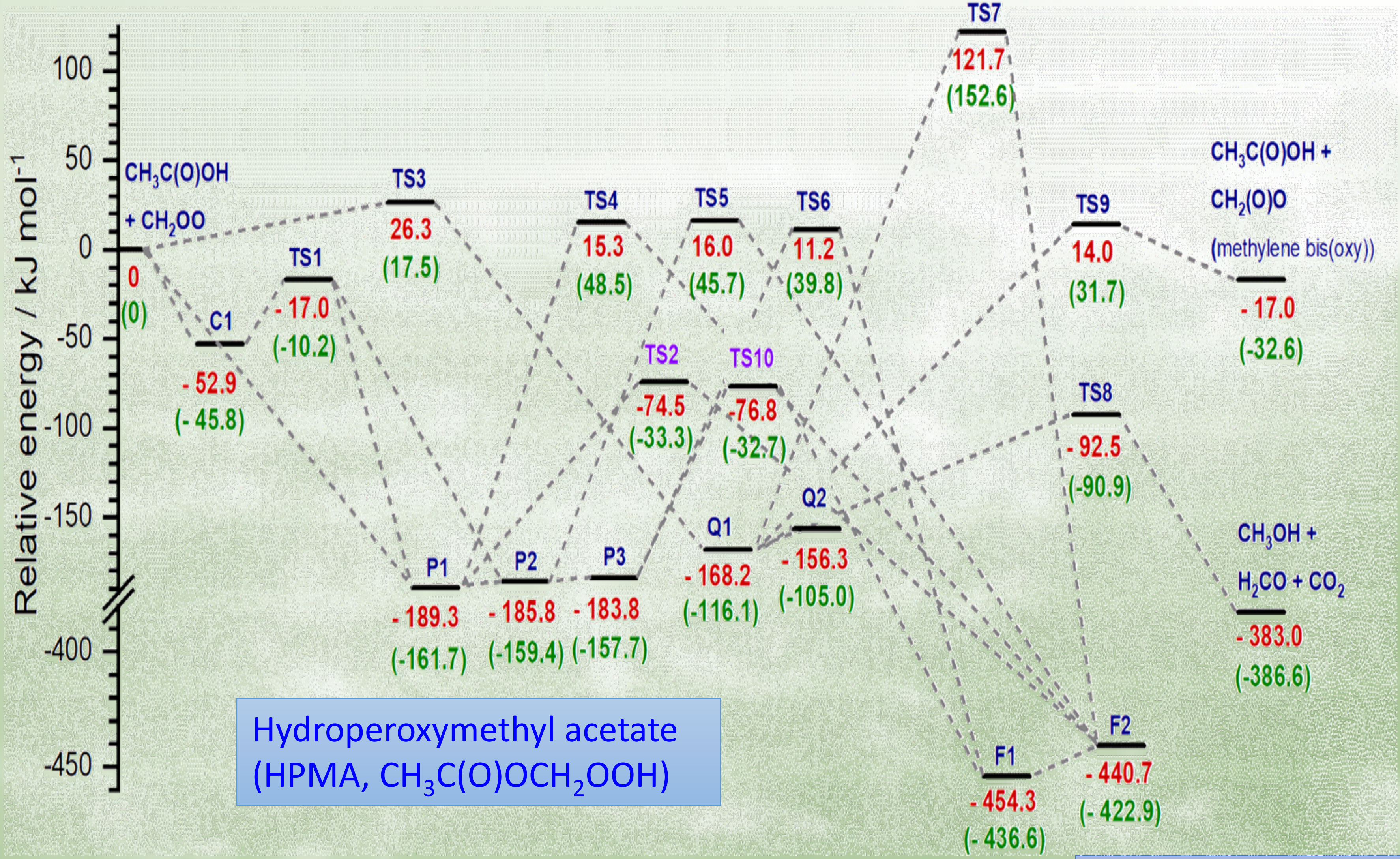

Hydroperoxymethyl acetate (HPMA, $CH_3C(O)OCH_2OOH$)

formic acetic anhydride (FAA, $CH_3C(O)OC(O)H$)

(P1)

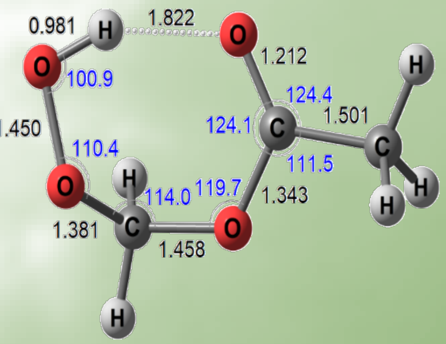

(P2)

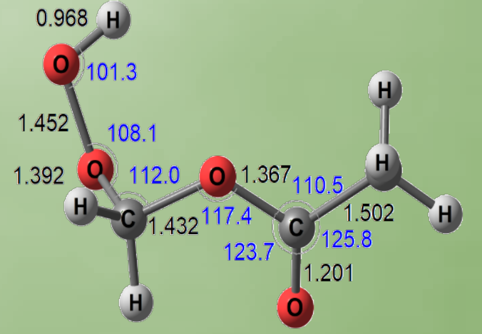

(F1)

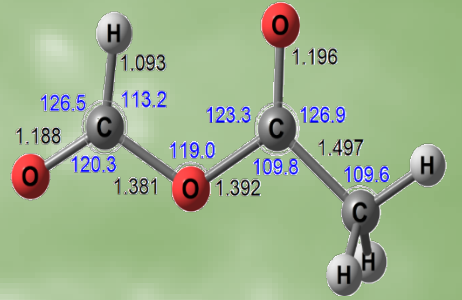

Identification of groups C & D to HPMA (P1 & P2)

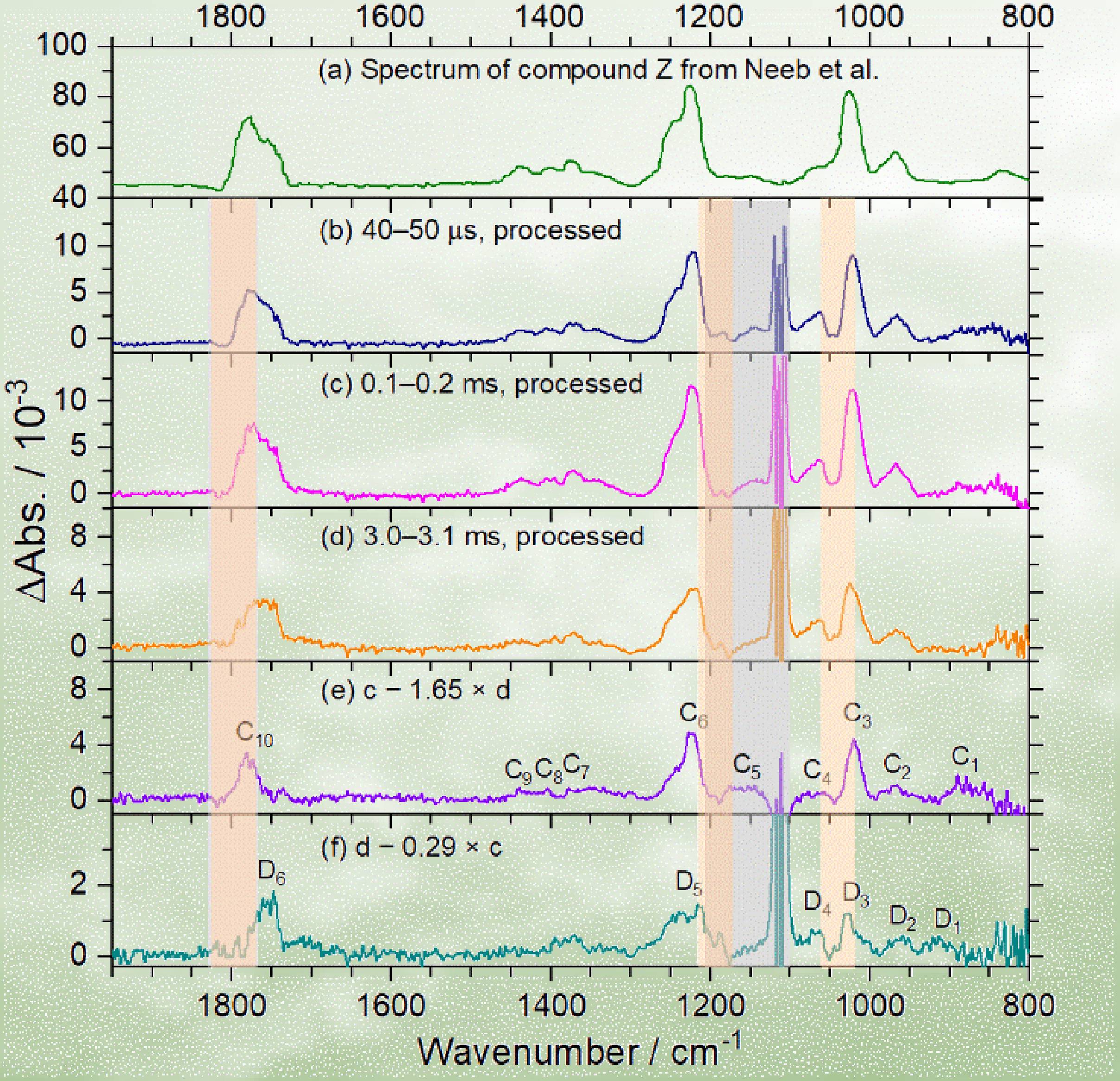

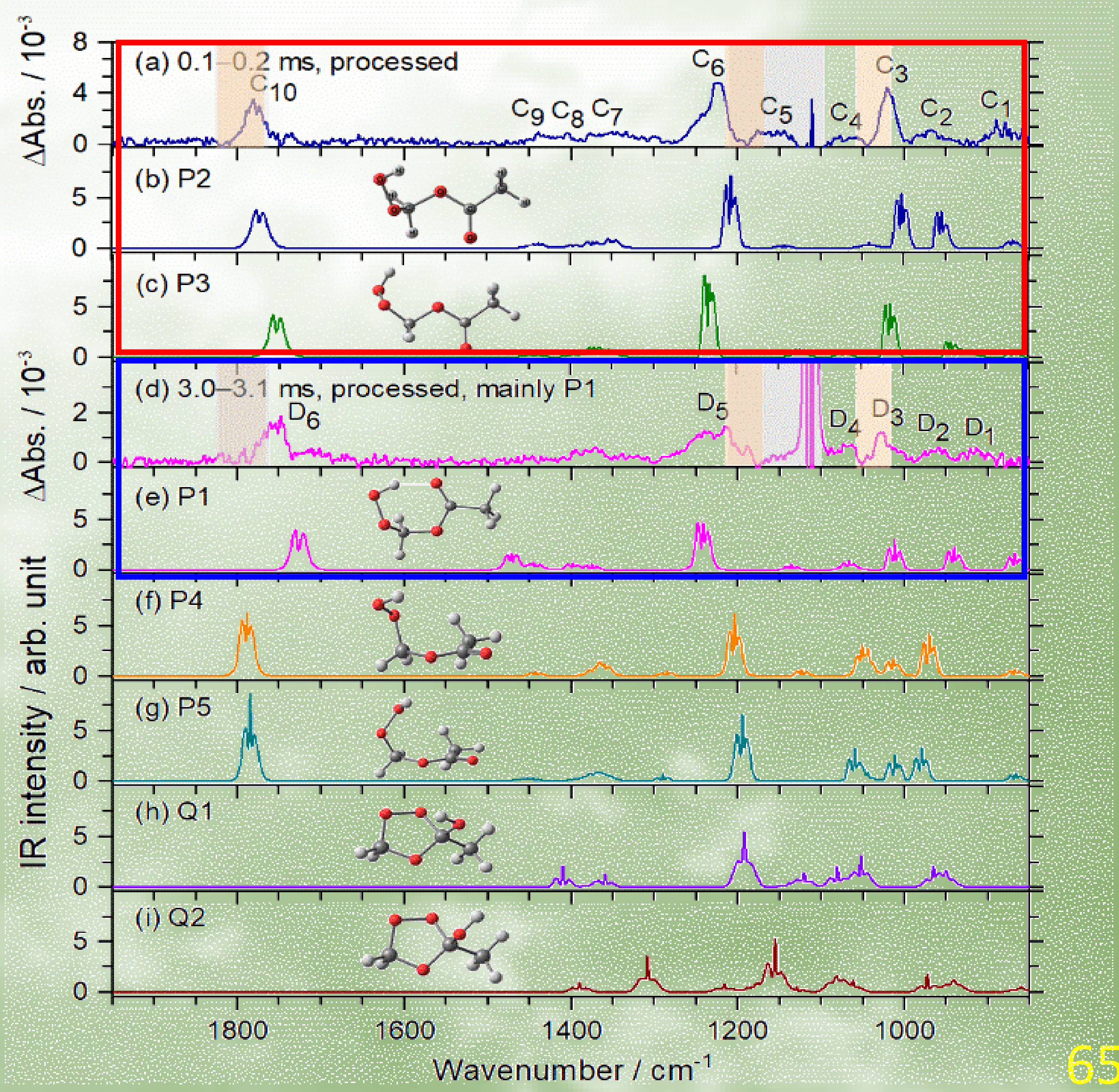

Decay of HPMA and Rise of FAA

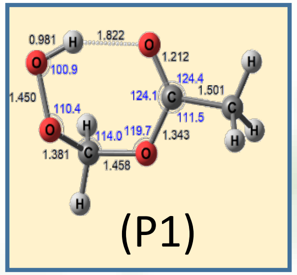

(P1)

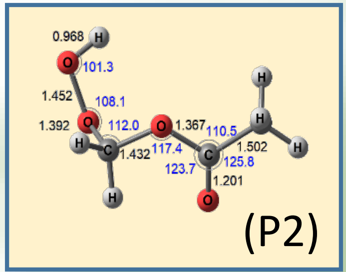

(P2)

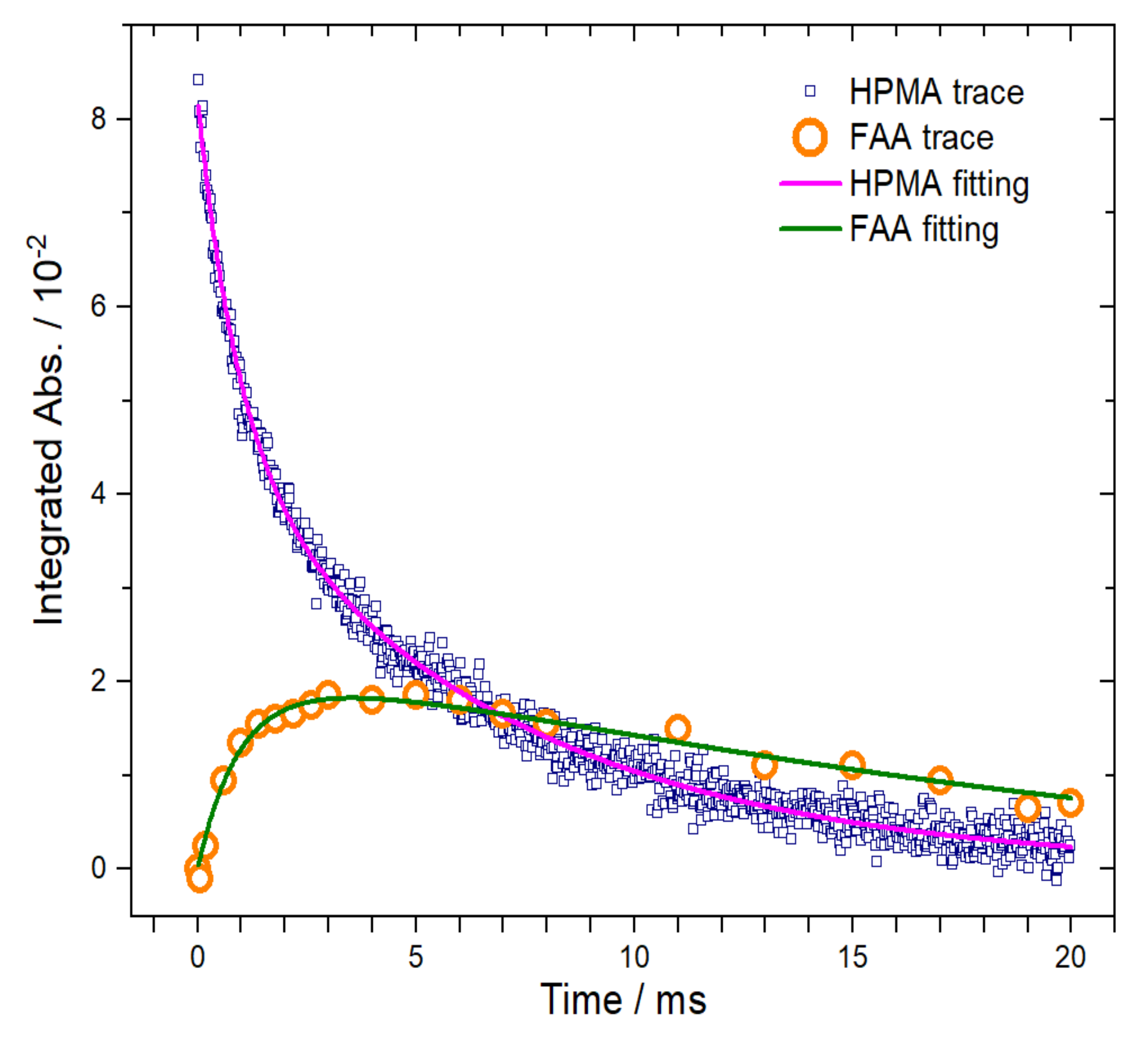

HPMA (P1) → FAA + H_2O, k_1

HPMA (P2) → FAA + H_2O, k_2

HPMA , FAA → pump away k_3

k_3 = 82 ± 2 s^{-1} (104 ± 25)
k_2 = 1000 ± 34 s^{-1} (983 ± 41)
k_1 = 67 ± 1 s^{-1} (44 ± 25)

Conformation dependent decay

2. Reaction of CH_3CHOO + HCl

conformation-independent products

interference by secondary reactions

CH_2OO + HCl

PCCP *23*, 11082 (2021)

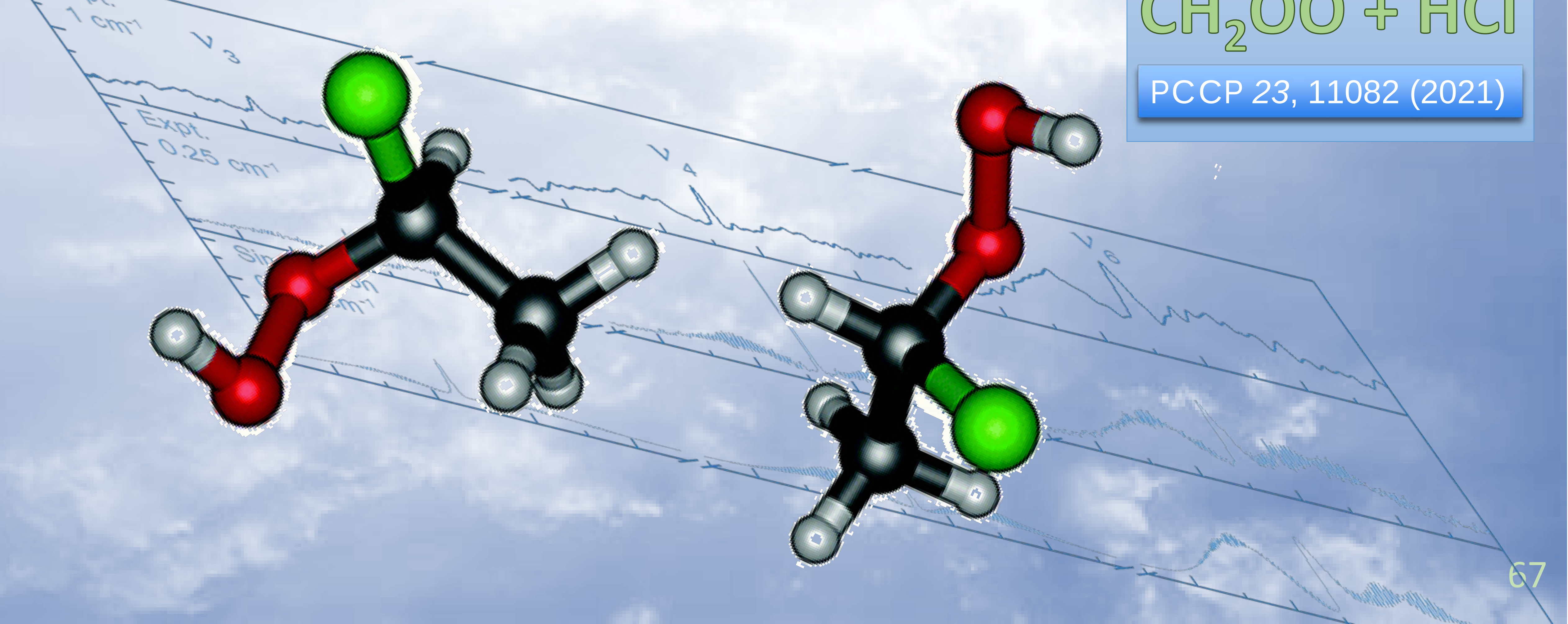

PES of $CH_3CHOO + HCl$

CCSD(T)/aug-cc-pVTZ//B3LYP/aug-cc-pVTZ

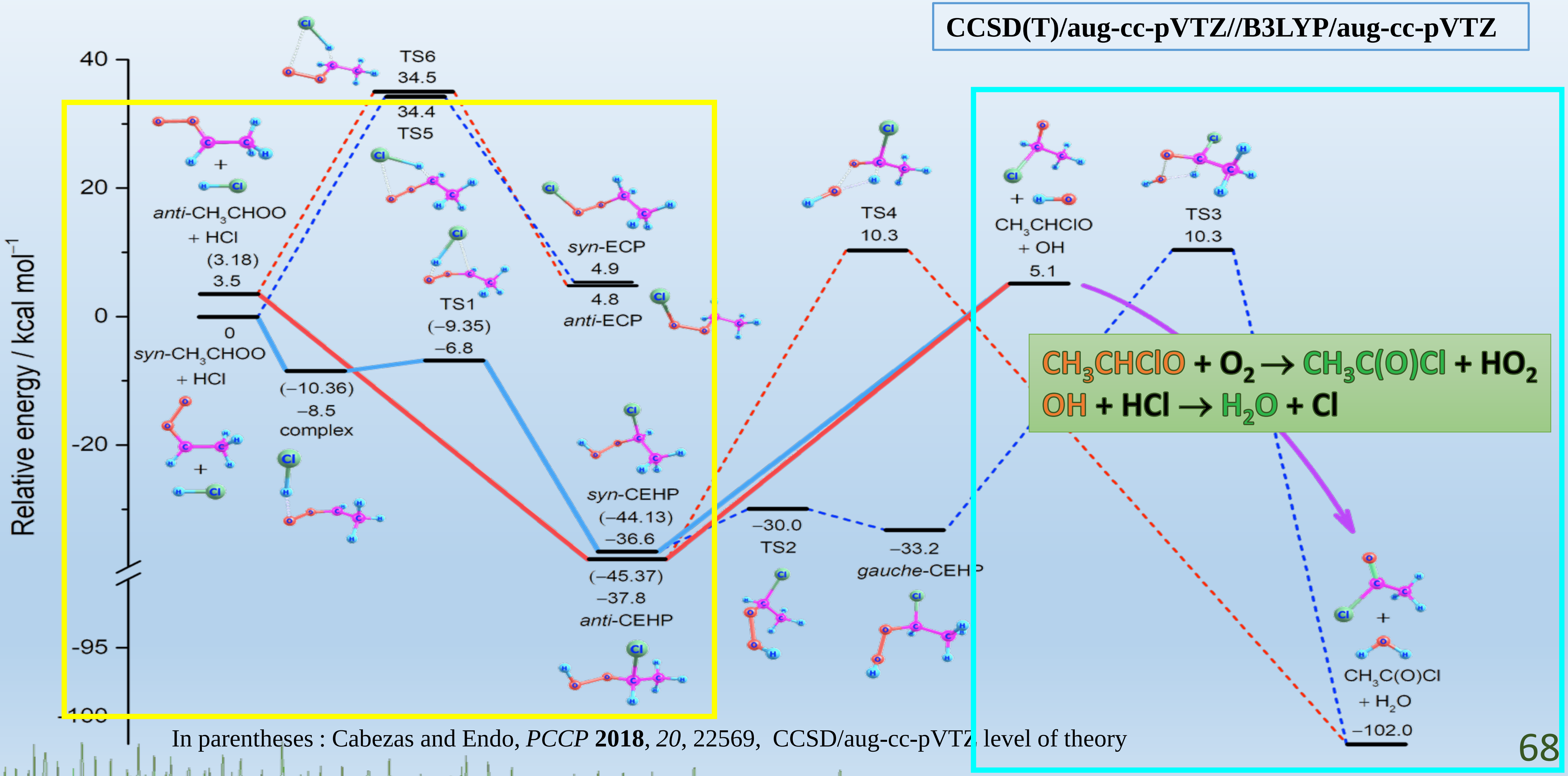

$CH_3CHClO + O_2 \rightarrow CH_3C(O)Cl + HO_2$

$OH + HCl \rightarrow H_2O + Cl$

In parentheses : Cabezas and Endo, *PCCP* **2018**, *20*, 22569, CCSD/aug-cc-pVTZ level of theory

Identification of group B: *anti*-CEHP

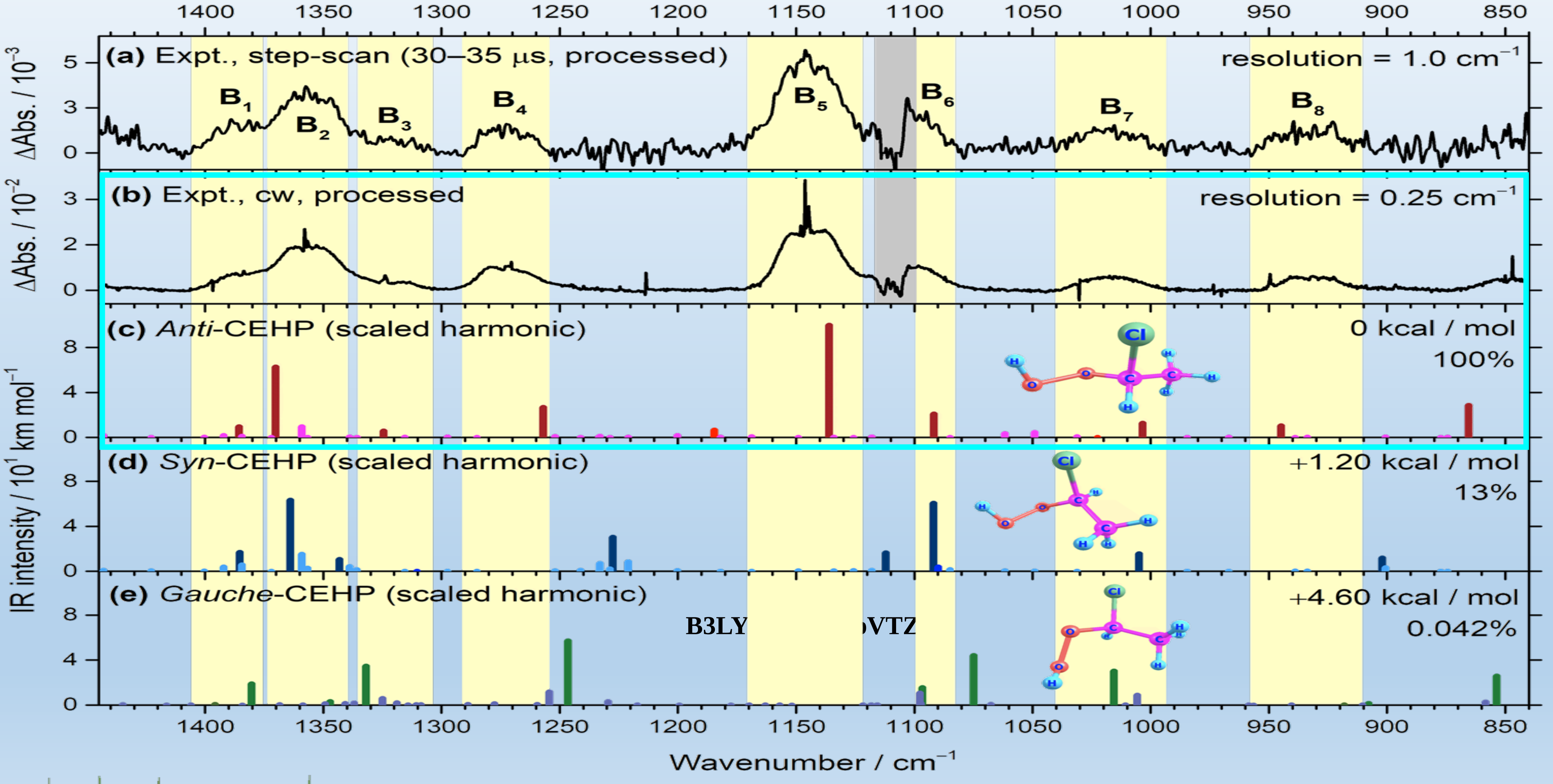

Identification of groups C & D: $CH_3C(O)Cl$ and H_2O

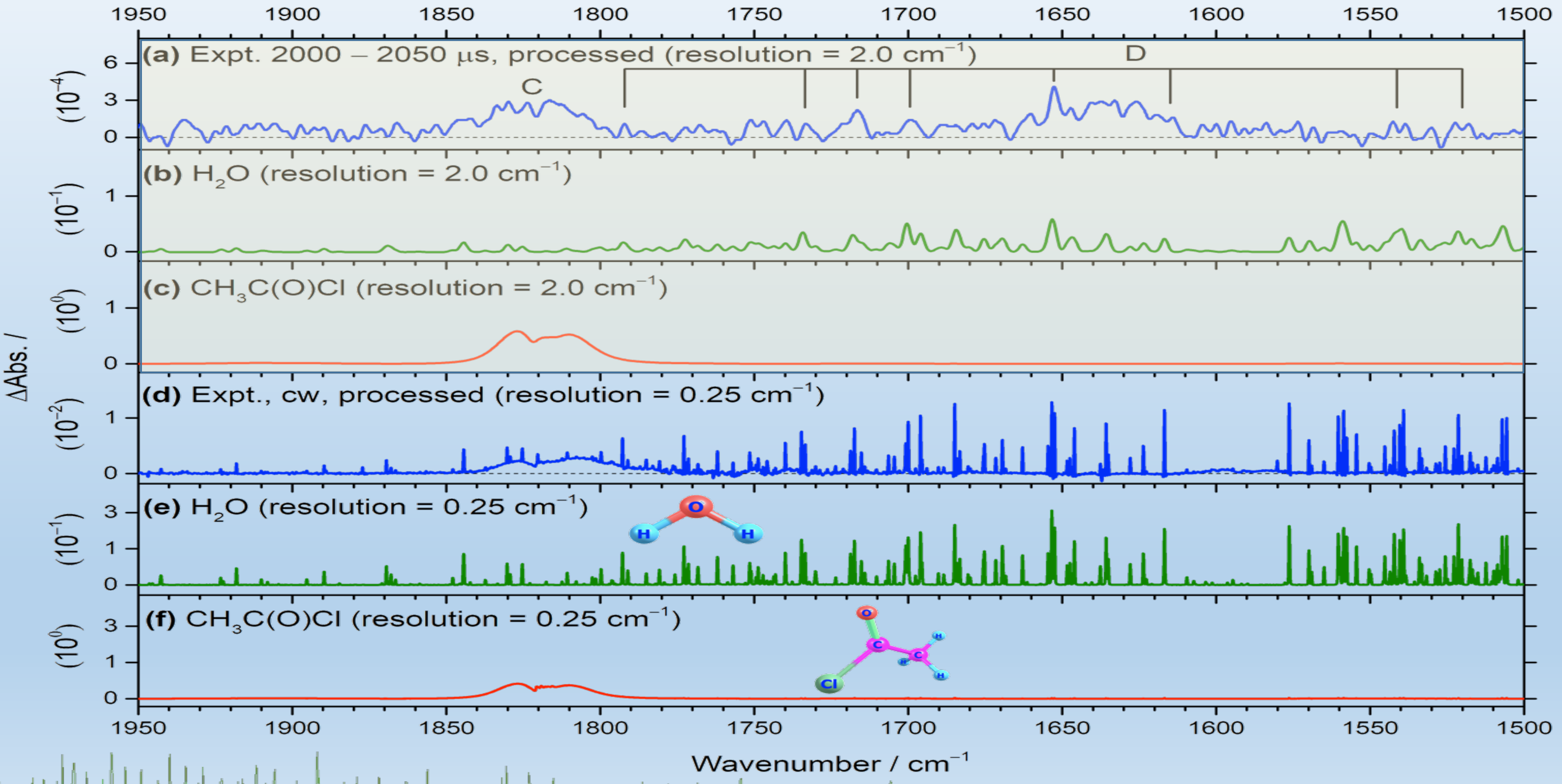

Summary of CH_3CHOO + HCl

CCSD(T)/aug-cc-pVTZ//B3LYP/aug-cc-pVTZ

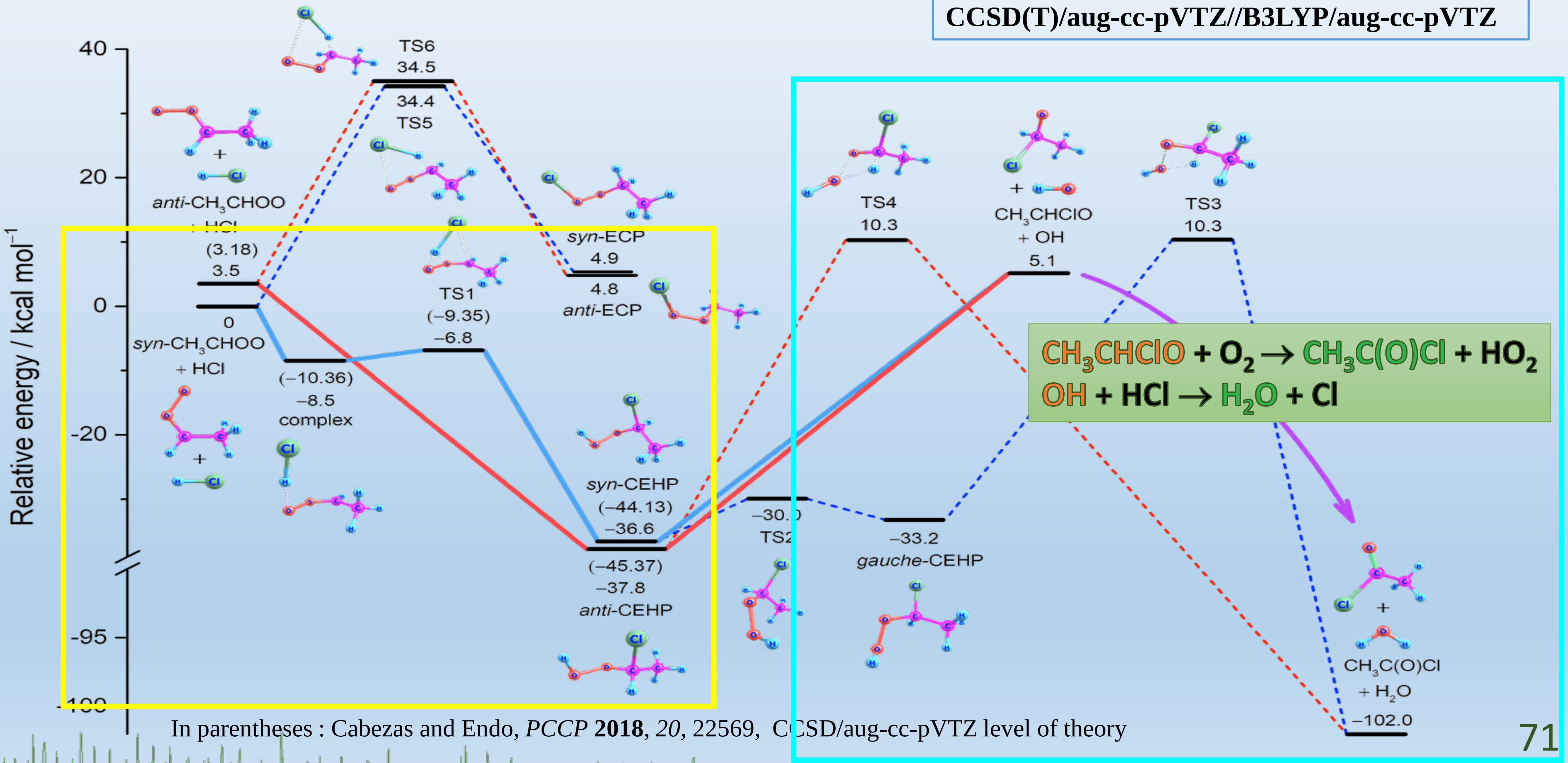

$CH_3CHClO + O_2 \rightarrow CH_3C(O)Cl + HO_2$

$OH + HCl \rightarrow H_2O + Cl$

In parentheses : Cabezas and Endo, *PCCP* **2018**, *20*, 22569, CCSD/aug-cc-pVTZ level of theory

High-resolution QCL Absorption System

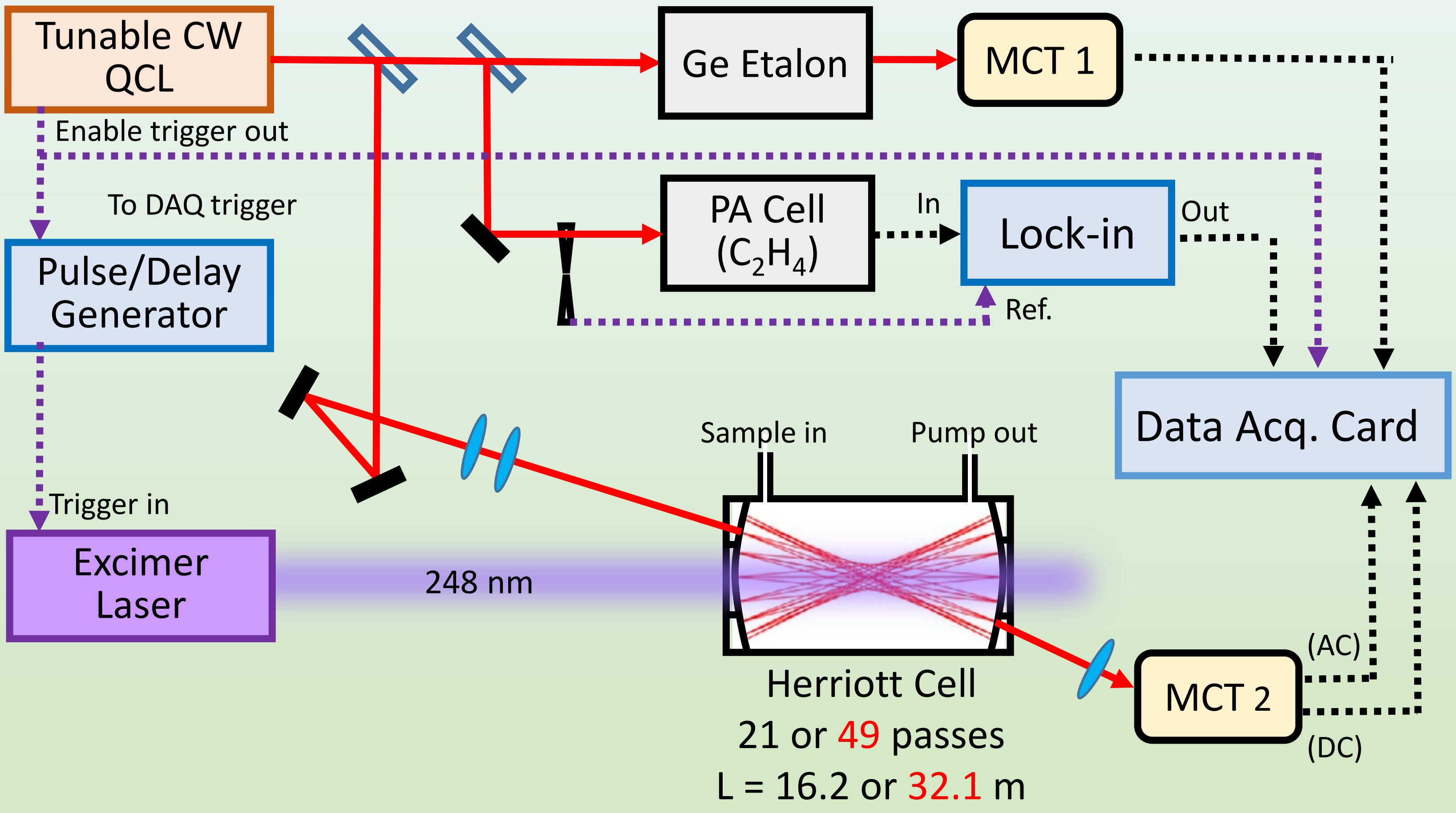

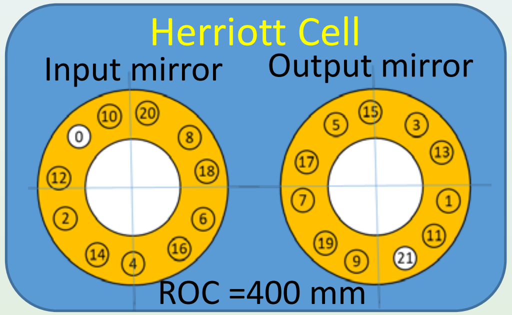

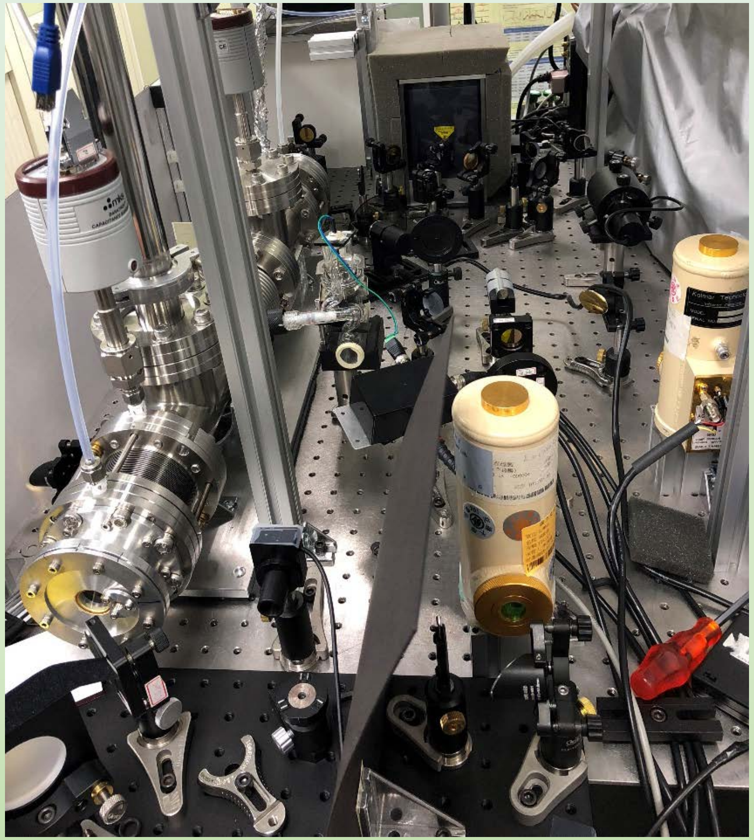

Tunable range: 880-932 cm^{-1}

1330-1260 cm^{-1}

Average power: ~ 40 mW

Line width : <5 MHz (over 100 ms)

Laser scan steps (min available): 0.0015 cm^{-1}

Spectrum of CH_2OO (ν_6) at 0.0015 cm^{-1}

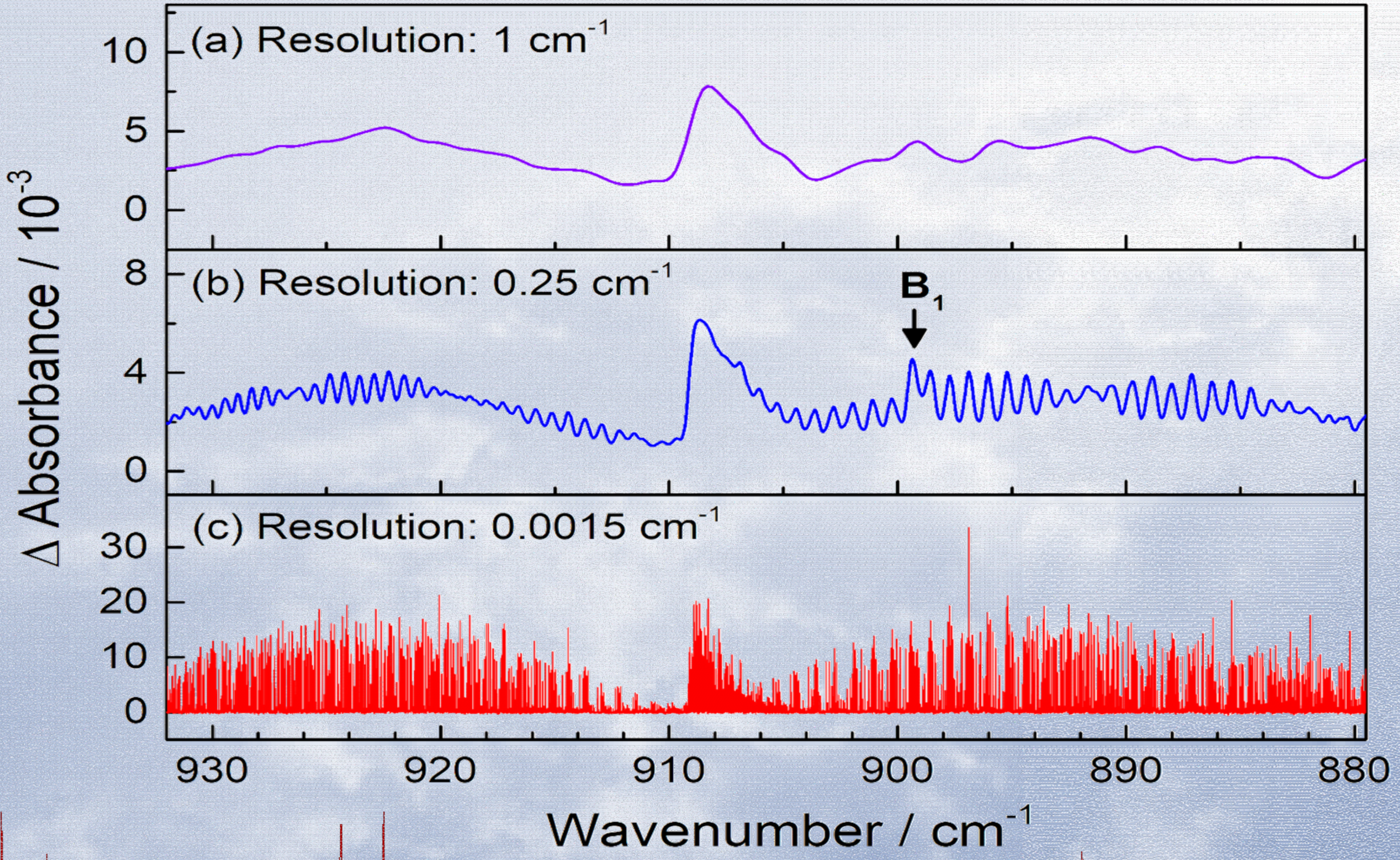

Science **340**, 174 (2013)
$CH_2I_2/N_2/O_2$ (1/20/760) at 94 Torr
$[CH_2OO]_0$ ~ 4×10^{13} mol/cm^3
340 K **(ss-FTIR)**

J. Chem. Phys. **142,** 214301 (2015)
$CH_2I_2/N_2/O_2$ (1/389) at 15 Torr
$[CH_2OO]_0$ ~ 5×10^{13} mol/cm^3
343 K **(ss-FTIR)**

PCCP, **20**, 25806 (2018)
CH_2I_2/O_2 (1/30) at 3.2 Torr
$[CH_2OO]_0$ ~ 1.2×10^{12} mol/cm^3
298 K **(QCL)**

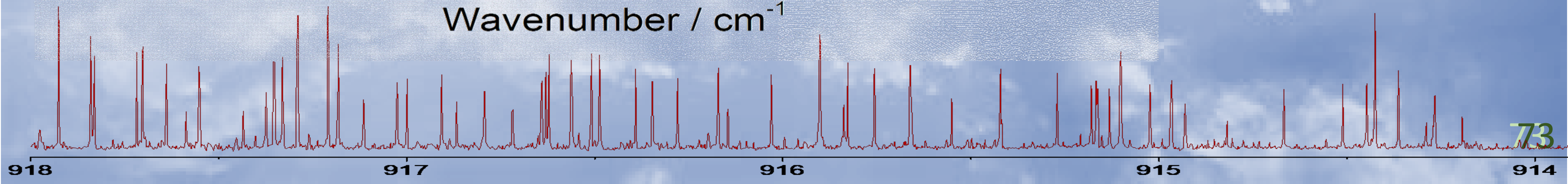

Rotational Perturbations

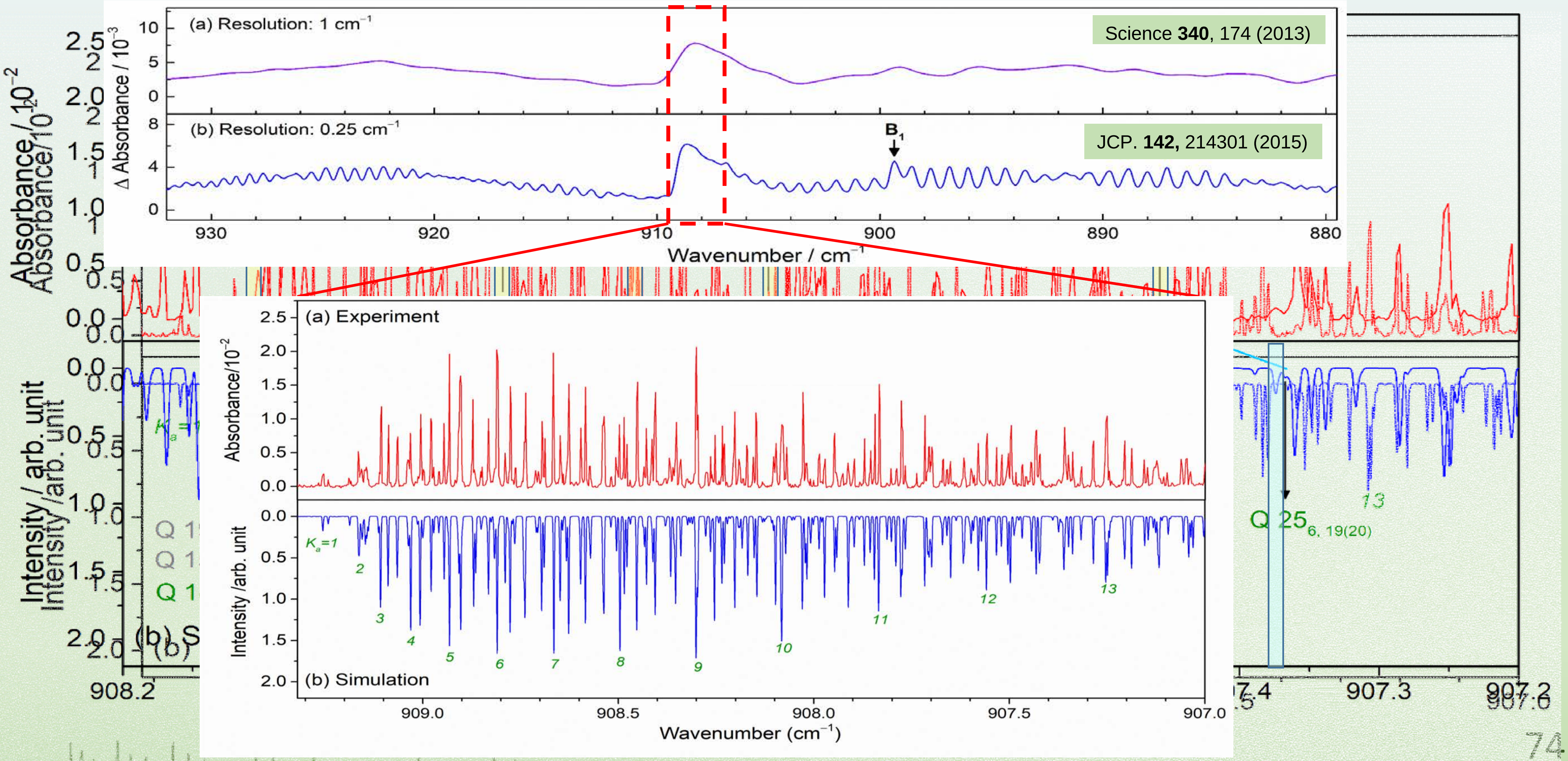

Analysis of Perturbation

Interaction between levels K_a = 6 of mode v_6 (O−O stretching) and levels K_a = 8 of mode v_8 (CH_2-wagging)

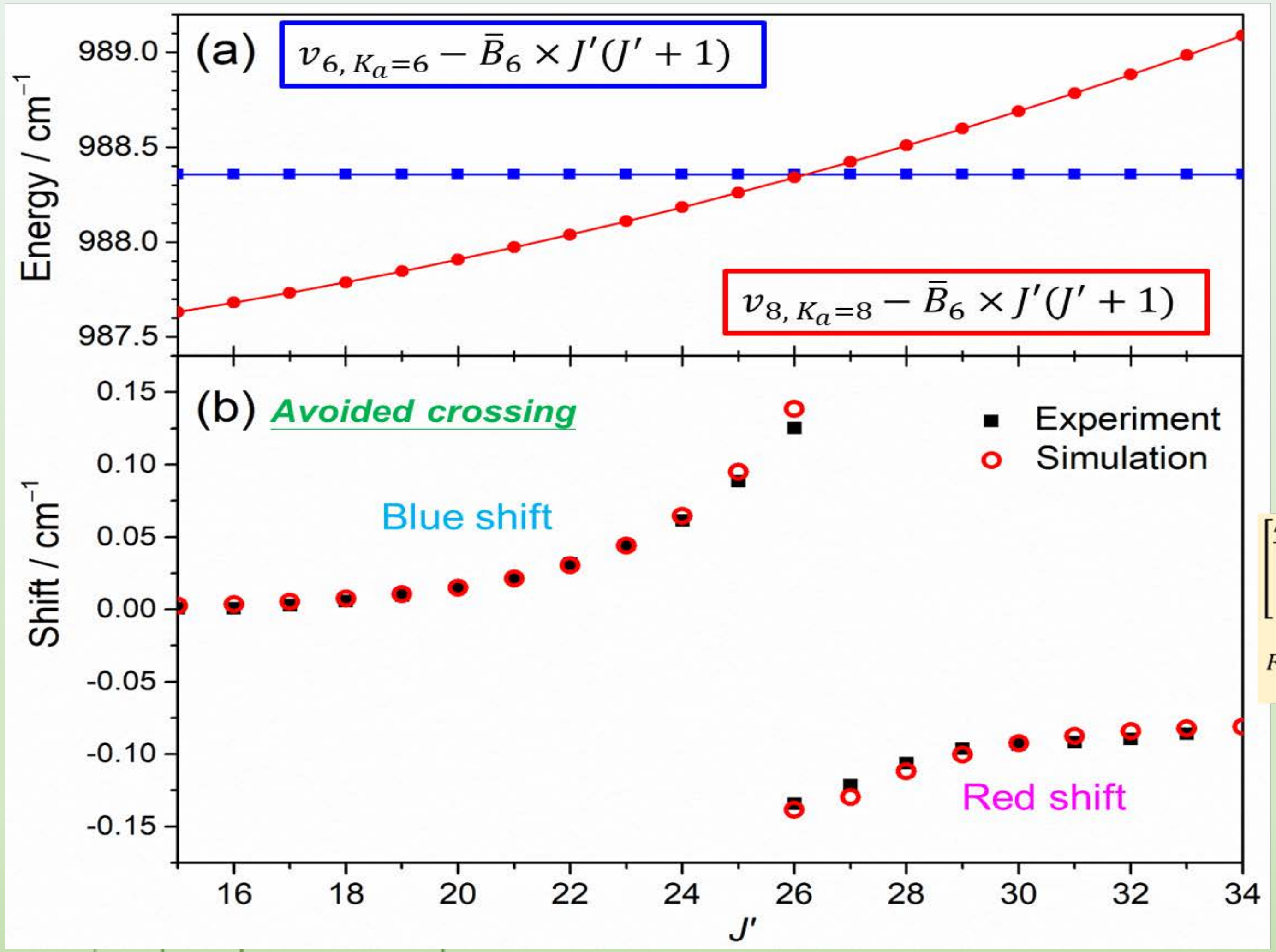

$$v_{6,\,K_a=6} = v_{6,0} + (A_6 - \bar{B}_6)\,K_a^2 + \bar{B}_6 \times J'(J'+1)$$

$$v_{8,\,K_a=8} = v_{8,0} + (A_8 - \bar{B}_8)\,K_a^2 + \bar{B}_8 \times J'(J'+1)$$

$$where\ \bar{B} = (B+C)/2$$

$v_{6,0}$ = 909.20995 cm^{-1}
A_6 = 2.5828784 cm^{-1}
$\bar{B}_6$ = 0.384336 cm^{-1}

$v_{8,0}$ = 847.095 cm^{-1}
A_8 = 2.576 cm^{-1}
$\bar{B}_8$ = 0.38587 cm^{-1}

$$\begin{bmatrix} \frac{\Delta E}{2} - x & \alpha \\ \alpha & -\frac{\Delta E}{2} - x \end{bmatrix} = 0 \qquad x = \pm\frac{\Delta E}{2}\sqrt{1 + \frac{\alpha^2}{(\Delta E/2)^2}}$$

$$For\ \Delta K_a = 2, \qquad \alpha = \alpha_0\sqrt{J'(J'+1) - K_a(K_a+1)}\sqrt{J'(J'+1) - (K_a+1)(K_a+2)}$$

Blue shift: $Shift = x - \frac{\Delta E}{2}$

Red shift: $Shift = -x + \frac{\Delta E}{2}$

Detectivity of CH_2OO

- **Welz et al.**

$\tau \cong 2$ ms

$[CH_2I]_0 \cong 9\times10^{11}$ molecule cm^{-3}

- **Our FTIR work**

$\tau \cong 50$ μs

$[CH_2I]_0 \cong 4\times10^{13}$ molecule cm^{-3}

detectivity $\cong 2\times10^{12}$ molecule cm^{-3}

- **Our QCL system**

CH_2I_2 = 7.6 mTorr

(2.4×10^{14} molecule cm^{-3})

O_2 = 3.2 Torr

$[CH_2OO] \cong 1.2\times10^{12}$ molecule cm^{-3}

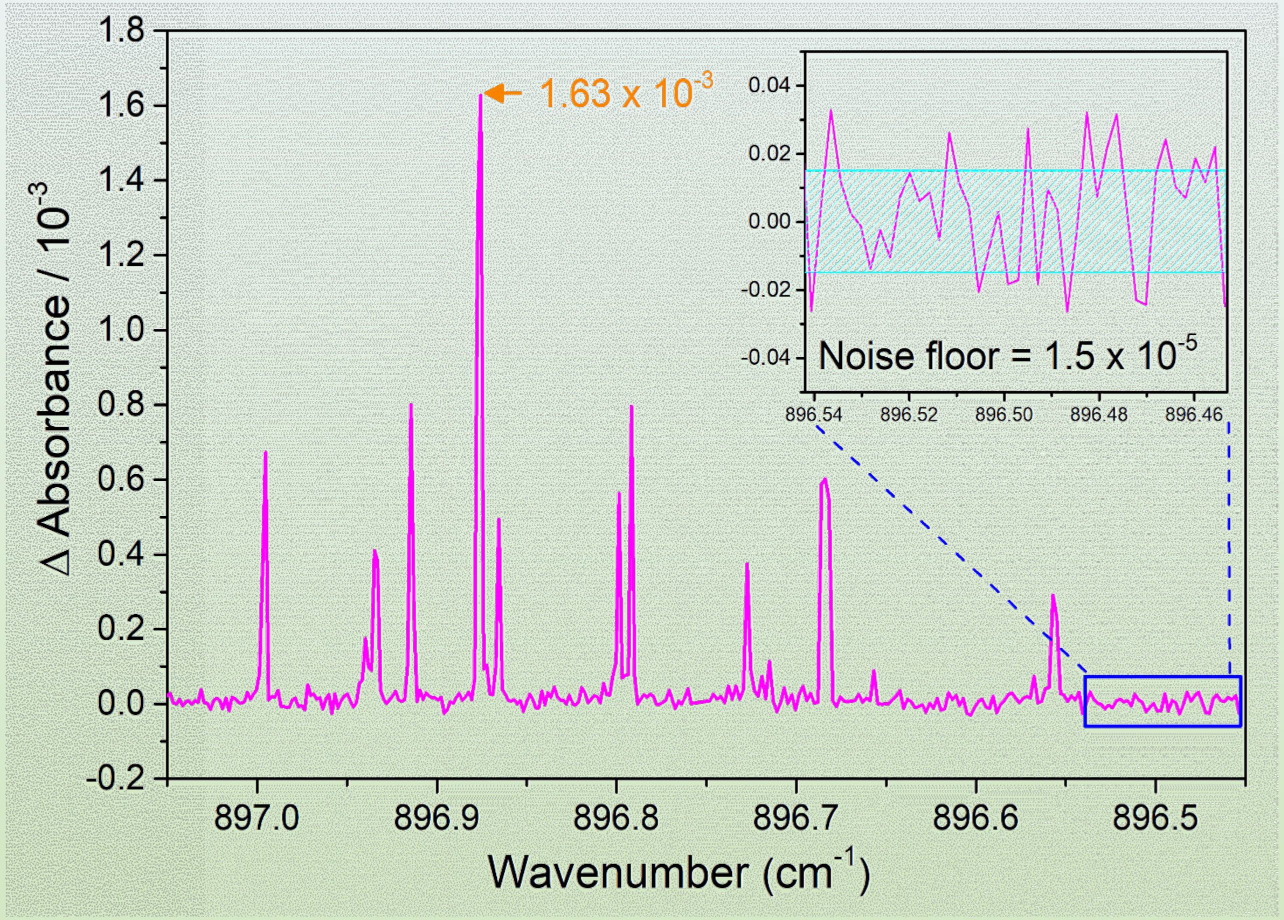

Min. detectivity $\cong 1.1\times10^{10}$ molecule cm^{-3}

~200 times better than FTIR

New Setup: Simultaneous IR/UV Absorption for Kinetics

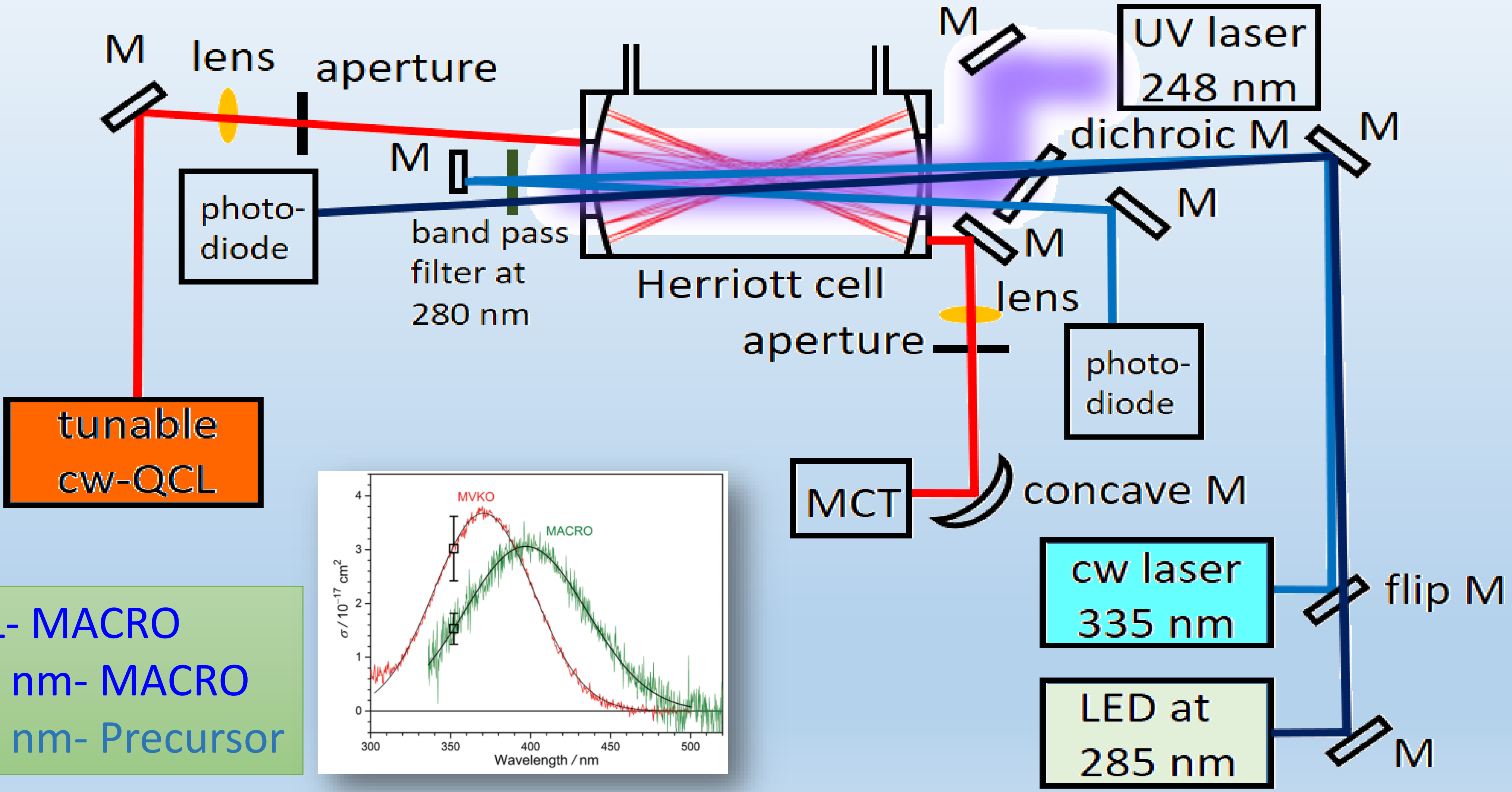

QCL- MACRO
335 nm- MACRO
285 nm- Precursor

Formation rate coefficient

Self-reaction rate coefficient

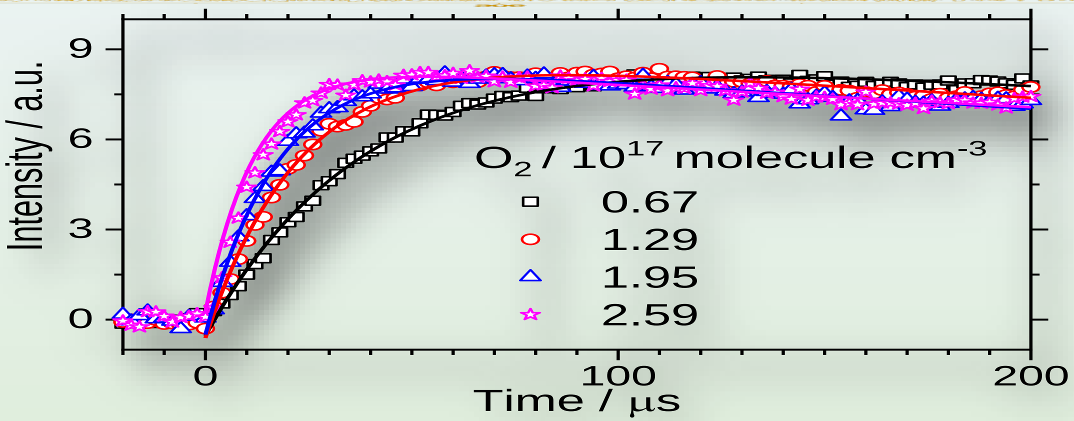

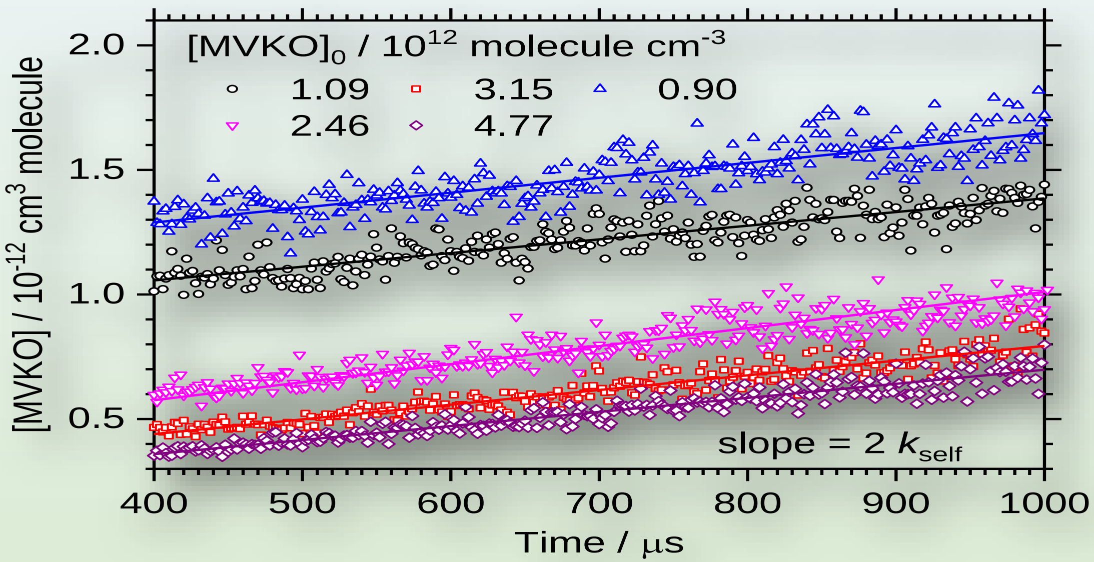

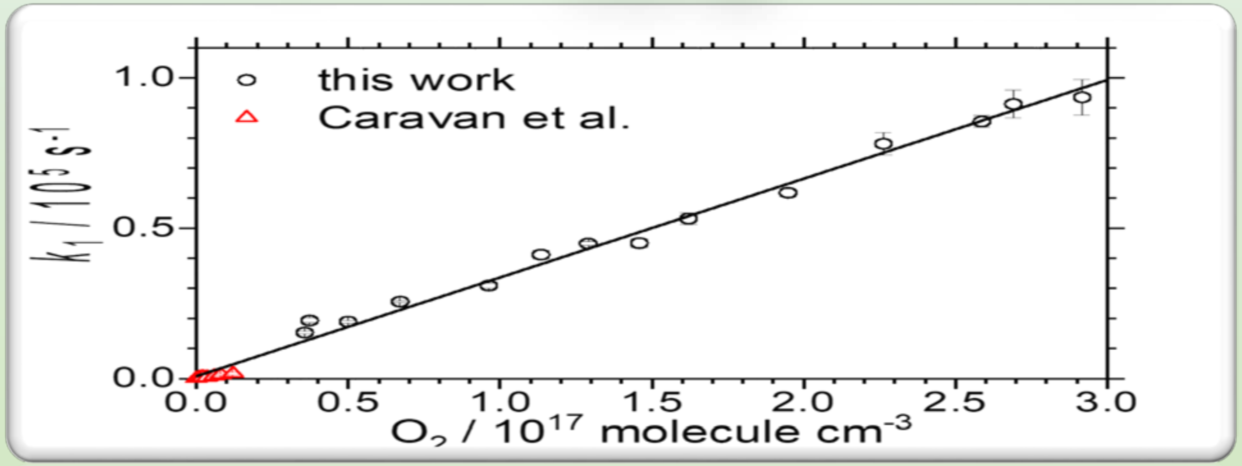

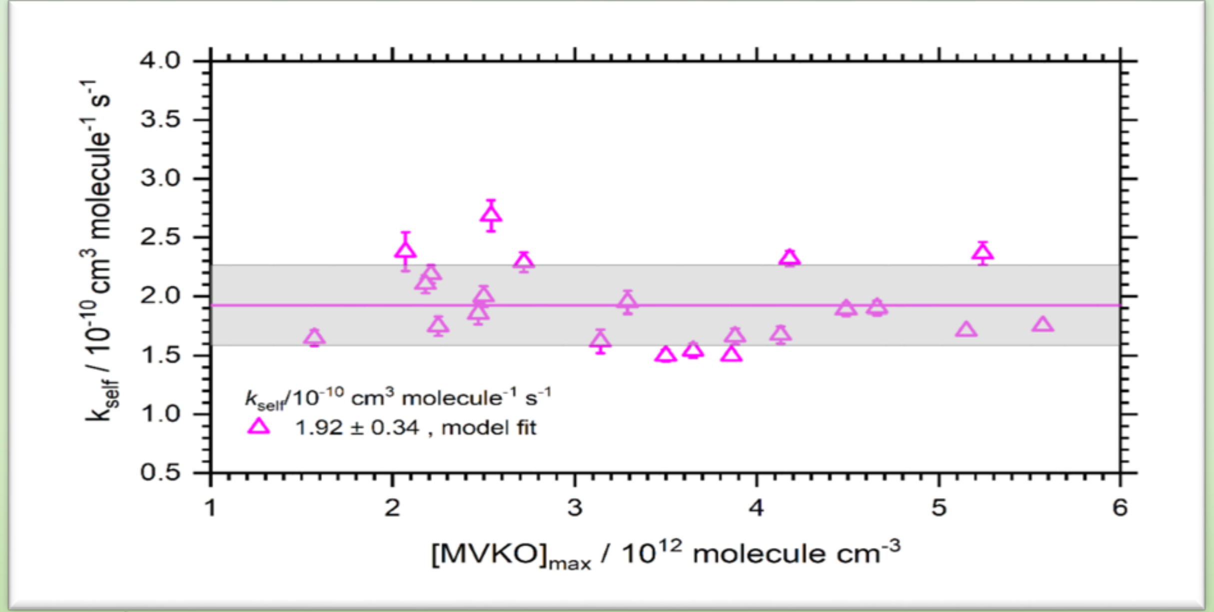

	this work	Caravan et al.
k_{O_2} / 10^{-13} cm^3 s^{-1}	2.8 ± 0.3	1.7 ± 0.1
O_2 / 10^{16} cm^{-3}	3.6–29.1	0–1.2

Caravan *et al.*, Proc. Nat. Acad. Sci. USA **117**, 9733 (2020).

Step-scan FTIR & QCL

J. Chin. Chem. Soc. *61*, 47 (2014)

Mini Review

JOURNAL OF THE CHINESE CHEMICAL SOCIETY

Transient Infrared Absorption Spectra of Reaction Intermediates Detected with a Step-scan Fourier-transform Infrared Spectrometer

Yu-Hsuan Huang,[a] Jin-Dah Chen,[a] Kuo-Hsiang Hsu,[a] Li-Kang Chu[b]* and Yuan-Pern Lee[a,c]*

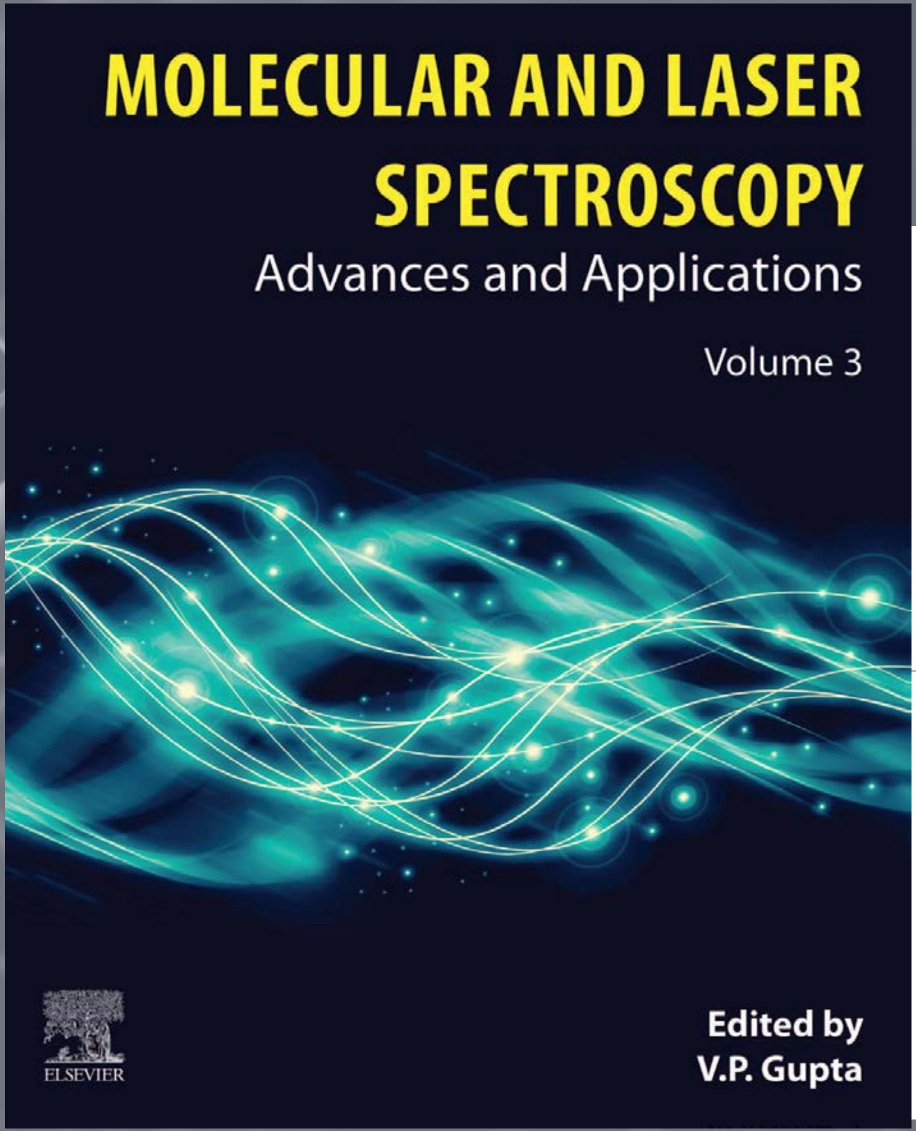

CHAPTER 14

Step-scan FTIR techniques for investigations of spectra and dynamics of transient species in gaseous chemical reactions

Li-Kang Chu[1], Yu-Hsuan Huang[2] and Yuan-Pern Lee[3,4,5]

CHAPTER 15

Quantum cascade lasers and their applications to spectral and kinetic investigations of reactive gaseous intermediate species

Chen-An Chung[1] and Yuan-Pern Lee[1,2,3]

Future Perspectives

para-H_2 matrix isolation

- **Fundamental understanding of hydrogen diffusion/tunneling**
  - Detailed mechanism
  - Anonymous temperature behavior
  - Spectral (IR) signature of H and H^+
- **Protonated/cationic PAH**
  - Larger PAH (evaporation, new protonation/ionization methods)
  - UV-induced IR emission
  - Improved calculations (anharmonic, Fermi-resonance)
- **Hydrogen reactions**
  - Other hydrogen sources
  - More examples of H-induced uphill isomerization/fragmentation
  - More prebiotic reactions (RNA precursors, enantiomer-selectivity)
- **Electronic transitions**
  - More data for matrix shifts, relaxation, and phonon interactions
  - Real identification to DIB

Future Perspectives
gas-phase transient spectroscopy

- **Improved sensitivity of step-scan FTIR in absorption mode**
  - Hardware improvement (light source, digitizer, Herriott cell)
  - Data processing (2D-correlation, spectral reconstruction, linear prediction)
  - Supersonic jet or discharge jet
  - New digitizer (1 μs, 20 bit) for kinetics
  - AI-assisted data analysis

- **Quantum-cascade laser**
  - Improved lasers (fill the spectral gap, wider coverage, mode-hop free)
  - Built-in wavelength calibration (frequency comb)
  - Multiplex methods (UV, several QCL)
  - QCL-based dual-comb (spectral & temporal resolution)
  - AI-assisted spectral analysis

ACKNOWLEDGEMENTS

Post-doctors & visiting scientists are needed!

Funding:

MOST 科技部 Ministry of Science and Technology

Ministry of Education Republic of China (Taiwan)

新世代功能性物質研究中心

Center for Emergent Functional Matter Science, CEFMS